



Cite this: *RSC Appl. Polym.*, 2025, **3**, 43

## Recent progress in the development of porous polymeric materials for oil ad/absorption application

Hyejin Lee,<sup>a</sup> Guowei Chen,<sup>a</sup> Boon Peng Chang<sup>b</sup> and Tizazu H. Mekonnen   <sup>a</sup>

Porous polymer materials, including polymer foams and melt-blown fibers, have nano or micro-size pores and a large specific surface area that endows them with great potential as engineered oil ad/absorption materials. This review provides an overview of the recent developments in the processing of polymer foams and melt-blown fiber-based porous polymeric materials for oil absorption properties. Detailed processing and preparation methods of polymer foams utilized in oil absorption are scrutinized, along with the recent peer-reviewed published research on the development of new polymer foams, such as nanocomposite foams and biodegradable foams. Critical reviews are also conducted on the modification methods, such as employment of surfactants, coating, plasma treatment, and chemical grafting. In addition, the recent progress in the processing of melt-blown fibers and the potential applications for oil absorption are discussed. A comparative analysis of the strengths and weaknesses of porous polymer materials between polymer foams and melt-blown fibers is presented. Lastly, the potential for developing melt-blown non-woven fibers as a viable alternative for oil absorption materials is explored.

Received 25th June 2024,  
Accepted 13th November 2024

DOI: 10.1039/d4lp00211c

[rsc.li/rscapplpolym](http://rsc.li/rscapplpolym)

### 1. Introduction

With industrial growth and urbanization, there has been a substantial increase in petroleum usage in transportation, power generation, and the fabrication of plastics and chemicals. Petroleum is derived from organic substances, such as ancient plants and marine creatures that have been buried under sediment in the ocean and the land.<sup>1</sup> Petroleum is extracted and transported to refineries where it is processed into various petrochemicals, such as diesel, gasoline, asphalt and road oil, petroleum coke, hydrocarbon gas liquids, *etc.* However, oil extraction, upgrading, transportation, and processing often result in spills and a large amount of oily wastewater discharge, leading to significant marine pollution with detrimental impacts on the environment, and large economic losses.<sup>2</sup> Despite the improved production technologies and safety precautions that have reduced accidental spills from oil platforms to around 3% of the petroleum inputs worldwide,<sup>3</sup> major oil spill accidents continue to occur regularly around the world. Some of the most significant oil spill accidents that have occurred since 1970 include the collision of *Atlantic*

*Empress/Aegean Captain* (1979) that caused 160 000 metric tons of oil release, the major oil spill in the Gulf of Mexico (1979) of 450 000 metric tons (Fig. 1(a)), the *Exxon Valdez* oil spill that occurred in Prince William Sound, Alaska (1989) (Fig. 1(b)), the Gulf War oil spill in Kuwait (1991) that led to 1 million metric tons of crude oil release, the *Sea Empress* oil spill (1996) that spilled 3 million metric tons of crude oil, and *Deepwater Horizon* (2010) in the Gulf of Mexico of 680 000 metric tons oil spill.<sup>4–6</sup> Fig. 1(c) presents the satellite image of the Gulf Coast when the *Deepwater Horizon* oil spill happened in 2010, and the impact continues even after 10 years.

The consequences of oil spills can be severe, impacting both marine and terrestrial ecosystems for years and requiring billions of dollars for restoration efforts. In the advent of oil spilling over the ocean, it reduces the amount of dissolved oxygen in the water and blocks sunlight from penetrating the surface. This can have devastating effects on marine life, causing hypothermia and death among birds and mammals whose waterproofing and insulating properties are compromised by the oil.<sup>8</sup> Oil spills have caused serious water pollution to the environment as well and affected the global economy; thus, research and development into highly efficient oil spill cleanup methods have become of paramount importance.

In recent years, extensive studies have been conducted, and numerous oil spill cleanup methods have been developed with varying degrees of success. The choice of the methods is dependent on several factors, such as the amount and the type

<sup>a</sup>Department of Chemical Engineering, Institute of Polymer Research, Waterloo Institute of Nanotechnology, University of Waterloo, Waterloo, Ontario N2L 3G1, Canada. E-mail: [tmekonnen@uwaterloo.ca](mailto:tmekonnen@uwaterloo.ca)

<sup>b</sup>School of Materials Science and Engineering, Nanyang Technological University, 50 Nanyang Avenue, 639798, Singapore



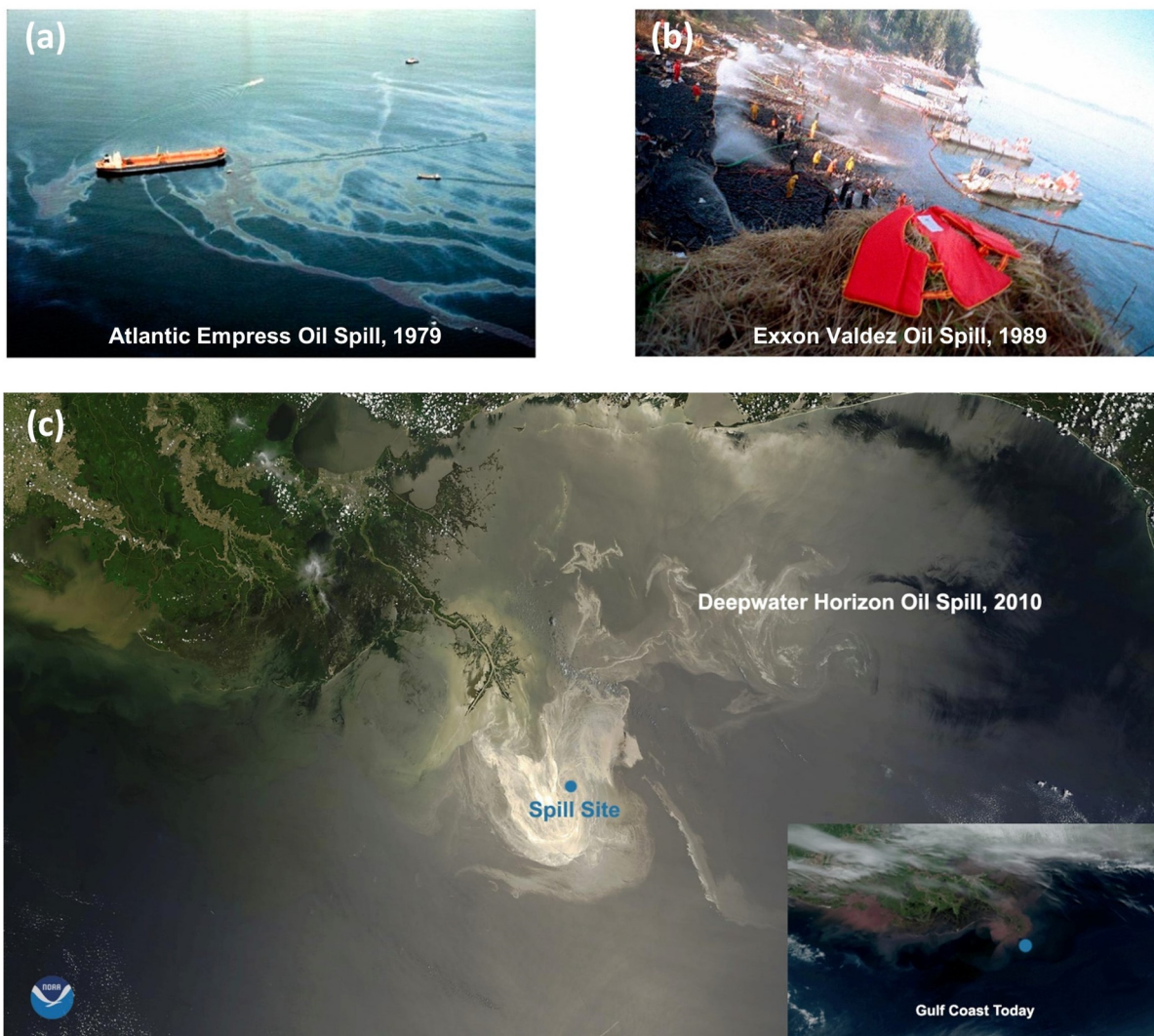


**Fig. 1** Some events of oil spills and clean-up efforts. (a) *Atlantic Empress*, 1979. (b) *Exxon Valdez*, 1989. (c) *Deepwater Horizon*, 2010. (Reproduced from ref. 7 for (a) and (b). Copyright 2018 Marine Science and Engineering; (c) is from the open-source year of 2020, credit to National Oceanic and Atmospheric Administration (NOAA).)

of discharged oil, the weather (wind and waves) conditions, and the surrounding environment (ecosystems and marine species) of the oil-spilled site. The major recovery methods include chemical methods, bioremediation, *in situ* burning, physical methods, and combinations.<sup>9</sup>

The chemical methods involve the use of chemicals that alter the physical and chemical properties of the oil, facilitating its containment and cleaning.<sup>10</sup> Dispersants and solidifiers are two major categories of chemicals commonly used for this method. Dispersants are surfactants that function by breaking down the oil slick into smaller droplets that can be dispersed in the ocean (Fig. 2). The diluted oil is then consumed by native marine microbes, as hydrocarbons are great sources of carbon and energy for them.<sup>11,12</sup> Solidifiers are hydrophobic granules that work as coagulants. When reacted with oil, they change the oil from a liquid to a rubbery state so that oil compounds can be efficiently removed. They are

usually employed along with physical clean-up methods, such as booms and skimmers. The advantage of chemical methods is that they can quickly prevent the spread of oil spills; however, those chemicals can be noxious and sometimes toxic to several marine organisms.

The bioremediation method employs the biodegradation capability of microorganisms, such as bacteria, fungi, protozoa, and nematodes that metabolize and degrade hydrocarbons in crude oil.<sup>13</sup> Organic substances are flocculated by aggregated microorganisms, and a form of sludge is generated. Through this process, the pollutants are degraded into non-toxic gases like  $\text{CO}_2$  and  $\text{H}_2\text{O}$ , which is helpful for restoring the marine/land environment.<sup>14</sup> Alkanes and aromatic compounds of low molecular weight are rapidly degraded by microbial enzymes; however, complex organic compounds require a longer time to degrade, as there are a smaller number of microorganisms that can break down large complex



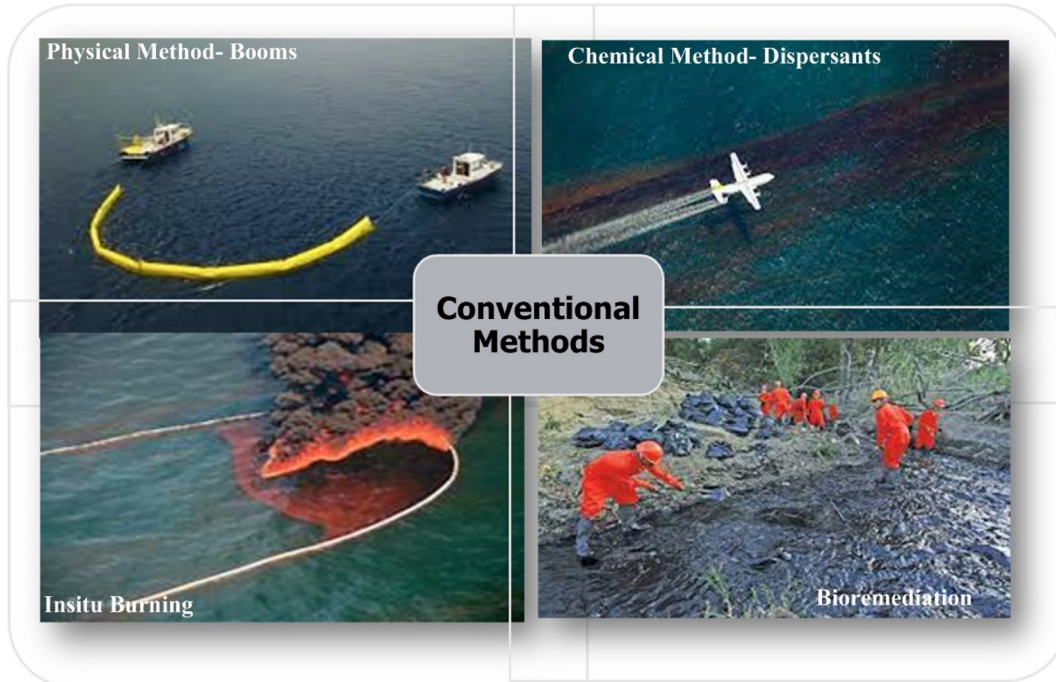


Fig. 2 The conventional oil spill remediation methods. (Reproduced from ref. 8. Copyright 2022 Elsevier Inc.)

hydrocarbons.<sup>15</sup> Bioremediation has the benefit of being a relatively inexpensive and eco-friendly technology. However, this method is not free of limitations; some organic components are only degraded by specific species of microorganisms, strict conditions need to be met for the microbes to proliferate, and depending on the oil concentration, inherent biodegradability, and biological environment, the biodegradation can take a long time, ranging from several weeks to months.<sup>16,17</sup>

As thermal remediation, *in situ* burning is widely practiced and considered an efficient method that prevents the environmental damage of oil discharged into sensitive aquatic ecosystems<sup>18</sup> (Fig. 2). It can be conducted rapidly in urgent situations where spilled oil poses a serious hazard to marine habitats and the environment. However, burning oil generates a wide range of air pollutants, such as smoke, carbon monoxide, sulfur dioxide, nitrogen oxides, and particulate matter, which can have a detrimental impact on the air condition.<sup>19</sup> Additionally, *in situ* burning typically requires some containment, has a limited window of opportunity, and might not be suitable for thick oil and unfavorable weather which can restrict its implementation.<sup>20</sup>

The physical cleanup method involves the application of mechanical means to remove oil without changing the chemical and physical properties of the oil.<sup>21</sup> Booms and skimmers are essential tools when it comes to containing and recovering oil spills. Booms are utilized to contain and control the spread of oil spills on the surface of the water, and they can be deployed quickly to form a barrier. A skimmer is another mechanical device often utilized in conjunction with a containment boom for effective oil cleanup. Fence booms, curtain

booms (inflated booms), and fire-resistant booms are some of the types available, and their effectiveness is determined by factors such as the type and concentration of the spilled oil<sup>22,23</sup> (Fig. 2). Unfortunately, their utilization has some downsides – for booms, much of the spilled oil sinks to the bottom, causing damage to marine life undersea and forming tar balls.<sup>24</sup> Skimmer technology is effective at mechanically extracting concentrated oil but is often inefficient; a large amount of oil is left mixed with water, resulting in high recycling costs and difficulties.

Meanwhile, employing sorbents (absorbents and adsorbents) has been widely accepted as the most efficient physical method for oil/water separation.<sup>25</sup> The sorbent materials generally offer advantageous properties such as cost-efficiency, light weight, high oil uptake capacity, and rapid oil sorption. Moreover, they have a great environmental benefit, as this approach does not involve chemicals during the oil cleanup process. Generally, oil sorbents fall into three main categories: natural organic materials (e.g., cotton, wool, kapok), synthetic organic materials (e.g., polypropylene, polyurethane), and inorganic minerals (e.g., zeolite, vermiculite, perlite, silica). Each category presents distinct advantages and limitations in oil spill remediation. Natural organic sorbents offer biodegradability and abundance, but typically exhibit low oil sorption capacity and poor reusability. In contrast, synthetic organic sorbents demonstrate superior oil selectivity and sorption capacity, although they face biodegradability challenges. Inorganic sorbents provide excellent stability but generally achieve lower sorption capacities than their organic counterparts. Recent research efforts are addressing these limitations

through innovative modifications across material types. For natural organic materials, chemical treatments enhance sorption capacity and selectivity, while synthetic organic materials are being optimized with biodegradable components to improve environmental compatibility without compromising performance. Additionally, inorganic mineral-based sorbents are undergoing nanoscale engineering to boost absorption efficiency while retaining their intrinsic stability and durability. Biochar and polymer aerogels are newer options with high surface areas and tunable properties. Though promising, they may still be limited by production costs or scalability. Building upon these approaches, various advanced sorbent materials, such as silica/graphene,<sup>26</sup> polypropylene nonwoven fibers,<sup>27</sup> kapok fiber,<sup>28</sup> cellulose aerogel,<sup>29</sup> polyurethane foam,<sup>30</sup> exfoliated graphite,<sup>31</sup> etc., have been developed and these materials possess great hydrophobicity and oleophilicity. Among these, hydrophobic polymeric foams and fibers have particularly been lauded for their porous structures and large surface area, providing them with enhanced sorption capacity and separation efficiency.<sup>32–35</sup>

The recent advances in research and applications of polymer foams and melt-blown fibers for oil absorption are reviewed in the following sections: (1) polymer foams as oil absorption materials, with a focus on the processing and the working mechanisms for oil absorption; (2) methods of preparation of polymer foams for oil absorption; (3) recent progress of the newly developed nanocomposite PU foams, biodegradable foams, and the surface modification methods for oil absorption are discussed; and (4) processing and applications of melt-blown fibers for oil absorption. This paper provides a brief overview of these topics and proposes some prospects of possible research interests in the future.

## 2. Polymeric foams as oil-absorbing materials

### 2.1. Role played by foams

Polymeric foam is a low-density porous material created by incorporating a large amount of entrapped gas or voids into a polymer matrix.<sup>36</sup> The presence of nano/micro-sized pores gives the polymeric foam a spongy, cellular structure that provides cushioning and buoyant properties. Also, polymeric foam is known to have many advantages over non-foamed polymers, which in turn allow the polymeric foam to be suitable for various applications. The low thermal conductivity of polymeric foams provides excellent insulation properties for applications such as building insulation and thermal packaging.<sup>37</sup> Their lighter weight compared with non-foamed polymers enables ease of handling and transport, while their cellular structure exhibits excellent shock-absorbing properties for cushioning and protecting fragile items during transport.<sup>38</sup> The versatility in formulation allows tunable physical and mechanical properties, enabling diverse applications from seating cushions to packaging materials.<sup>39</sup> Beyond these applications, the large surface area of polymeric foam serves as an

effective oil sorbent material due to the numerous sites available for oil absorption.<sup>40</sup> The foam's cellular structure provides abundant small voids that trap and retain oil, resulting in high sorption capacity. Furthermore, its lightweight and low-density characteristics enable efficient oil absorption as it floats on the surface, thereby containing and preventing oil spread.<sup>41</sup>

Polymer materials mainly used for the foaming process are thermoplastics and thermoplastic elastomers, due to their good melt-processability under heated conditions. Thermoplastics (TPs) have the ability to be repeatedly melted and molded without undergoing significant changes in chemical structure. Thermoplastic elastomers (TPEs) are a relatively new class of copolymers that display a unique combination of properties from both thermoplastics and elastomers.<sup>42</sup> These polymers incorporate the processing ease of thermoplastics, combined with the stretchability and rigidity of elastomer. TP and TPE foams are employed in various applications, among which TP foams investigated for oil sorption purposes include polyethylene, polypropylene, thermoplastic polyurethane,<sup>43–45</sup> poly(lactic acid),<sup>46,47</sup> polycarbonate, and polystyrene foams, and TPE foams, including ethylene propylene diene monomer (EPDM)<sup>32</sup> and ethylene vinyl acetate (EVA)-based foams.<sup>48</sup>

### 2.2. Oil sorption and separation mechanism of polymer foam

Polymer foam is a physical sorbent that possesses a remarkable oil spill cleanup ability, which minimizes environmental damage cost-effectively. Sorbents remove the oil with typically two mechanisms: adsorption and absorption. Adsorption involves the adhesion of atoms, ions, or molecules from a gas, liquid, or dissolved solid to the surface of a material, and is a surface-based phenomenon driven by physical forces.<sup>49</sup> Absorption, on the other hand, involves the diffusion of the absorbate throughout the absorbent's body, including the surface and interface, driven by both physical and chemical forces.<sup>50</sup>

Polymeric foams are effective materials for oil/water separation due to their hydrophobic and oleophilic properties, which allow them to selectively ad/absorb oil while permitting water to pass through the vacant voids in the polymer. The oil absorption mechanism in polymer foams is governed by several key parameters and physical phenomena. The primary driving forces include capillary action – a phenomenon where liquids are drawn into small spaces between cell walls without dissolving the foam structure. Due to the capillary action, polymeric foams can absorb significantly higher volumes of oil than non-foamed polymers.<sup>51</sup>

The capillary pressure ( $P_c$ ) in polymer foams, is described by the Young–Laplace equation:

$$P_c = 2\gamma \frac{\cos \theta}{r} \quad (1)$$

where  $\gamma$  is the surface tension of the oil,  $\theta$  is the contact angle between the oil and the polymer surface, and  $r$  is the radius of the pore. While this equation indicates that smaller pores generate higher capillary pressure, it does not necessarily follow that foams with smaller expansion (and thus smaller pores) exhibit



superior oil absorption capabilities. This equation alone doesn't account for other crucial factors such as the total surface area for interaction and pore connectivity effects.

The Washburn equation provides additional insights into the capillary action governing oil absorption:

$$h^2 = \frac{r\gamma \cos \theta}{4\eta} t \quad (2)$$

where  $h$  is the height of oil rise,  $r$  is the pore radius,  $\gamma$  is the surface tension,  $\theta$  is the contact angle,  $\eta$  is the oil viscosity, and  $t$  is time. This equation demonstrates that the absorption rate depends on both geometric ( $r$ ) and surface ( $\gamma, \theta$ ) parameters. Higher viscosity oils are absorbed more slowly, while improved wettability (smaller  $\theta$ ) enhances the absorption rate. Notably, larger pore sizes result in greater oil rise height, suggesting that increased foam expansion leads to enhanced oil uptake due to the larger pores present in the system.

Furthermore, the expanded surface area provides additional contact points for oil imbibition. Darcy's law (eqn (3)) illustrates how increased surface area ( $A$ ) enhances flow rate through the foam structure, helping explain why higher expansion foams achieve superior overall absorption despite lower capillary pressure per individual pore.

$$Q = -\frac{kA}{\mu} \left( \frac{\Delta P}{L} \right) \quad (3)$$

where  $Q$  is the volumetric flow rate,  $k$  is the permeability,  $A$  is the cross-sectional area,  $\mu$  is the fluid viscosity, and  $\frac{\Delta P}{L}$  is the pressure gradient.

While real-life foams possess more complex characteristics such as interconnected pore networks (rather than isolated pores), multiple oil flow pathways, and dynamic absorption processes where initial uptake influences subsequent absorption, the aforementioned equations can provide a foundational understanding of the oil absorption mechanism.

When it comes to the foam's porosity, this structural parameter plays a crucial role in determining the maximum oil absorption capacity. The porosity ( $\phi$ ) of a polymer foam is defined as the volume fraction of void spaces:

$$\phi = \frac{V_{\text{total}} - V_{\text{solid}}}{V_{\text{total}}} \quad (4)$$

where  $V_{\text{total}}$  is the total volume of the foam and  $V_{\text{solid}}$  is the volume of the polymer matrix. Higher porosity values indicate more available space for oil storage, directly correlating with the foam's maximum absorption capacity.

Adsorption and absorption processes effectively remove oil without dissolving the polymer sorbent. On the other hand, gelation is another method that involves dissolving the polymer sorbent. Polymer sorbents that employ gelation interact with oil when they come into contact, dissolving the polymer to form a gel that selectively removes oil from oil-water mixtures.<sup>52</sup> The gelation process is driven by non-covalent interactions such as hydrogen bonding,  $\pi$ - $\pi$  stacking, and van der Waals forces, without involving a chemical reac-

tion.<sup>53</sup> The chemical compounds responsible for the gelation process are commonly known as organogelators. Organogelators used in oil spill cleanups primarily include low molecular weight substances like amino acid-, fatty acid-, and sugar alcohol-based gelators.<sup>54,55</sup> However, researchers have also demonstrated the successful use of high molecular weight polymers for selective gelation of hydrocarbon oil.<sup>53,56,57</sup> Recently, an innovative triblock elastomer foam was developed that combines both absorption and gelation mechanisms – initially absorbing oil before transforming into a semi-solid gel upon oil interaction. This dual-function foam leverages both the excellent oil absorption capabilities of foams and the sealing effect of physical gels, effectively preventing oil leakage.<sup>58</sup>

Polymer foams, like PU, polyethylene (PE), and polystyrene (PS), often show limitations in real-world oil sorption and separation because of challenges in their porous structure and interfacial properties. Most commercial foams are not optimized for specific oil sorption applications and may have irregular, interconnected pores, which can limit oil uptake. Ideal sorption would require highly interconnected, uniform pores with high surface area at the nano or microscale, enhancing oil retention. In real-life foams, the variability in pore sizes can trap air pockets and reduce effective oil uptake. In addition, polymer foams often have low surface energy, making them hydrophobic but not necessarily oleophilic enough to effectively adsorb oils over long periods. Surface modifications are often required to make the foam more oleophilic, allowing it to attract and retain oils more effectively. Even with modifications, creating a stable oleophilic surface across a complex porous structure remains challenging. During adsorption, the foam structure can collapse under pressure, reducing the number of available pores for oil sorption and resulting in lower performance. Furthermore, reusability and structural integrity often degrade with repeated absorption cycles, making foams less practical for prolonged real-world applications. Another associated challenge is polymer foams can become quickly saturated, after which they may release absorbed oil, especially under pressure. This limits their utility in dynamic environments like ocean oil spill recovery. Efficient sorbents need high absorption capacity along with structural properties that prevent oil leakage upon compression or shaking, which can be difficult to achieve in flexible foams. Fig. 3 presents the simple polymeric foam's selective oil absorption mechanism and associated challenges. These challenges can be mitigated through mechanisms such as surface modifications, the introduction of nanoscale porosity, or by adding fillers that can increase foam's surface area and oleophilicity. However, achieving an ideal balance between absorption efficiency, structural stability, and reusability in polymer foams remains a complex engineering challenge.

### 2.3. Basic structure–properties of foams

The structure of foams can vary depending on the level of expansion and specific formulation. A general characterization of foam should consider a combination of cell structure, cell size/density, and expansion ratio factors.

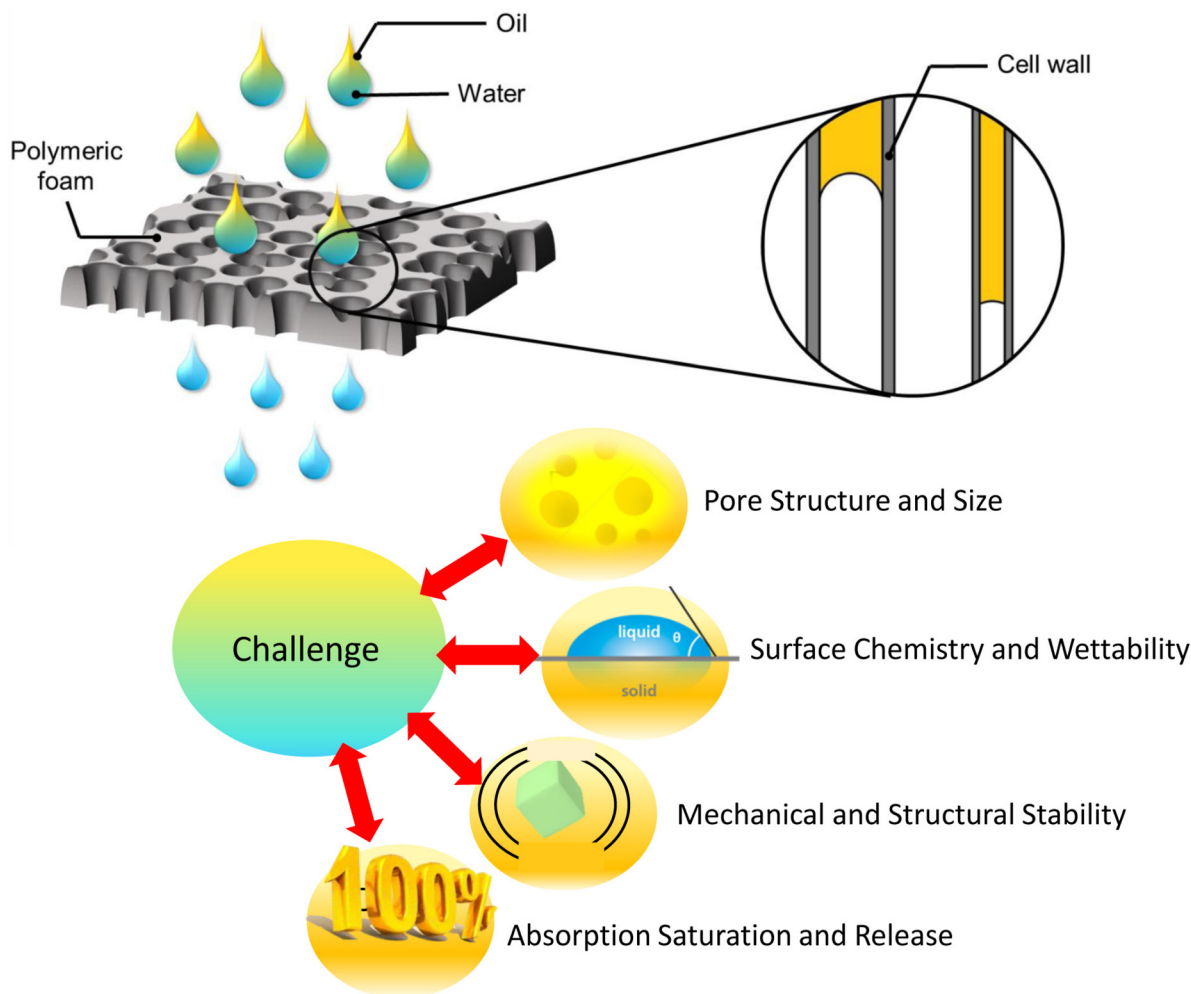


Fig. 3 Schematic illustration of polymeric foam's selective oil absorption mechanism and associated challenges.

Polymer foam can be classified into closed-cell, partially open-cell, and open-cell structures. Closed-cell foams generally have open-cell content below 10 vol% and open-cell foams

have an open-cell content above 90 vol%.<sup>59,60</sup> Fig. 4(a) depicts the open-cell structures of polymeric foams, where the cells are connected, and the air is free to flow throughout the

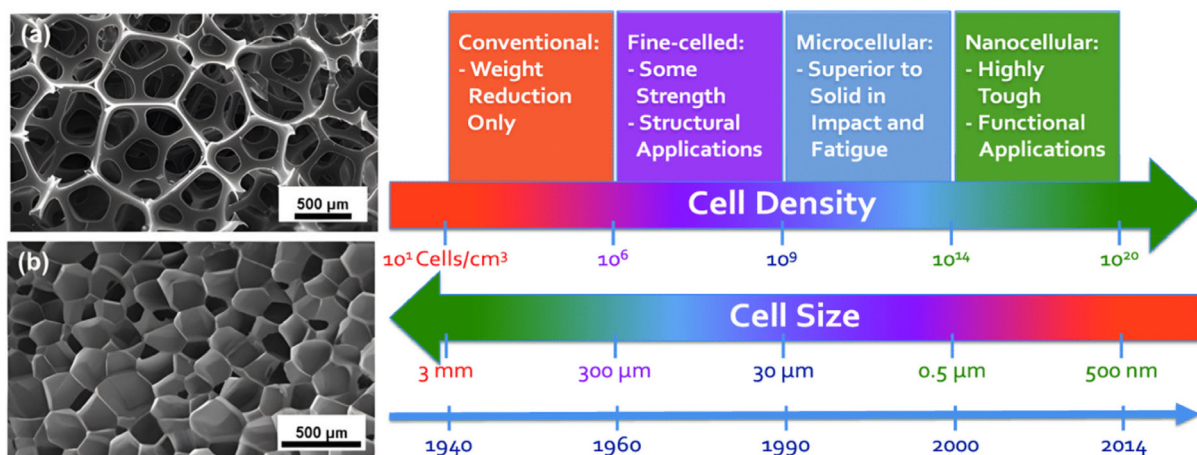


Fig. 4 (a) Open-cell<sup>59</sup> and (b) closed-cell<sup>60</sup> structures of polymeric foams; (c) cell sizes and cell density of the developed foams over time.<sup>66</sup> (Reproduced from ref. 59, 60 and 66. Copyright 2004 and 2005 Elsevier Inc.)

volume. The closed-cell structure is shown in Fig. 4(b), where the cellular structure is separated into independent bubble units and there is no air tunnel between the adjacent cells. It is important to consider cell morphology and open/closed-cell content in determining the properties and applications of polymer foams. Open-cell foams have broken cells that allow air to occupy the spaces within, which results in a lightweight, less dense material with a soft, sponge-like appearance. On the contrary, closed-cell foams have intact cells and are dense, and they are commonly used for heat and sound insulation. For specific applications, such as oil sorption, it is crucial for the sorbent to have an optimal open-cell ratio, as a high open-cell content enhances oil/water permeation, but excessive open-cell content can have low efficiency of oil sorption and low mechanical properties.

Cell size, which is a crucial property of foams, can be measured by counting the number of cells intersecting a specific area, as described in ASTM D3576. Microcellular and nanocellular foams are characterized by their mean cell size and cell density, as can be seen in Fig. 4(c). Microcellular foams have a mean cell size of less than 10  $\mu\text{m}$  and cell density of between  $10^9$  and  $10^{12}$  cells per  $\text{cm}^3$ , while nanocellular foams have a mean cell size of less than 1  $\mu\text{m}$  and cell densities greater than  $10^{15}$  cells per  $\text{cm}^3$ .<sup>61–63</sup> The variation in cell sizes in foams is due to both random nucleation and growth of cells through the diffusion of gas from smaller to larger cells. This process leads to an unstable structure, characterized by a non-uniform cell size distribution. Eqn (5) describes the pressure inside a bubble surrounded by molten (or softened) polymer, which explains the mechanism of gas diffusion.<sup>64,65</sup>

$$\Delta P = \frac{2\alpha}{r} \quad (5)$$

where  $\Delta P$  is a pressure difference between gas and molten polymer,  $\alpha$  is surface tension, and  $r$  is the radius of a spherical bubble.

Expansion ratio refers to the relative increase in the volume of polymer foam during the foaming process and is expressed as eqn (6).

$$\phi = \frac{\rho_1}{\rho_2} \quad (6)$$

where  $\phi$  is an expansion ratio and  $\rho_1$  and  $\rho_2$  are densities of the polymer before and after foaming. The expansion ratio is an important parameter that can affect the final properties of the foam, such as cell size, cell density, and mechanical properties. For example, a higher expansion ratio results in foam with larger cell sizes and lower cell density, while a lower expansion ratio regards smaller cell sizes and higher cell density or less efficient foaming in the matrix. The expansion ratio can be controlled by adjusting the conditions of the foaming process, such as temperature, pressure, and chemical composition.<sup>67</sup>

## 2.4. Processing of polymer foams

### 2.4.1. Foaming agents.

Foaming agents are integral components in the fabrication of polymer foams, possessing light-

ness, thermal insulation, and cost-effectiveness.<sup>68</sup> These additives facilitate the formation of fine and uniform pores within the polymer, leading to a diverse range of foaming applications, ranging from rigid thermoset resins to easily softening thermoplastics. Apart from polyurethane foam, which employs water to react with isocyanate to release  $\text{CO}_2$  gas for the foaming, foaming agents are often divided into two categories: physical and chemical foaming agents.

Physical foaming agents (PFAs) function by undergoing a change in their physical state, which involves the vaporization of liquid or depressurization of gas bubbles embedded in the polymer system.<sup>69</sup> PFAs that create foaming expansion through liquid vaporization include water, short-chain hydrocarbons, and halogenated hydrocarbons, and PFAs that create foam by undergoing depressurization use relatively inert gases, such as  $\text{CO}_2$  and  $\text{N}_2$ .<sup>70</sup> Nowadays,  $\text{CO}_2$  and  $\text{N}_2$  are highly regarded as effective foaming agents for their eco-friendliness, cost-efficiency, foamability, and safety.

The relatively low critical temperature and pressure of  $\text{CO}_2$  and  $\text{N}_2$  make it easy for them to enter the supercritical state, enabling them to serve as highly effective foaming agents.<sup>71</sup> A supercritical state is a state of matter that occurs when a substance is maintained at a certain point of temperature and pressure above its critical temperature and pressure. In this state, the substance has properties of both a liquid and a gas, with high fluidity and low surface tension. Therefore, the solubility of  $\text{CO}_2$  and  $\text{N}_2$  in this state increases significantly in the polymer system and this results in a decrease in the glass transition temperature of most polymers.<sup>72</sup> When a molten polymer is saturated with a supercritical fluid, cell nucleation takes place at a high concentration, and cell growth persists until the polymer solidifies. This makes it beneficial for fine-adjustment of the size of the pores from nano to macroscale. Furthermore, the modest critical temperature and pressure of  $\text{CO}_2$  (31.1 °C and 7.38 MPa) make the rapid depressurization step relatively easier for the polymer foaming without requiring a high processing temperature.<sup>64</sup>

However, the major challenge of physical foaming is the volume shrinkage of the polymeric foam, especially elastomers.<sup>73,74</sup> Unlike thermoplastics, TPEs are difficult to foam with large expansion due to their elasticity and low modulus. During the foaming process, gas bubbles are entrapped in the TPEs to create pores within the polymer matrix. However, once TPEs are exposed to ambient temperature and pressure after the foaming process, they become elastic and lack the necessary modulus to withstand the compressive force from the air. As the air pressure is higher than the gas pressure within the polymer, the gas bubbles shrink by the compressive force, and this restricts the foaming expansion.<sup>36</sup> To enhance the modulus of TPEs and mitigate the issue of volume shrinkage, the use of rigid fillers, such as silicate, carbon fiber, and carbon black has been studied.<sup>75</sup> Also, crosslinking (or vulcanization) is an effective way to increase the modulus of such polymers, which involves the formation of covalent bonds between polymer chains and creates an interconnected structure. In the physical foaming method,

crosslinking must take place prior to the foaming process. However, this pre-crosslinking often impedes cell growth and restrains foam expansion due to TPEs' enhanced rigidity.<sup>36</sup> In this case, utilizing a chemical foaming agent can probably facilitate the process. In addition, the foaming speed has to be balanced with the curing rate of the elastomer matrix, which normally requires a high temperature, *via* the optimization design of the foaming temperature and dwelling time.

Chemical foaming agents (CFAs) are thermally decomposable foaming agents that decompose into gases upon heating. They are mostly solid at room temperature, but when exposed to a heat with a specific temperature (above decomposition temperature) they decompose and release gas such as N<sub>2</sub>, CO<sub>2</sub>, or CO. The process of using a CFA involves blending, heating, expansion, and solidification.<sup>37</sup> A blend of the polymer material and the CFA is prepared, and then it is heated under pressure. The heat melts or softens the polymer, and simultaneously decomposes the foaming agent to release gas *via* a heat-mediated chemical reaction, and the evolved gas subsequently forms cells within the softened/melted polymer.<sup>38</sup> If desired, the polymer/gas mixture can be placed in a mold with a designed shape by which the expanded foam forms the desired shape. The mold is then cooled, allowing the polymer to solidify and maintain the cell structure created during the foaming process.<sup>37</sup>

CFAs can be largely classified into two groups: exothermic and endothermic chemical foaming agents.<sup>76,77</sup> Exothermic CFAs generate a large amount of heat when they decompose and cause an exothermic chemical reaction. They are usually organic compounds, such as azodicarbonamide (ADC), *p*-toluenesulfonyl hydrazide (TSH), and 4,4'-oxybis(benzenesulfonyl hydrazide) (OBSh). Endothermic CFAs, on the other hand, absorb heat when they decompose, causing an endothermic reaction. Examples of endothermic foaming agents include inorganic salts such as sodium bicarbonate and ammonium sulfate.

One of the main advantages of CFAs is their ability to create a uniform foam structure. This allows manufacturers to produce consistently sized and shaped foams. Also, using CFAs is cost-effective, because most CFAs are easy to obtain and store, and it reduces capital cost as it requires simple incorporation into the existing thermoplastic processing facilities. CFAs can be added to a solid polymer before heating, whereas PFAs require the polymer to be already molten (or softened) before they can be injected. This makes CFAs advantageous to use in a variety of processing methods, such as compression, injection molding, extrusion, and calendaring without requiring special processing equipment, treatment, storage, or handling.<sup>78</sup>

Moreover, the chemical foaming method addresses the volume shrinkage issue of the physical foaming method on TPEs. As mentioned, improving the modulus of elastomers requires additional modulus enhancement treatment such as crosslinking. In the physical foaming process, crosslinking must be done before the foaming process, but this pre-cross-linked network often inhibits foam expansion.<sup>37</sup> On the other hand, chemical foaming allows crosslinking and foaming to

happen simultaneously, therefore it can benefit from the cross-linking with the enhanced melt strength that maintains the foam structure, thus minimizing post-shrinkage and improving the elastomers' dimensional stability.<sup>36</sup>

Despite their many advantages, there are disadvantages to using chemical foaming agents. When using these foaming agents, it is important to pay close attention to the foaming agent's decomposition temperature, as the polymer can decompose before the foaming agent is fully activated.<sup>78</sup> Additionally, CFAs can cause contamination if unreacted or solid residue stays in the product. This residue can lead to discoloration, unpleasant odor, and corrosion of the polymer. Also, the gases released by foaming agents such as NO<sub>x</sub>, SO<sub>x</sub>, and a large amount of CO<sub>2</sub> can cause environmental pollution; therefore, it is important to limit the use of CFAs to the minimum concentrations required for the foaming operations to minimize the problem.<sup>79</sup>

**2.4.2. Foam cell formations.** The formation of foam involves the creation and expansion of gas bubbles in a polymer matrix resulting in a system of dense polymer matrix with spherical pores filled with gas. The transformation of a foaming agent from free gas molecules to spherical bubbles occurs with the rapid change of temperature and pressure, causing a reaction in the polymer system.<sup>71</sup> When the polymer matrix surrounding the gas bubbles solidifies quickly enough before the gas condenses, the foam becomes stable. It is crucial that this solidification process happens faster than the gas phase condensation, as otherwise, the size of gas bubbles reduces, causing the shrinkage of the polymer foam.<sup>80</sup> Fig. 5 describes the general foaming process in four stages, (1) gas diffusion, (2) cell nucleation, (3) cell growth, and (4) cell stabilization.

**(1) Gas diffusion:** A pressured gas is injected into a molten polymer (for physical foaming) or a decomposed gas from a chemical reaction is introduced to a molten polymer (for chemical foaming). The gas diffuses throughout the molten polymer until saturation is reached. The gas solubility during physical foaming normally relies on high temperature and pressure. For chemical foaming, the blowing agent dispersion, and the mixing parameters (*e.g.*, mixing speed and blowing agent concentration) are the keys to control and gas source diffusion.<sup>81</sup>

**(2) Cell nucleation:** The formation of microcellular nuclei starts with the addition of gas to a saturated polymer/gas mixture, causing gas to escape from the single-phase polymer/gas mixture and form the cell nucleus. The thermodynamic change, a driving force of the cell nucleation, is often brought about by a decrease in the solubility of the gas, which can be achieved through a pressure drop or a temperature increase.<sup>82</sup> If the foaming process involves rapid depressurization, cell nucleation and the cell growth occur simultaneously, as the escaping gases within the polymer system swiftly expand to create larger cells. The relationship between solubility and pressure is an important factor in the foaming process as this stage influences the final shape and characteristics of the material. The use of fillers and nucleating agents can help enhance the nucleation process during foaming. They provide



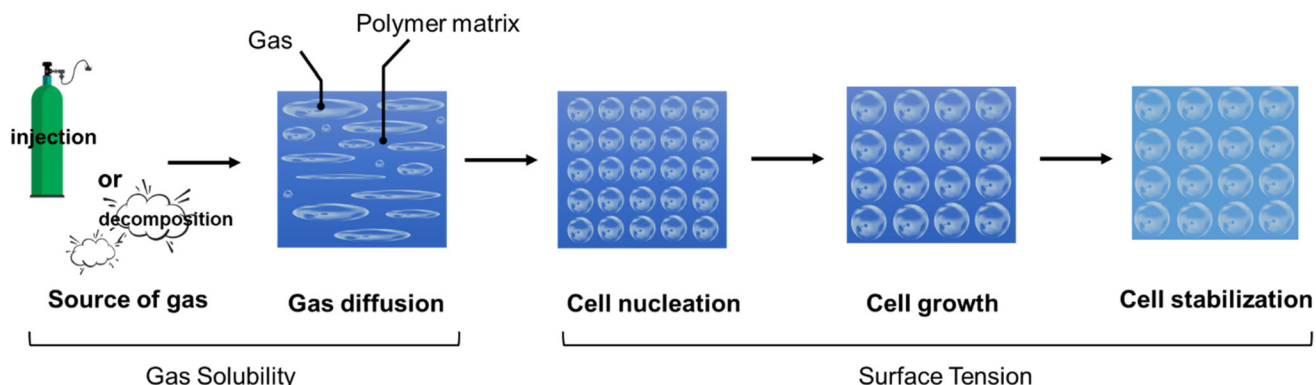


Fig. 5 Cell-formation procedure of polymeric foam.

additional sites for bubble formation during foaming, which facilitates the creation of gas bubbles, leading to a more controlled and efficient foaming process. The use of these additives allows for better control over the foaming process and can contribute to achieving desired foam properties for specific applications.

(3) **Cell growth:** Cell nucleation results in the creation of cells with varying sizes. The pressure within a small cell is higher compared with larger cells, causing the smaller cells to coalesce with the larger cells through a pressure gradient. This, in turn, contributes to the expansion of cells. Cell growth is dependent on various factors, such as temperature, pressure, and viscoelastic properties of the polymer/gas mixture during the processing.<sup>67</sup>

(4) **Cell stabilization:** The solidification of the molten polymer occurs through cooling and the use of surfactants or curing agent(s). For an open-cell system, once solidification takes place, the gas inside the cells gradually diffuses out, creating room for air to enter. The mutual diffusion between gas and air continues until the gas has completely been replaced by air, leading to cell stabilization.<sup>83</sup> For the closed-cell system, the cells stabilize as separated units as soon as the matrix cools down or the vulcanization/crosslinking finishes,<sup>36</sup> and the gas within the closed cells will be eventually replaced by air as time passes.

### 3. Polymer foam preparation methods for oil sorption

As shown in Fig. 6, the commonly used preparation methods for polymer foam processing involve but are not limited to extrusion foaming, batch foaming, foam injection molding, compression foaming, freeze-drying, and reactive foaming. They are discussed in detail below and their advantages and limitations are listed in Table 1.

#### 3.1. Extrusion foaming

Extrusion foaming is a process where a foaming agent (gas) is injected into the molten polymer through an extruder. The gas

is introduced into the polymer through either the thermal decomposition of a chemical foaming agent or the direct injection of a physical foaming agent, with the principles being similar for both methods. Rizvi *et al.*<sup>91</sup> presented extrusion foaming of PP/PTFE blends using a physical foaming agent ( $\text{CO}_2$ ) in two-step single-screw extruders (Fig. 7). The solid polymer (usually pellet or powder form) is fed through the hopper and the polymer melts as it passes the heated screw where shear heating is generated by the screw motion.  $\text{CO}_2$  is then introduced into the first single-screw extruder barrel *via* a syringe pump, ensuring a constant flow rate. The rotating screw inside the barrel creates high shear and high pressure, facilitating the dissolution of  $\text{CO}_2$  in the molten polymer through convective diffusion. It is crucial to maintain high pressure throughout the extruder and die to delay bubble nucleation until the polymer emerges from the die. Upon exiting the die, the molten polymer experiences a sudden pressure drop, leading to supersaturation with gas. This phenomenon triggers the nucleation and formation of bubbles within the material. The foam structure stabilizes as it rapidly cools down. This method requires pressure control, and the final size and shape of extruded foam samples are limited by the nozzle size and the foaming temperatures.

A type of continuous extrusion foaming for open-cell polypropylene/polyolefin elastomer (PP/POE) blend foams was reported by Pang *et al.*<sup>84</sup> Foams of PP/POE prepared at temperatures of 180 °C, 178 °C, 176 °C, and 174 °C were characterized and results revealed that the lower temperatures (174 °C and 176 °C) investigated in this study were more conducive to achieving well-foamed PP/POE blends with increased open-cell contents and thinner cell walls. On the contrary, the higher foaming temperatures led to cell coalescence resulting in closed cells. In the same study, the authors investigated oil sorption kinetics and displayed that the higher open cell-containing samples corresponded to an increased sorption rate and sorption capacity.

#### 3.2. Batch physical foaming

The production of polymeric foam through batch physical foaming can be classified into two methods based on how



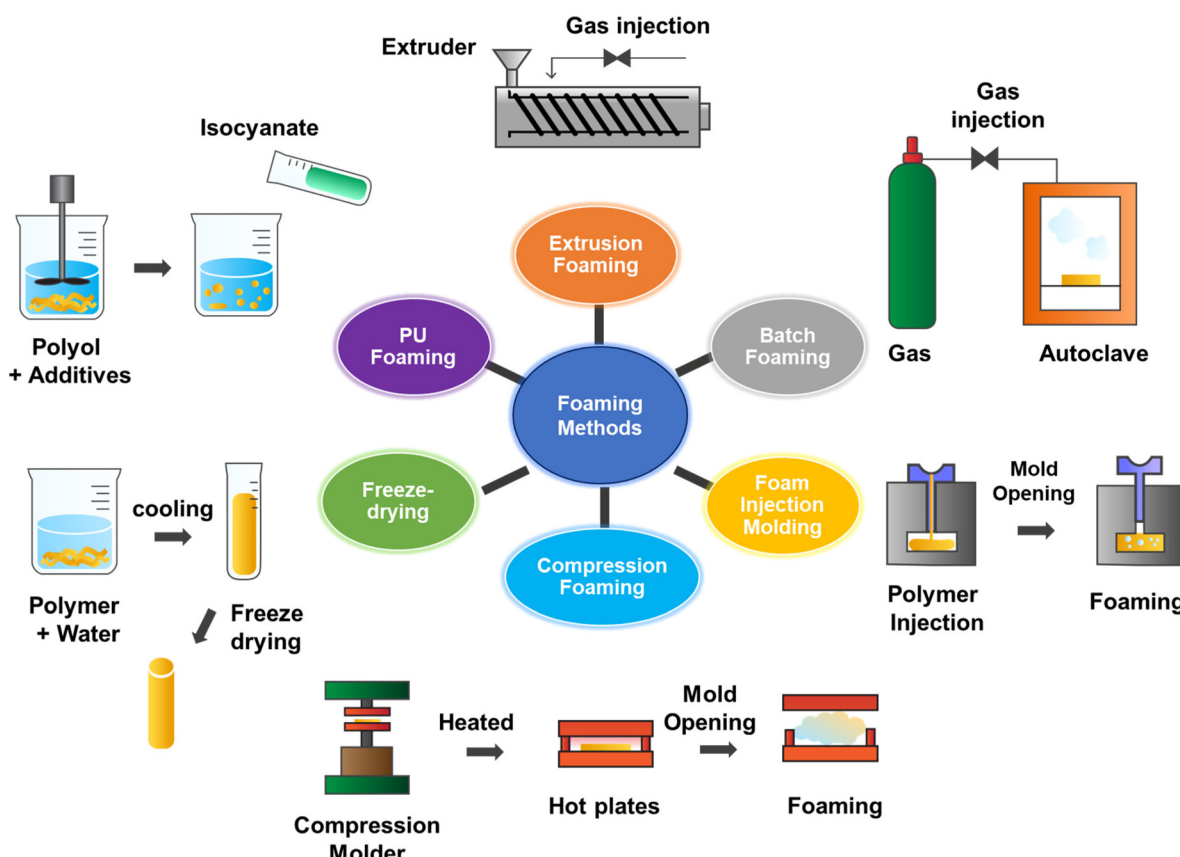


Fig. 6 Various foaming process methods to develop porous polymeric materials for oil spill cleanups.

Table 1 Advantages and limitations of the various foaming methods

Foaming methods	Advantages	Limitations	Ref.
Extrusion foaming	Suitable for both chemical and physical foaming	Limited sample sizes and shapes	84
Batch foaming	For physical foaming process only and no chemical reaction required	High pressure and temperature required	85 and 86
Foam injection molding	Quick and precise molding	Premixed masterbatch required	85 and 87
Compression foaming	High pressure and temperature not required	Premixed masterbatch required	85
Freeze-drying	Low temperature: no foaming agent is required	Solvent required; time-consuming	88 and 89
Reactive foaming (e.g., PU foaming)	High pressure and temperature not required	Reactions between the foaming agent and the reactants; not for oil absorption if without modification	90

pressure and temperature are controlled.<sup>92</sup> The first method, heating foaming, involves saturating the elastomer with foaming agents at low pressure and temperature, then expanding the gas-saturated elastomer to a higher temperature for a set amount of time. The second method, cooling foaming, involves first heating and melting the elastomer with foaming agents at high pressure and temperature, then cooling it down to the foaming temperature and expanding it by releasing the pressure. Fig. 8 shows a batch foaming system with a cooling foaming method.<sup>93</sup> The foamed polymer was a chain-extended polylactide with CO<sub>2</sub> used as a foaming agent. The maximum

processing temperature and pressure in the autoclave were 350 °C and 200 bars, respectively, and the pressure was rapidly dropped (at the rate of 20 bar min<sup>-1</sup>) for the foam expansion. To accomplish the foaming, both the heating and cooling foaming require specific and complicated control of the pressure and temperature. As a comparison, the first method, heating foaming, shows fewer steps and is more straightforward for pressure control.

For instance, high-melt-strength polypropylene (HMSPP) and linear polypropylene (PP) were compounded at different ratios and subsequently batch-foamed by supercritical CO<sub>2</sub> at



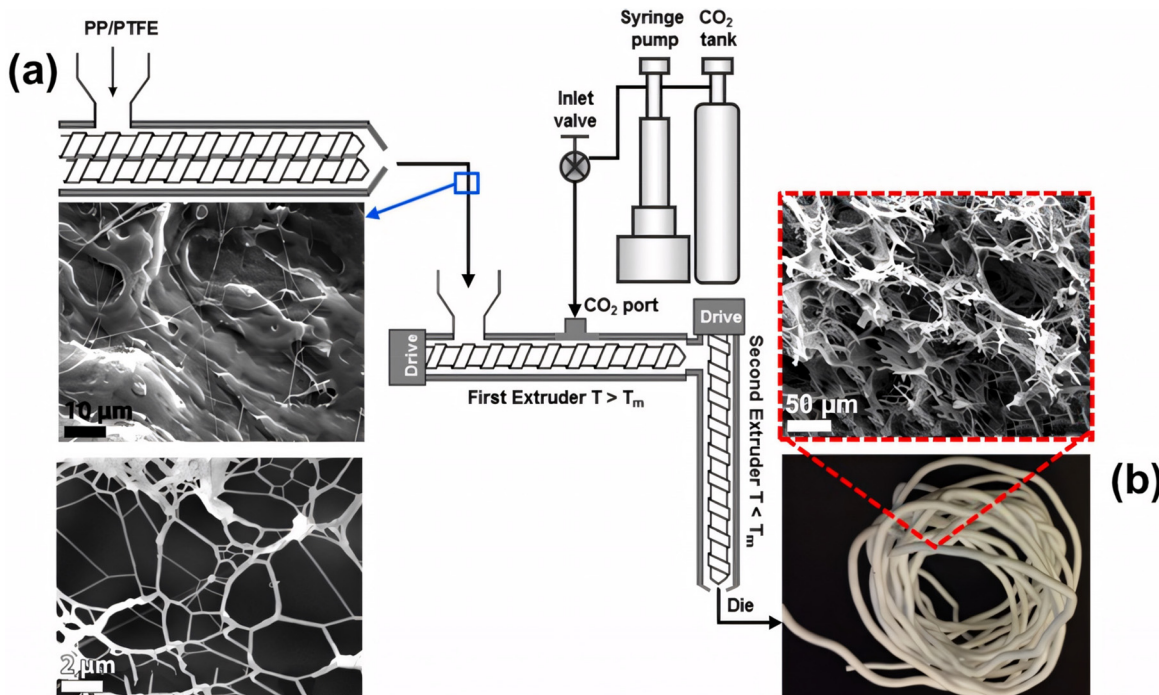


**Fig. 7** Extrusion foaming of PP/PTFE fibrillar blends: (a) PP-homopolymer blended with PTFE in a twin-screw extruder; (b) images of an open-cell foam filament produced via extrusion. (Reproduced from ref. 91, Copyright 2014 American Chemical Society.)

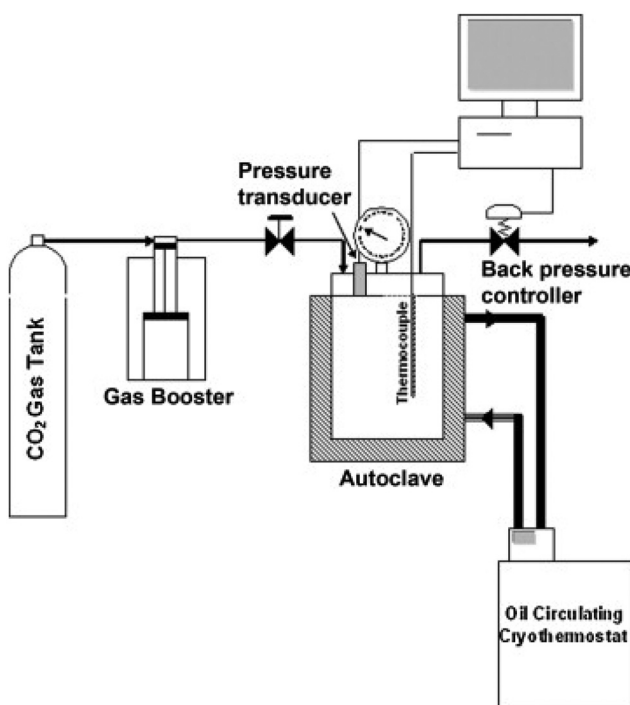


**Fig. 8** Batch foaming equipment (reproduced from ref. 93, Copyright 2011 Elsevier Inc.).

different temperatures and pressures to develop open-cell foams tailored for oil absorption applications.<sup>94</sup> The findings revealed that the incorporation of HMSPP into PP not only

broadened the processing window for foaming but also amplified the foam's expansion ratio. Moreover, both the expansion ratio and open-cell content exhibited an increase with saturation pressure. In the absence of any surface modification for the blended polymer foams, the oil absorption capacity for gasoline reached a noteworthy 35 g g<sup>-1</sup> after a 24-hour exposure period.

Batch physical foaming typically involves the use of a high-pressure vessel and a control system to achieve the desired foaming conditions. The need for specialized equipment and control systems can result in higher processing costs compared with other foaming methods, such as chemical foaming or extrusion foaming. The complexity and cost associated with the equipment and control systems are factors that should be considered when choosing a foaming method for polymer processing.

### 3.3. Foam prepared by injection molding

Foam injection molding is a quick and economical method of producing foam products with consistent and uniform characteristics. This is because the process grants a level of precision in the molding process, such as the amount of material used, the foam density, and the product's shape. Additionally, it requires minimal tooling and results in low scrap rates. The injection molding shows quick foaming; however, it requires the premixed polymer/foaming agent compounded as the masterbatch.

Hopmann *et al.*<sup>95</sup> conducted a foam injection molding of ethylene propylene diene monomer (EPDM) using water as a foaming agent, to determine that water vaporization can replace the chemical decomposition foaming method for a



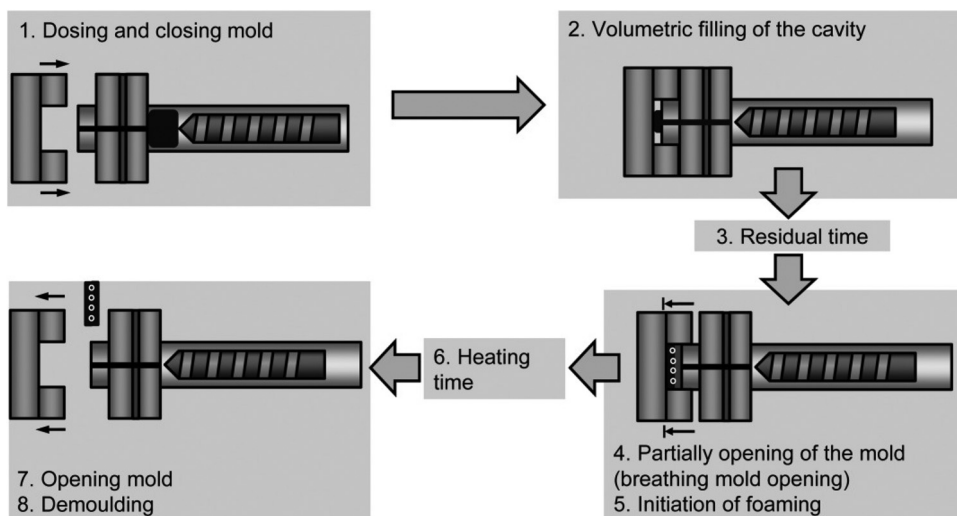


Fig. 9 Process sequence of the breathing mold technique in injection molding (reproduced from ref. 95, Copyright 2016 John Wiley & Sons, Inc.).

TPE. The EPDM samples were made using a breathing mold technique as shown in Fig. 9. This technique involves the injection of the melt into a compression mold, followed by a residual time of 100 seconds and the opening of the mold by 2 mm. The opening initiates foaming, after which the sample is demolded. The main benefit of this concept is the controlled foaming after a set time and temperature. The pressure within the cavity increases due to thermal expansion, preventing premature foaming until the mold is opened. The injection was carried out with a mold temperature of 180–210 °C and a maximum injection pressure of 75 bar. No foaming agents were added in this study; however, product control would be a challenge if the foam were solely dependent on the mold partially opening and breathing.

The chemical and physical foaming methods for injection molding of thermoplastic PU were compared by Kharbas and McNulty.<sup>96</sup> The results showed that the use of physical blowing agents yielded softer foams, while the use of CO<sub>2</sub> and N<sub>2</sub> as co-blowing agents helped to manufacture foams with lower bulk densities, better microstructures, and lower hysteresis loss ratios. In another study, CO<sub>2</sub> was applied as the foaming agent in the microcellular injection molded PP/PTFE foams, and the developed foam showed outstanding hydrophobicity and re-usability of oil uptake.<sup>97</sup>

Process parameters such as chemical blowing agent dosage, shot size, mold temperature, injection speed, packing pressure, and core-back speed possess significant effects on the produced foam's density and mechanical properties. The customizable, scalable, and cost-effective injection molding foam technology shows a promising future in the manufacture of microcellular polymer foam for oil absorption.

### 3.4. Compression foaming

Compression foaming is another quick foaming process that involves compressing a foamable polymer at high temperatures and a certain dwell time to decompose the foaming

agent (*i.e.*, CFAs) in compression molding. The compression step involves applying pressure to the material to reduce its volume before expansion. The control of pressure in compression foaming can influence the density and properties of the resulting foam. A controlled compression step helps in achieving uniform foaming and desired characteristics in the final product. The level of pressure applied, the compression time, and the subsequent release conditions can be factors that affect the foaming process, and the quality of the foam produced.<sup>98</sup> While pressure control might not be necessary throughout the entire foaming process, it is often a critical parameter during the compression phase to achieve consistent and controlled foam expansion. The specific requirements can depend on the material being foamed and the desired properties of the final foam product.

Recent studies reported by Lee *et al.* showed the compression foaming of ethylene propylene diene monomer (EPDM)-based rubber composites, and the final batch displayed mechanical and oil absorption properties.<sup>99</sup> ADC was used as a foaming agent, and it was premixed with the rubber *via* a softened-state batch mixing. The compounds were then compression molded into sheets and high temperature was applied successively for the foaming. The foaming process required no pressure control but only adequate temperature to decompose the foaming agent. The drawback is similar to the injection molding that will need extra premixing for the preparation of the masterbatch.

### 3.5. Freeze-drying

Freeze-drying, also known as lyophilization, is an industrial process that consists of removing water from a frozen sample by sublimation and desorption under a vacuum.<sup>100</sup> Preparing polymer foams *via* freeze-drying can be a simple method that entails freezing and solvent replacement<sup>89,101</sup> as displayed in Fig. 6. Firstly, the polymer is completely dissolved *via* an appropriate solvent, and then the solution is frozen. The



frozen solvent can then be immersed in 0 °C distilled water to replace the solvent. Lastly, the water–polymer mixture will be dried at a higher temperature for a period of time (e.g., 60 °C for 12 h). For the process of freeze-drying foaming, there will be no foaming agent or high temperature required. However, the foaming process can be a time-consuming and labor-intensive process. Finding a substitute solvent that is as eco-friendly as water and shortens the foaming time would be a future research topic.

### 3.6. PU foaming

PU foaming is listed separately because the foaming mechanism is different from conventional physical or chemical foaming methods, for which pressure and temperature control are prerequisites. The PU foams (PUFs) are groups of expanded polymer materials, and the synthesis results from the combination of two steps, including the polymerization (reaction between isocyanate and polyol) as the first step and expansion (reaction between isocyanate and water) as the second step. The foaming process can take place almost simultaneously with the polymerization at room temperature with appropriate catalysts.<sup>102</sup>

The foaming process of reacting PUFs was *in situ* monitored in a recent study,<sup>90</sup> and it was found that the foam's structure was primarily influenced by the mixing process and subsequent bubble coarsening. In cases where no air bubbles were introduced during the mixing phase (a slower mixing rate), the formation of new bubbles arising from the reaction of CO<sub>2</sub> with water and pentane was observed. Additionally, both bubble fusion and the process of Ostwald ripening were identified as mechanisms contributing to the coarsening of the foam structure, with the latter showing reduced effectiveness in the context of polyisocyanurate foams.

PUFs are commonly used in comfort applications or as thermal and sound insulation materials, contributing to the second largest portion of the US plastic foam market.<sup>103</sup> However, because of the formed functional groups, neat PUFs are not suitable for oil absorption unless there are some modifications to alter the hydrophilic nature, which will be discussed in the following sections.

### 3.7. Other foaming methods

Besides the conventional foaming techniques discussed earlier, there are alternative methods to introduce pores or voids into a polymer matrix, such as template-based routes. These methods offer significant advantages in customizing the porous structure, allowing for controllable hierarchical porosity, precise pore size, and intricate microstructures without the need for chemical or physical foaming agents.<sup>104–106</sup> This approach is particularly promising for creating polymer foams tailored for oil absorption and adsorption applications. However, despite these advantages, template-based techniques also have some notable limitations: (1) the size scale of the foams is typically constrained by the dimensions of the template used. This limitation can hinder the production of large-scale foams required for industrial applications; (2) the

process often involves the use of solvents or soluble salts within the matrix, which can introduce complications related to the removal of these materials and potential contamination; and (3) the method can be time-consuming, particularly during the template removal phase, which can impact the overall efficiency of the production process. Addressing these limitations should be a focus of future research to make template-based methods more viable for large-scale, practical applications in oil absorption and adsorption.

## 4. Recent progress of polymer foam for oil sorption

### 4.1. Nanocomposite polyurethane foam (PUF) for oil sorption

Polyurethane foams (PUFs) have been one of the major material options for effective oil absorption, due to several combinations of desirable properties, such as ease of modification, processibility, recyclability, high oil absorption capacity, stability, and exceptional mechanical properties. Moreover, PU materials can be readily produced on a significant industrial scale, which establishes them as a highly promising option for the absorption of oil and organic solvents.

Nevertheless, the hydrophilic nature induced by polar groups like carboxyl and amino groups in PU hinders its selectivity and overall effectiveness in oil/water separation processes. To address this concern, recent studies have focused on incorporating additives into PU foams to achieve hydrophobic surfaces, which would increase the oil/water selectivity. Various materials have been used for this purpose, including Al<sub>2</sub>O<sub>3</sub>,<sup>107</sup> ZnO,<sup>108</sup> SiO<sub>2</sub>/MnO<sub>2</sub>,<sup>109</sup> lauryl methacrylate,<sup>110</sup> and carbon-based materials.<sup>111–113</sup> Among the materials used for the hydrophobic functionalization of polyurethane sponges, carbon-based nanomaterials, such as nanotubes, nanofibers, nanoparticles, and graphene (2D nanocarbon) have been proved to be effective as filler additives in PUF. These fillers not only increase the hydrophobicity of the foam but also improve their overall performance.

Keshavarz *et al.*<sup>114</sup> studied multi-walled carbon nanotube (MWCNT)-modified PUF and the results showed that the addition of MWCNTs on the PUF surface improved its thermal and mechanical resistance and increased its light crude oil sorption capacity by 21.44% at a concentration of only 1 wt% MWCNT. The sorbent's reusability was also tested through four cycles of chemical regeneration and 85.45% of its initial oil sorption capacity was retained after regeneration. Another noticeable work of MWCNT-incorporated PUF material was reported by He *et al.*<sup>112</sup> Their work indicated that the modified foam had a high-water contact angle of 159° and an improved oil absorption of up to 60 g g<sup>−1</sup>. It was confirmed to be highly effective and reusable (900 cycles) in various oil/organic-water systems such as engine oil, silicone oil, and kerosene. Also, the modified materials showed 27% higher tensile strain, and 35% lower compressive strain compared with regular PUs,



indicating they possessed enhanced mechanical properties and larger foam expansion.

Visco *et al.*<sup>111</sup> investigated PU-based foams filled with carbon nanofibers (CNF) to enhance their oil selectivity and mechanical durability. The samples were characterized through various physical and mechanical tests, including contact angle measurement, absorption tests, optical microscopy observation, and compression fatigue tests. The results showed that the addition of CNF to the foam led to an increased hydrophobicity (contact angle of 111–114°) and a better oil separation (22.85% improvement in oil/water selectivity compared with a non-modified PUF). The optimal filler amount was found to be around 1 wt% for a homogeneous distribution within the foam. Furthermore, the fatigue test results showed that the mechanical properties of the foam improved with increasing amounts of carbon filler, leading to greater resistance to fatigue and increased elasticity.

Nanomaterials with high surface area, high aspect ratio, and excellent mechanical, electrical, and thermal properties can enhance the surface properties of PU foam by making it more hydrophobic and oleophilic, which results in enhancing the adsorption capacity of foams towards oil and reducing the water uptake. Besides better absorption capacity, the incorporation of nanomaterials in foams would have a reinforcing effect with improved mechanical strength, which helps the foam to withstand repeated compression and recovery cycles without losing its shape and absorption capacity.<sup>111,113</sup>

The study of Anju *et al.*<sup>115</sup> presented a novel graphene-meso FeO<sub>2</sub> composite-incorporated polyurethane foam (GPUF) as a highly efficient sorbent for organic contaminants and oils. The foam's surface was modified by anchoring the graphene-meso FeO<sub>2</sub>, which endowed high porosity, increased hydrophobicity, and great magnetic properties to the polyurethane foam. The effectiveness of the GPUF was demonstrated by its ability to remove oil rapidly and selectively from water using a magnetic field, while its magnetic properties also enabled it to be easily directed to specific areas and quickly recollected after use. The

3D porous PU scaffold and graphene-mesoporous FeO<sub>2</sub> composite were found to have a cooperative effect on the adsorption dynamics, leading to selective adsorption capacity for a wide variety of oils and organic pollutants in the range of 90–316 g g<sup>-1</sup>. The GPUF was also easily recoverable by manual squeezing, with the reusability of over 150 cycles (for chloroform), and maintained its high adsorption capacity (Fig. 10).

The potential of PUF nanocomposites for oil absorption and adsorption is promising due to their high oil absorption capacity, stability, and exceptional mechanical properties. These foams are highly modifiable because their large surface area and embedded nanofillers provide numerous reactive sites. However, future research must address three significant challenges. (1) Processability: nanofillers often agglomerate, which hinders their uniform dispersion within the polymer matrix. This challenge necessitates specific treatments, complicating the production process. (2) Recyclability: if not properly recycled, treated, and reused, many nanofillers pose serious environmental risks. Effective strategies for recycling are essential to mitigate these impacts. (3) Cost: the manufacturing and recycling of nanofillers increase the overall cost of producing PUF nanocomposites. Incorporating bio-based polymers and fillers may offer a solution to improve both cost efficiency and recyclability. To enhance the application of PUF nanocomposites for oil absorption and adsorption, future research should focus intensively on improving their cost-effectiveness, recyclability, and processability.

#### 4.2. Sustainable polymer-based foam for oil sorption

The extensive use of conventional petroleum-derived polymers led to significant consumption of non-renewable resources and the production of large amounts of difficult-to-degrade plastic waste, resulting in severe environmental pollution. This contradicts the goals of sustainable development and the primary purpose of oil–water separation, which is to conserve energy and safeguard the environment. As a result, there is a

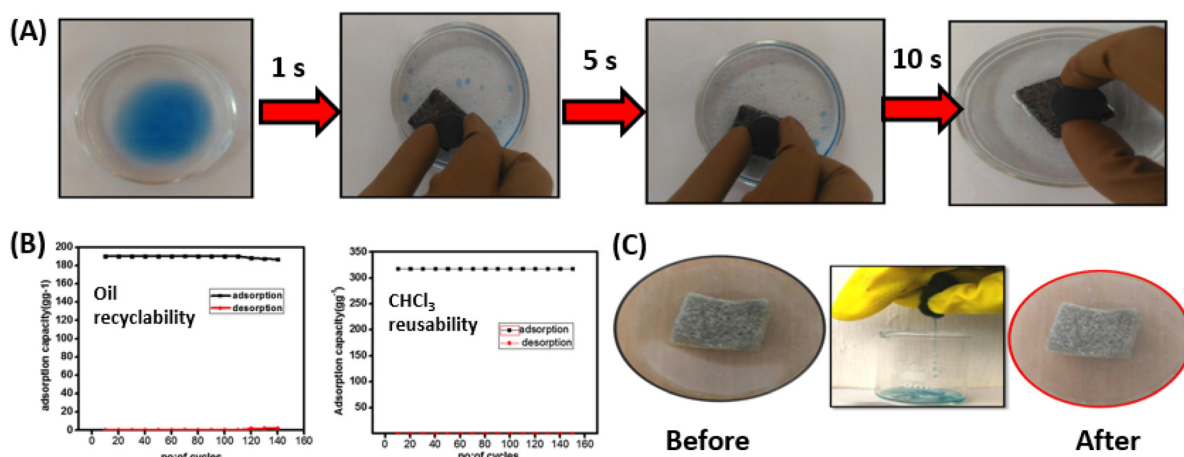


Fig. 10 (A) Oil removal by magnetically driven GPUF over time; (B) adsorption capacity of GPUF in cycles of adsorption and desorption of diesel oil and chloroform; (C) digital images of GPUF before and after reusability studies using diesel oil (reproduced from ref. 115. Copyright 2020 Elsevier Inc.).



growing interest in oil-absorbing polymeric foams made from sustainable (*e.g.*, bio-based and biodegradable) polymers.

**4.2.1. PLA foams.** Poly(lactic acid) (PLA) is among the most extensively studied biodegradable polymers. PLA foam with an open-cell structure and high expansion ratio possesses a 3D structure with a large specific surface area and increased porosity, which provides high buoyancy in the water and efficient oil sorption.<sup>116,117</sup> With its strong oleophilicity and hydrophobicity, PLA serves as an excellent material for oil absorption. Moreover, the porous nature of PLA foam allows for easier degradation compared with solid PLA (Fig. 11).

The high-expansion open-cell PLA foams can be prepared by a cooling batch foaming process under supercritical  $\text{CO}_2$  based on a pre-melted non-crystalline state.<sup>99</sup> This method achieved an impressive maximum expansion ratio of 59.7-fold, coupled with an exceptional adsorption capacity of  $15 \text{ g g}^{-1}$  for  $\text{CCl}_4$ . Mechanical property modifications were introduced by blending PLA with poly(butylene succinate) (PBS) and subsequently batch-foaming with supercritical  $\text{CO}_2$ . The resulting foams demonstrated varying oil adsorption capacities ranging from 7.9 to  $21.9 \text{ g g}^{-1}$  for different oils.<sup>118</sup> *Calotropis gigantea* fiber-reinforced PLA foams were produced using a freeze-drying method, exhibiting a stable porous structure withstanding pressures up to 185 kPa and showcasing an impressive oil capacity of  $48.3 \text{ g g}^{-1}$ .<sup>89</sup> Recent studies have shown the promising applications of PLA foams as oil absorption materials. However, the PLA foams inherit drawbacks from their matrix,

which are low thermal stability and brittleness, and the cost is much higher than regular engineering polymers. Thus, future work for PLA foams may need to be focused on mitigating these challenges.

Table 2 presents studies of sustainable polymer-based foams designed for oil sorption applications. Wang S *et al.*<sup>117</sup> and Li *et al.*<sup>118</sup> successfully fabricated PLA foam and PLA/PBS foam, respectively, employing the supercritical  $\text{CO}_2$  foaming method. Both PLA-based foams exhibited great recyclability for  $\text{CCl}_4$ . Wang X *et al.*<sup>101</sup> employed a water-assisted thermal phase separation to prepare superhydrophobic PLA foam in a simple and facile method, which showed great sorption capacity at around  $12\text{--}31 \text{ g g}^{-1}$ . In Table 2, the recyclability item indicates the number of sorption and desorption cycles during which the foam preserved its structural integrity and oil sorption capacity.

Although PLA foams exhibit strong oleophilicity, high expansion ratios, and impressive oil sorption capacities, they suffer from low thermal stability and brittleness. These issues can limit their performance in varying environmental conditions and reduce their lifecycle during repeated usage. Introducing nanopores and fibers, or blending with some modifiers (*e.g.*, chain extender) may help increase the toughness of PLA-based foams.

**4.2.2. PBS foams.** Poly(butylene succinate) (PBS), alternatively known as poly(tetramethylene succinate), belongs to the polyester family and is a biodegradable thermoplastic polymer

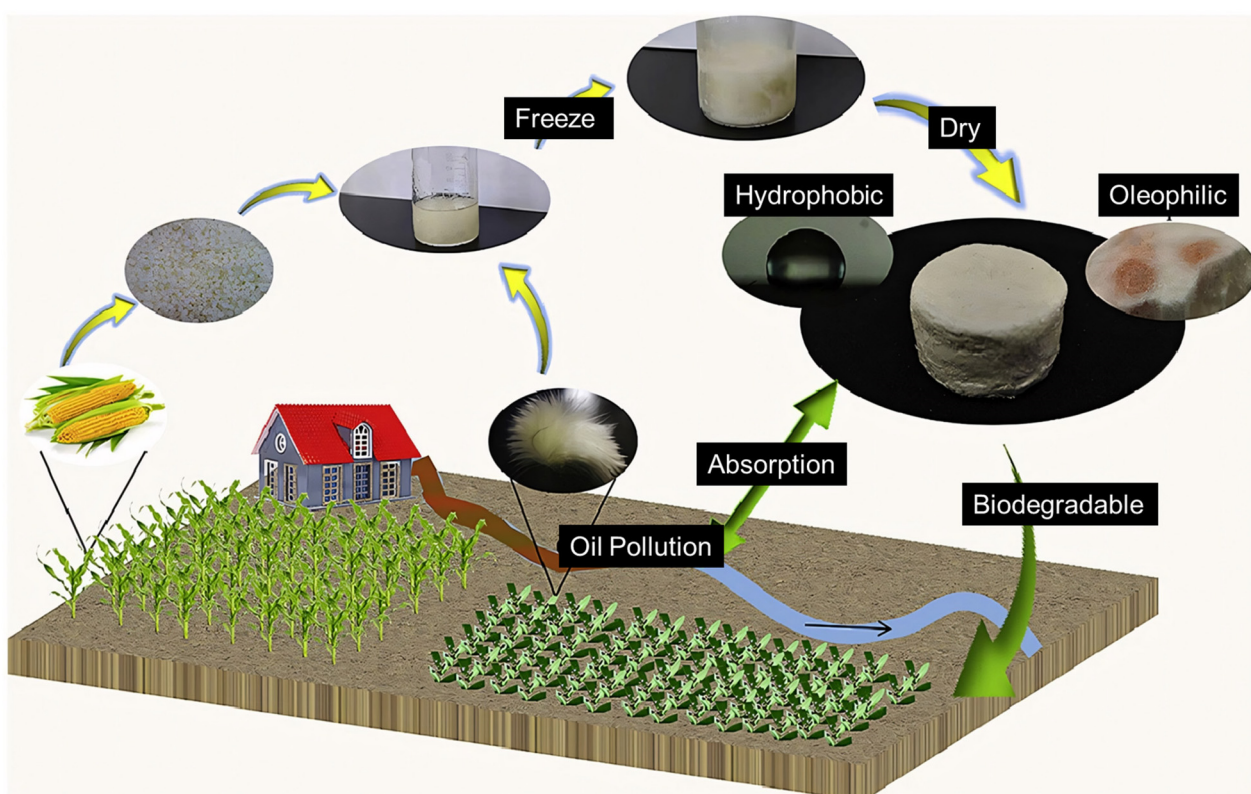


Fig. 11 The eco-cycle of PLA foams as oil absorption materials (reproduced from ref. 89 Copyright 2021 Elsevier Inc.).



Table 2 Sustainable polymer foams developed for oil-absorbing applications

Type	Material	Fabrication method	Type of oil/solvent	Sorption capacity (g g <sup>-1</sup> )	Reusability (cycle)	Ref.
PLA	PLA foam	scCO <sub>2</sub> foaming	CCl <sub>4</sub> , ethyl acetate, N-octane, etc.	4.6–15.1	20 (CCl <sub>4</sub> )	117
	PLA/PBS foam	scCO <sub>2</sub> foaming	CCl <sub>4</sub> , ethyl acetate, silicone oil, etc.	7.9–21.9	20 (CCl <sub>4</sub> )	118
PBS	PLA foam	Water-induced phase separation and freeze-drying	Engine oil, silicone oil, cyclohexane, etc.	Around 12–31	10 (ethanol and cyclohexane)	101
	PBS foam	scCO <sub>2</sub> foaming	CCl <sub>4</sub> , cyclohexane, peanut oil, silicone oil	6.8–34.3	10 (CCl <sub>4</sub> )	120
PBAT	PBS/PLA foam	scCO <sub>2</sub> foaming	CCl <sub>4</sub> , silicone oil	19.2–50.4	20 (CCl <sub>4</sub> )	121
	PBAT foam	Freeze-drying	Engine oil, silicone oil	N/A	N/A	51
PVA	BNNFs/PVA foam	Freeze-drying	Silicone oil and pump oil	19.8–61.1	—	125
	PVA-based porous gel TiO <sub>2</sub> /PVA foam	SAW-induced bubble generation and freeze-drying	Fluorocarbon solvent/oil and silicon oil	Around 4–8	10 (fluorocarbon oil)	129
Others	PVA modification with TiO <sub>2</sub> anchoring	PVA modification with TiO <sub>2</sub> anchoring	PEG, CCl <sub>4</sub> , ethanol, etc.	4.3–13.6	15 (n-hexane and CCl <sub>4</sub> )	128
	NR/CNF foam	CNF modification with NR anchoring	Diesel, pump oil, silicone oil, etc.	Around 40 (silicone and pump oil)	20 (THF, chloroform, and toluene)	130
	Lignin/PU foam	Lignin modification with PUF	Crude oil, olive oil, pump oil, etc.	Around 6–9	50 (crude oil and olive oil)	131

resin that has garnered considerable research attention. This focus stems from its outstanding melt-processability, remarkable insulation capabilities, and commendable toughness characteristics. However, challenges arise in the fabrication of open-cell PBS foam with a stable structure and high porosity due to its linear configuration, low molecular weight, and relatively rapid crystallization rate.<sup>119</sup> Zhu *et al.*<sup>120</sup> studied the oil absorption characteristics of amphiphilic open-cell PBS foams, where glycerin monostearate and chain extender were used to improve hydrophobicity and the molecular weight. The oil absorption capacity of the prepared PBS foam was up to 34.33 g g<sup>-1</sup> for carbon tetrachloride. PBS blended with PLA nanofibers<sup>121</sup> and poly(hexamethylene(iso-co-terephthalimide) (PA6IcoT)<sup>122</sup> showed improved foamability since the melt strength had been increased. Accordingly, the blended PBS foam showed smaller pore sizes, a much more stable pore structure, and improved oil adsorption capacity. While PBS foams offer good melt-processability and biodegradability, achieving a stable open-cell structure with high porosity remains challenging due to PBS's linear configuration and rapid crystallization rate. These factors can lead to variability in foam properties and potential inconsistency in oil sorption performance. Blending the PBS matrix with other polymers or introducing reinforcing fillers may help improve the dimensional stability and modify the crystallinity.

**4.2.3. PBAT foams.** Polybutylene adipate terephthalate (PBAT) is a biodegradable random copolymer, specifically a copolyester of adipic acid, 1,4-butanediol, and terephthalic acid (from dimethyl terephthalate). It is generally marketed as a fully biodegradable alternative to low-density polyethylene, having many similar properties including flexibility and resilience, allowing it to be used for many similar uses such as food packaging, containers, and automobile applications.<sup>121,122</sup> Though PBAT is foamable, its matrix shows weak mechanical

properties, and its considerable shrinkage limits its application as an oil-removal material.<sup>123</sup> Shrinkage-free fully biodegradable PBAT/PBS blend foams were reported by Hu *et al.*<sup>124</sup> by employing supercritical CO<sub>2</sub> foaming. The results showed that the addition of PBS facilitated cell nucleation and increased CO<sub>2</sub> solubility resulting in an open-cell structure with improved stiffness. A directional freezing process was used to develop PBAT foams with aligned channels, and the biodegradable biomimetic hydrophobic PBAT foams showed fast and efficient oil absorption properties that were comparable to their non-biodegradable counterparts (e.g., PET).<sup>51</sup> PBAT foams, despite their biodegradability and flexibility, have weak mechanical properties and significant shrinkage, restricting their use in oil sorption applications. Enhancing the mechanical properties without compromising biodegradability is essential for expanding their application range. Blending with other bio-degradable polymers and fillers might be one of the solutions.

**4.2.4. PVA foams.** Polyvinyl alcohol (PVA) is an affordable, non-toxic, and biocompatible polymer that has attracted significant interest due to its ease of fabrication, slight biodegradability, and suitability for environmental remediation.<sup>125</sup> PVA foam, with its high porosity and low density, exhibits outstanding adsorption performance and the durability of PVA-based foam is essential for sustained oil-water separation applications.<sup>126</sup> However, the hydrophilicity of PVA foam limits its application in oil-water separation.<sup>127</sup> This issue can be addressed by fabricating nanocomposites often through the incorporation of surface-modified nanostructures. Pristine PVA foam typically contains numerous hydroxyl groups, which enable active site reactions with nanoparticles, resulting in hierarchical structures on the PVA foam's framework.<sup>128</sup>

Gao *et al.*<sup>125</sup> combined porous boron nitride nanofibers (BNNFs) with PVA to create a composite foam using a freeze-



drying method. An increase in BNNF content resulted in a larger specific surface area and significantly increased oil sorption capacity. Jin *et al.*<sup>129</sup> fabricated a PVA-based porous gel with a surface acoustic wave (SAW) microfluid generation method, which allowed for improved control and flexibility in manipulating the microfluid. He *et al.*<sup>128</sup> prepared superhydrophobic and superoleophilic TiO<sub>2</sub>/PVA foam by anchoring TiO<sub>2</sub> to the surface of PVA foam with chemical modification. For other biomass-derived foam modification, Lorevice *et al.*<sup>130</sup> fabricated cellulose nanofibril (CNF)-based foam incorporated with natural rubber (NR), and Hwang *et al.*<sup>131</sup> created PU foam combined with hydrophobized lignin particles, which both showed great reusability.

PVA foams are known for their affordability and biocompatibility, but their inherent hydrophilicity limits their effectiveness in oil–water separation. Additionally, their mechanical stability during extended oil sorption cycles requires improvement to ensure long-term usability. Some modifications, for instance, chemical treatments (*e.g.*, grating, coating) to hydrophobize the foam surface may help to improve structural stability.

**4.2.5. Eco-sustainability of biodegradable polymer foams for oil ad/absorption.** Despite the significant progress in developing sustainable polymer-based foams for oil sorption, several challenges remain that need addressing in future research, including:

**4.2.5.1. Environmental impact and degradation.** The degradation rates and mechanisms of these foams can vary significantly depending on environmental conditions such as temperature, presence of microbes, and exposure to sunlight.<sup>132</sup> This variability can affect the predictability of foam performance and environmental impact over time. The degradation products of some biodegradable polymers may still pose environmental hazards if not managed properly.<sup>133</sup> Comprehensive studies on the environmental impact of degradation by-products are necessary to ensure that these materials provide a truly sustainable solution.

**4.2.5.2. Materials and manufacturing costs.** The raw materials for bio-based polymers can be more expensive and less readily available than those for petroleum-based polymers. Exploring alternatives, more abundant bio-based sources, or enhancing the efficiency of existing sources could help mitigate these cost issues. The production costs of sustainable foams, such as PLA and PBS, are generally higher than conventional petroleum-based.<sup>134</sup> Innovations in manufacturing processes, as well as the development of cost-effective and scalable production techniques, are needed to make these foams more commercially viable.

**4.2.5.3. Process optimization.** Achieving uniform and controlled foam structures, particularly in terms of pore size and distribution, is critical for consistent oil sorption performance.<sup>51</sup> Advanced manufacturing techniques and precise control over processing conditions are necessary to enhance the structural properties of these foams. Additionally, incorporating various additives to enhance the properties of these foams, such as nanofillers for mechanical strength or hydro-

phobic agents, can lead to compatibility issues. Ensuring that these additives do not compromise the biodegradability or recyclability of the foams is crucial.

**4.2.5.4. Recyclability and reusability.** Developing efficient recycling processes for these foams that maintain their structural integrity and oil sorption capacity is essential. Current recycling methods may not fully recover the properties of the foams, leading to diminished performance over multiple cycles. The reusability of these foams in practical applications, including their resistance to fouling and degradation after multiple oil sorption and desorption cycles, needs to be thoroughly evaluated. Ensuring long-term effectiveness and durability will enhance their practical application potential. Previous literature demonstrates that many polymers, including polyolefins, undergo chain scission degradation during repeated melt-recycling.<sup>135</sup> This degradation limits the number of times a polymer can be effectively recycled and thermoformed into foam. For biodegradable polymers, recyclability and reusability need further research.

**4.2.5.5. Environmental footprint.** A comprehensive life cycle assessment (LCA) of these foams from production to disposal, including their environmental footprint compared with conventional materials is necessary. This assessment will help in understanding the true environmental benefits and trade-offs involved in using these sustainable foams for oil ad/absorption applications. Addressing these challenges will be pivotal in advancing the application of sustainable polymer-based foams in oil sorption and ensuring their practical, environmental, and economic feasibility.

### 4.3. Surface modifications to improve oil-sorbing properties

The PU and the biodegradable foams reviewed above showed promising applications as oil absorption materials. However, they still suffer from lower oil absorption capacity. The exposed functional groups such as ether, ester, and amide groups may force the foams to absorb both oil and water. Surface functionalization can improve the oil absorption capacity of polymer foams by modifying the surface chemistry of the foam to enhance its hydrophobicity. Some of the relevant literature is listed in Table 3 to show the improvements in oil-sorbing properties after surface modifications.

The surface modification technique usually involves coating a pre-existing polymer foam with a hydrophobic and oleophilic layer to enhance its oil absorption capacity and selectivity. This technique can improve the performance of various types of polymer foams, such as melamine, PU, and polystyrene.<sup>136</sup>

**4.3.1. Surface modification with surfactants.** Surfactants can be used to modify the surface chemistry of the foam by reducing the surface tension and increasing the surface energy. This can enhance the wettability of the foam surface and improve its oil absorption capacity. Silanization has been used as a convenient way to do surface modification for melamine foams in some previous studies.<sup>140,141</sup> In these cases, the foams were soaked in silane solution to modify the surface wettability and water contact angle. The treated foams can get



**Table 3** Improvement of oil-sorbing properties after surface modifications

Surface modification methods	Oil type	Before (g g <sup>-1</sup> )	After (g g <sup>-1</sup> )	Improvement (%)	Ref.
Surfactants	Diesel oil	32	38	19	137
Coating with hydrophobic materials	Edible oil	25	53	112	45
Plasma treatment	Diesel oil	30	47	57	138
Chemical grafting	Heavy crude oil	28	58	107	139

an oil absorption capacity of up to 90 g g<sup>-1</sup>, and the reusability was also improved. However, the surfactants used to cover the foams may be taken away with the oil in the desorption process. Surfactant-based modifications, while effective in enhancing surface wettability, are often not durable. The surfactants can be washed away or degraded during oil desorption, leading to a loss of modification efficacy over repeated cycles. Strategies to create more permanent chemical bonds or use more robust surfactants could be explored to enhance durability.

**4.3.2. Coating with hydrophobic materials.** To make the PBAT open-cell foam superhydrophilic, the foam doped with iron-pillared bentonite (IPB) was prepared by using sugar as a foaming agent and solution phase separation and then combined with a solution dipping method to coat the foam surface with polyacrylamide/SiO<sub>2</sub>.<sup>142</sup> Superhydrophilicity enables the foam to perform better in oil/water separation applications. A two-step dip-coating procedure with oleophilic molecules was used to modify melamine foams, and the treated foams reached an improved oil absorption capacity of up to 100 g g<sup>-1</sup>.<sup>143</sup> Dip-coating is a quick and accessible method to do surface modification; however, it requires a large amount of solvent, which can be environmentally harmful and pose safety risks. Developing solvent-free or low-solvent modification methods could mitigate these environmental impacts. Additionally, while hydrophobic coatings can significantly improve oil absorption, their longevity is often a concern. The coatings may degrade or wear off over time, particularly under harsh conditions or repeated use. Additionally, controlling the uniformity and thickness of coatings during dip-coating processes can be challenging, which may lead to inconsistent performance.

Chemical vapor deposition (CVD) has been used to establish an extremely thin hydrophobic layer on the PU foam surface in an environmentally friendly way, as shown in Fig. 12.<sup>45,144</sup> Different chemicals can be used to functionalize the PU foams, and both the foam structure stability and the oil absorption capacities were improved after modification. While CVD provides a precise and environmentally friendly method for surface modification, it requires significant investment in equipment and maintenance. Additionally, the use of chemicals in CVD processes may still pose environmental and health risks that need to be managed carefully.

**4.3.3. Plasma treatment.** Plasma treatment can modify the surface chemistry of the foam by introducing functional groups, such as carboxylic or amine groups, that can enhance its oil absorption capacity. A two-step atmospheric pressure plasma process to modify the surface properties of a PU foam was reported.<sup>145</sup> The treated PU foam showed selective absorp-

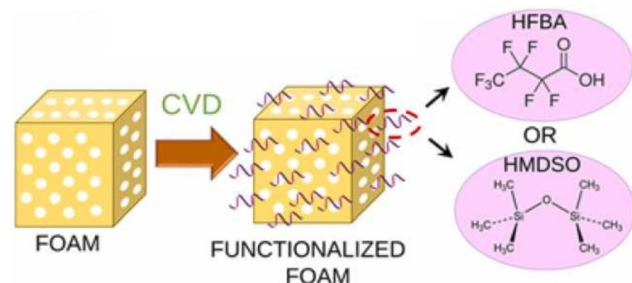


Fig. 12 The CVD coating process for PU foams. Reproduced from ref. 144, Copyright 2022 Elsevier Inc.

tions of various kinds of oil up to 23 times its own weight. In addition, the plasma-treated foam could remove mineral oil while floating on the surface of oil/water mixtures with a separation efficiency greater than 99%. In another study, atmospheric pressure plasma was used to modify the commercialized polymer foam or fiber mesh (e.g., PU sponge),<sup>145</sup> and the treated foam showed improved oil–water separation efficiency. Though the plasma treatment can induce oxygen-containing groups into the polymer foams, the modified foams can repel water completely. To cover the exposed oxygen-containing groups, the melamine sponge (MS) modified by Argon plasma treatment was then coated with Polydimethylsiloxane (PDMS).<sup>138</sup> The modified foam showed superhydrophobicity and reusability with exceptional sorption capabilities.

The disadvantages of plasma treatment include (1) the possibility of introducing hydrophilic groups and (2) the high investment required. Plasma treatment can sometimes introduce hydrophilic groups onto the foam surface, which can counteract the intended increase in hydrophobicity. Ensuring that the plasma treatment parameters are optimized to minimize this effect is crucial. Plasma treatment facilities require significant investment and expertise to operate, which limits their accessibility for widespread use. Simplifying the process and reducing costs could make plasma treatment a more viable option for commercial applications.

**4.3.4. Chemical grafting.** Chemical grafting involves the covalent attachment of functional groups onto the surface of the foam. This can modify the surface chemistry and increase its affinity for oils. PU foams were grafted using polystyrene as absorbent materials for the oil spills in an earlier study,<sup>139</sup> where the chemical grafted foams showed enhanced oil absorption, and doubled the baseline foam. However, the oil absorption capacity started decreasing after 3 cycles. In



another study, a superhydrophobic/superoleophilic PU sponge was fabricated by environmentally friendly surface grafting polymer molecular brushes (grafting with a solution of 1,3-oxazolidin and grafting with a solution containing 1,4-dioxane, stearoyl chloride, and  $\text{NaHCO}_3$ ).<sup>146</sup> The grafted PU foam showed high absorption capacity (23 times its weight), high oil retention (93%), high mechanical strength, and good recyclability (up to 400 times).

To improve the oleophilic/hydrophobic properties of PU foams for oil absorption, PU foams were modified by grafting with oleophilic monomer Lauryl methacrylate (LMA)<sup>147</sup> and coating with LMA microspheres through heating and curing.<sup>110</sup> After modification, the water sorption of modified PU foams was decreased by 24–50%, while the diesel or kerosene sorption of modified samples was increased by 18–27%.

Toward controllable oil/water separation, PU foams were grafted using a block copolymer comprising pH-responsive poly(2-vinylpyridine) and oleophilic/hydrophobic polydimethylsiloxane (*i.e.*, P2VP-*b*-PDMS).<sup>148</sup> The modified PU foams had pH-responsive switchable wettability in aqueous media and showed great potential for various underwater applications. Another study regarding the modification of melamine foams also showed the switchable wettability by pH values when the foams were grafted by poly(4-vinyl pyridine).<sup>149</sup> These studies showed a promising research trend for the future, since the absorption and desorption processes should all be covered in real-life applications.

Chemical grafting methods can be complex and may suffer from process costs and issues with reproducibility and control over the extent of grafting. Ensuring consistent grafting across large-scale production is challenging but necessary for practical applications. Furthermore, the grafted functional groups or polymers might degrade or lose their effectiveness over time, especially under prolonged exposure to oils, and harsh chemical or environmental conditions. Developing more stable grafting techniques or materials could enhance the longevity of these modifications.

#### 4.3.5. Challenges and future directions in surface-modified foams for oil absorption

**4.3.5.1. Selectivity and efficiency.** Although surface-modified foams have demonstrated enhanced oil absorption capacities, their ability to selectively absorb a broad range of oils while repelling water remains inconsistent. To improve their utility across various scenarios, future research must focus on developing modifications that offer universal oil selectivity and performance. Additionally, these foams need to be tested under diverse environmental conditions, including temperature fluctuations and the presence of contaminants, to ensure their effectiveness and reliability in practical applications.

**4.3.5.2. Cost and scalability.** The complexity and expense of many surface modification techniques currently limit the scalability and commercial viability of modified foams. For large-scale industrial deployment, it is essential to identify and develop more cost-effective modification methods that do not compromise performance. Research should prioritize creating scalable methods that maintain efficiency and effectiveness

while minimizing costs, thereby facilitating broader adoption in various industries.

**4.3.5.3. Real-world testing and validation.** Much of the existing research on modified foams has been conducted in controlled laboratory settings. To validate their effectiveness in real-world conditions, extensive field testing is necessary, particularly for applications like marine oil spills and industrial oil–water separation. Moreover, ensuring that these foams comply with regulatory standards for environmental safety and performance is crucial for their commercialization. Further studies should focus on regulatory compliance and environmental impact assessments to support the transition from laboratory research to practical use.

## 5. Melt-blown fibers for oil sorption

### 5.1. Role played by melt-blown fibers

Melt-blowing is a manufacturing process used to produce fine fibers from thermoplastic resins. The process involves melting a polymer resin and then extruding it through small nozzles, where high-velocity fluid, typically air, is blown through the nozzles to break up the molten polymer stream into tiny droplets.<sup>150</sup> These droplets then solidify into fibers as they encounter a conveyor or take-up screen.<sup>151</sup> The resulting fibered web is self-bonded, so the fibers stick together without the need for adhesives. The fibers produced by the melt-blowing process are typically very fine, with diameters ranging from sub-microns to nanometers.

The melt-blowing process is applied in various fields, including automotive components, filtration, thermal insulation, geotextiles, drug delivery systems, and garments.<sup>152,153</sup> The resulting fibered web can be used as a filter medium in air or liquid filtration systems, as the small fiber diameters provide a high surface area, which increases filtration efficiency.<sup>154</sup> Melt-blowing can also be used to produce non-woven fabrics for use in clothing and protective gear, as well as in medical applications like wound dressings and surgical masks.<sup>154,155</sup> Melt-blown fibers have also been found to be effective in oil sorption due to their porous structure. In producing melt-blown fibers, the use of hydrophobic polymers like PP can result in a membrane that repels water due to its low-surface-energy fibers with varying diameters. The rough and porous structure created by these interwoven fibers allows for the selective permeation of oil instead of water.<sup>154,156</sup> This property is useful in oil spill cleanup, where melt-blown fibers can be used to adsorb oil and/or filter the contaminated water. The efficiency of the melt-blowing process and the quality of the fibers primarily depend on the spin head, which pushes the molten polymer through a row of closely spaced fine holes.<sup>157,158</sup>

### 5.2. Melt-spinning and melt-blowing

Melt-spinning and melt-blowing are two common techniques used to produce fibers from polymer materials. Although they share similarities, there are some differences in the process of



fiber formation. Melt spinning is a process in which polymer resin is melted and extruded through a spinneret to form a fiber. The spinneret contains numerous holes or orifices, and the extrusion process produces continuous filaments. The diameters of the fibers produced in melt spinning can be varied by adjusting the size of the orifices in the spinneret.<sup>159</sup>

Melt-blown, on the other hand, is a one-step process in which the molten polymer is blown into ultrafine fibers by hot and high-velocity air. The fiber is then collected on a rotary drum or a forming belt with a vacuum underneath the surface to form a non-woven web. In melt-blowing, the die assembly is different from the melt-spinning process, as hot air converges with the fiber as it emerges from the die.<sup>160</sup> The fibers produced in melt-blowing are typically smaller in diameter, typically ranging from 1 to 10  $\mu\text{m}$ , which allows melt-blown fibers to have superior filtration properties, while conventional melt-spun fibers have a coarser fiber structure, higher tensile strength, and lower pressure drop.<sup>161</sup> The diameters of the fibers produced in melt-blowing can be varied by adjusting the air pressure, temperature, and distance between the die and the collector.

### 5.3. Melt-blowing process

In the present day, there exists a multitude of designs for melt-blowing processes, yet a set of fundamental components is commonly shared among the majority of such processes. These components include (1) polymer feed, (2) a metering pump system, (3) die assembly, (4) air assembly, and (5) fiber collection and a winding system.<sup>162</sup> The schematic diagram of melt-blowing is described in Fig. 13.

The extrusion process begins by feeding the polymer pellets or granules into the extruder hopper, where they are conveyed along the hot walls of the barrel between the screw flights. As the polymer flows through the barrel, it becomes molten due to the combined effects of high temperature, friction, and shear heating as the screw rotates inside the barrel. The molten polymer is then pushed towards the metering zone, which applies the greatest pressure during the extrusion process. This high-pressure molten polymer is regulated by a breaker plate with a screen pack that is positioned near the screw discharge. The molten polymer is then transferred to the metering pump which precisely controls the flow rate of the

molten polymer, which is essential for creating uniform fibers. The metering pump works by measuring and delivering a fixed volume of polymer melt per unit of time and ensures consistent polymer flow under process variations in viscosity and temperature. The most crucial component of the melt-blowing process is the die assembly, which comprises three essential parts: polymer feed distribution, die nosepiece, and air manifolds.<sup>163</sup> The polymer feed distribution is designed in a way that polymer distribution is not heavily influenced by the shear properties of the polymer, allowing for the melt blowing of a wide range of polymeric materials with one distribution system. Once the polymer melt exits the feed distribution channel, it directly flows to the die nosepiece, which is a broad, hollow, and tapered metal piece containing several hundred holes or orifices spread across its width. The orifices or holes in the die nosepiece release the polymer melt, which then solidifies into thin strands. These strands are then drawn out and stretched into fine fibers (attenuation) by high-velocity hot air (typically at 230 °C to 360 °C and 1/2 to 4/5 the speed of sound in commercial processes).<sup>164</sup> A spin head enables the extrusion of low-viscosity molten polymer through a single row of fine holes that are closely spaced, typically ranging from 1000 to 4000 holes per m. To solidify and draw the extruded fibers, high-velocity hot air is used and then cooled by entrained air (winding process). The collected fibers are subsequently formed into a fiber mat on the collector.

### 5.4. Melt-blowing dynamics

A considerable amount of theoretical and experimental research has been conducted on the mechanisms of fiber dynamics during melt-blowing.<sup>165,166</sup> Understanding fiber dynamics is critical in controlling the properties of melt-blown nonwoven fibers.

**5.4.1. Fiber motion.** Whipping is a phenomenon that occurs in the melt-blowing process when the polymer fibers undergo lateral oscillations due to aerodynamic forces.<sup>165</sup> The theory of aerodynamically driven jet bending was developed by Entov and Yarin,<sup>166</sup> who stated that if the velocity of the flow exceeds a certain critical value, any small disturbance in the flow will grow and result in instability. According to the online measurement conducted by Xie and Zeng,<sup>167</sup> the area between 0 to 5 cm at the centerline experienced high air velocities and

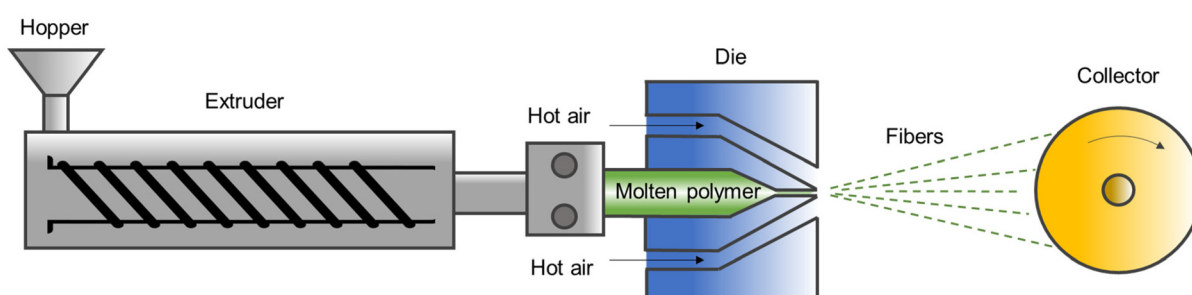


Fig. 13 Melt-blowing process from the extruder.



significant turbulent fluctuations when the polymer melt was discharged from the die. Measurement of turbulence quantities is crucial in the melt-blown process to understand fiber motion and formation. Also, it can prevent operational problems caused by strong velocity fluctuations, such as fibers sticking to the die face or becoming entangled with themselves or adjacent fibers. Xie and Zheng's observation of fiber whipping amplitude and frequency showed that whipping occurs more intensely with an increase in distance from the die, while the frequency of the whipping action decreased as the distance from the die increased.

One of the factors that influence fiber motion is the airflow field created near the melt-blowing die. The airflow field can be modified by using different die designs, such as slot die and annular die (or swirl die). A slot die is a type of melt-blowing die that has a rectangular opening for airflow. The airflow field near the slot die is important for fiber formation and quality because it determines the degree of fiber attenuation, whipping motion, entanglement, and cooling. Xie *et al.*<sup>168</sup> discussed the measurement and analysis of the three-dimensional jet flow field under a common slot-die using a hot wire anemometer, three-dimensional traverse equipment, and a stepper motor. Their results showed that the velocity of airflow is significantly reduced near the slot end face, which affects the distribution of the flow field. The characteristics of the flow field led to inconsistencies in fiber diameter and strength. In the center area and its vicinity, air velocities were high with little difference between them, while distant areas had lower velocities and no drafting effect on the fiber. The velocity on the spinning line decreased sharply as the distance to the die increased, and the instantaneous speed fluctuated rapidly, which could cause fiber whipping and hinder smooth drafting.

On the other hand, a swirl-die (annular-die) can produce a swirling diffused airflow that can induce helical fiber motion and result in fibers with specific patterns. Moore *et al.*<sup>169</sup> reported that the inner annular wall of the die creates significant variations in turbulence behavior, including the formation of a recirculation region due to the center wall effects. In addition, the annular orifice generates a substantial amount of turbulence in its immediate vicinity, which is much greater than that generated by a circular orifice. The flow properties of a swirl die are significantly different from those of a more extensively studied slot die. Zhu *et al.*<sup>170</sup> studied the relationship between the lateral swirling diffusion of airflow and fiber distribution in the unique swirl-die melt-blowing process. The three-dimensional resultant velocity of air ( $v$ ) in the swirl-die melt blowing was three-dimensionally decomposed into its lateral velocities ( $v_r$  and  $v_s$ ) and the downward velocity ( $v_z$ ), which was directed toward a fiber collector. The fiber path in the swirl-die melt blowing was captured using high-speed photography. It was found that the critical boundary of the air lateral diffusion velocity ( $v_r$ ) played a significant role in controlling the lateral fiber distribution during melt-blowing. However, most of the twisting velocity ( $v_s$ ) was located outside the conical fiber envelope and had little contribution

to the continuing helical motion of the fiber below 6 mm from the die.

Fiber morphology in the melt-blowing process is shaped by airflow characteristics, die design, and distance from the die. High air velocities and turbulence near the die, as in slot dies, induce intense fiber whipping and can lead to inconsistencies in fiber diameter and strength. Slot dies create linear airflow fields, resulting in fiber attenuation and possible entanglement. In contrast, swirl dies produce diffused, swirling airflow that promotes helical fiber motion and unique patterns. Turbulence around swirl dies also enhances fiber distribution control but limits twisting effects close to the die. Overall, die structure and airflow dynamics play crucial roles in fiber formation and stability.

**5.4.2. Fiber diameter.** Numerical simulation has been used in several studies to predict the diameter of melt-blown fibers during the melt-blowing process. The first model, developed by Uyttendaele and Shambaugh,<sup>171</sup> was based on equations used in the melt-spinning process and simulated fiber dynamics in one dimension. Shambaugh and his team later improved the model by expanding it to two-dimensional and three-dimensional models,<sup>172,173</sup> allowing the fibers to experience lateral velocity perturbations and simulate the whipping phenomena observed during melt-blowing.

The distance between the die and collector (DCD) affects the diameter of melt-blown fibers, as it impacts the fiber attenuation rate due to aerodynamic drag and fiber entanglement.<sup>174</sup> The effect of DCD on melt-blown fiber properties depends on intrinsic material properties, such as crystallization kinetics, viscosity, and relaxation time.<sup>154</sup> Fibers produced at larger DCDs tend to have smaller diameters due to greater deformation from high-speed hot air drag. DCD also influences the mat thickness and pore size of melt-blown fibers. Fiber speed is generally independent of diameter, except near the die where entanglement is low.<sup>175</sup> It is therefore anticipated that during melt-blowing, fine fibers will have a lower temperature compared with coarse fibers due to their faster cooling rate and similar exposure time to cool air.

Air temperature and air pressure are critical parameters in melt-blowing that can influence fiber diameter. Studies have shown that as the air temperature increases, the average fiber diameter tends to decrease.<sup>176,177</sup> This is because higher temperatures soften and melt the polymer resin to the required viscosity for efficient extrusion in melt-blowing.<sup>178</sup> Also, air temperature affects the processability of the material and the physical properties of the polymer melt. Lower polymer flow rate and higher initial temperature have been shown to decrease the fiber diameter.<sup>177</sup> An increase in air pressure can also lead to a decrease in fiber diameter. The shape of fibers produced in melt-blowing is affected by both air pressure and air velocity, which are linked to the rate of airflow. When air velocity is increased during the process, it leads to greater attenuation and results in a smaller fiber diameter.<sup>154</sup> However, generating excessive air pressures during the process can result in fiber breakage and the production of loose fibers. In order to minimize the significant energy cost associated with the use of pressurized hot air in melt-



blowing, it is important to develop a technique to produce melt-blown fibers with low air velocity.<sup>174</sup>

Tan *et al.*<sup>179</sup> examined how the linear viscoelasticity of polymer melt impacts the diameter and diameter distribution of melt-blown fibers. Polystyrene of varying molecular weights was added to control the viscosity and elasticity of the testing samples. The average diameter and fiber diameter distribution, or the coefficient of variation were used and calculated with the following equations.

$$\text{the } f(d) = \frac{1}{(d \cdot \sigma \sqrt{2\pi})} \exp \left[ -\frac{1}{2\sigma^2} \left\{ \ln \left( \frac{d}{d_{av}} \right) \right\}^2 \right] \quad (7)$$

where the  $f(d)$  is lognormal distribution,  $d$  is the fiber diameter,  $d_{av}$  is the average diameter, and  $\sigma$  is the standard deviation.

$$CV = \sqrt{\exp(\sigma^2) - 1} \times 100\% \quad (8)$$

where  $CV$  is the coefficient of variation.

The study found that increasing viscosity resulted in an increase in average fiber diameter, with minimal effect on  $CV$ . Conversely, increasing elasticity above a certain threshold value decreased  $CV$  while increasing average diameter, as illustrated in Fig. 14. The figures show the average diameter ( $d_{av}$ ) and coefficient of variation (CV) of melt-blown polystyrene samples (of almost constant viscosities) as a function of the longest melt relaxation time ( $\lambda_1$ ), which are associated with elasticity. A notable increase in average diameter was observed at the highest elasticity (highest  $\lambda_1$ ) and a decline in  $CV$  beyond a specific threshold value ( $1 \text{ ms} \leq \lambda_1 \leq 10 \text{ ms}$ ) was observed along with the increase in elasticity.

To summarize, fiber diameter in melt-blowing is influenced by factors including die–collector distance (DCD), air temperature, air pressure, and polymer properties. Larger DCDs yield finer fibers due to extended aerodynamic drag, while higher air temperatures reduce fiber diameter by softening the polymer. Increased air pressure and velocity also lead to finer fibers but risk breakage if excessive. Polymer viscosity and elasticity further impact diameter and distribution; higher viscosity increases fiber diameter, while higher elasticity initially

reduces variation in diameter before increasing average diameter at high elasticity levels. These factors collectively shape fiber size, distribution, and consistency in melt-blown processes.

**5.4.3. Crystallization.** Crystallinity is also an important physical property in understanding melt-blown fibers. Uyttendaele and Shambaugh<sup>171</sup> analyzed the crystallinity of melt-blown PP using a differential scanning calorimeter (DSC) with a  $20 \text{ }^{\circ}\text{C min}^{-1}$  scan rate of 5–6 mg sample. A single peak was found at  $159 \text{ }^{\circ}\text{C}$  which was caused by the monoclinic crystal structure due to the high spinning speed and the tested polymer's relatively low melt flow index (35 g per 10 min). Bresee and his team observed fiber crystallization behavior through successive investigations of melt-blown fibers. They reported that fiber attenuation mostly occurred close to the die area before the fibers had solidified, while most of the molecular orientation and crystallization occurred further from the die after the fibers had solidified.<sup>180</sup> The fiber array structure was found to be less complex near the die but exhibited greater complexity further away from the die. In their later work, wide-angle X-ray diffraction (WAXD), small-angle X-ray scattering (SAXS), and optical microscope measurements were taken at various locations between the die and collector, as well as from a web retrieved from the collector by Bresee *et al.*<sup>175</sup> to investigate the crystallization of PP during melt-blowing. The WAXD measurements revealed that fibers between the die and collector were mostly smectic mesophase, while the web from the collector exhibited a well-defined monoclinic crystalline structure. This suggested that the majority of fibers did not crystallize until they reached the collector. The SAXS measurements further supported this observation, indicating that fibers 25 cm from the die showed little lamellar stacking, while fibers retrieved from the collector contained well-stacked lamellae. Moreover, optical microscope images showed that no spherulites were present in fibers retrieved at any location between the die and collector, whereas coarse fibers retrieved from the collector contained large spherulites.

The effects of various melt-blowing parameters on the structure of PP fibers were studied by Kara and Molnár.<sup>174</sup> It

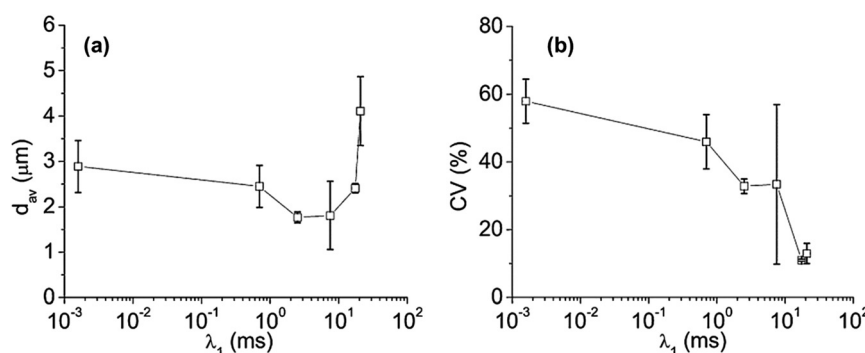


**Fig. 14** (a) Average diameter ( $d_{av}$ ) and (b) coefficient of variation (CV) of melt-blown polystyrene fibers at approximately constant viscosities. Reproduced from ref. 179. Copyright 2010 Elsevier Inc.



was observed that lower air velocity, pressure, and temperature led to slower cooling rates and higher fiber crystallinity. The tensile behavior of the fibers changed from malleable to brittle as the air temperature and pressure increased, due to increased fiber entanglements and a crystalline structure change. The structure of melt-blown fibers was analyzed using WAXD, which showed the formation of crystalline, amorphous, and mesomorphic phases. The content of these phases varied depending on the processing conditions and the temperature gradient between DCDs. They found that it was essential to minimize the temperature difference between the fiber and its surroundings to generate high-strength melt-blown fibers with a perfect crystalline structure, and high air stretching was also required to reduce crystallite size and improve molecular orientation.

Therefore, fiber morphology in melt-blowing is influenced by crystallinity, air parameters, and cooling rates. Higher air velocity, pressure, and temperature decrease fiber crystallinity by increasing cooling rates, leading to smaller, more brittle fibers with reduced lamellar structure. Most crystallization occurs near the collector, where molecular orientation and crystalline phases, such as monoclinic structures, become prominent. Slow cooling enables higher crystallinity and larger spherulites, enhancing fiber strength. Techniques like WAXD and SAXS reveal that fibers further from the die exhibit complex structures, while those closer remain less organized. Optimal temperature control and stretching improve fiber orientation and crystallinity, enhancing strength and consistency.

**5.4.4. Porosity and pore size.** The functionality and filtration performance of melt-blown fibers is greatly affected by their pore size. Fabrics produced by melt blowing have a range of porosity from 70 to 99%, and fiber diameters from 500 nm to hundreds of microns exhibit alignment and anisotropy.<sup>181</sup> The pore size can be controlled by adjusting the production parameters such as fiber diameter, air pressure, temperature, and polymer melt viscosity.<sup>174,182,183</sup> High-speed air jets also lead to the formation of finer fibers and smaller porosities, which in turn reduces the size of pores of the fiber web.<sup>184</sup> The thickness of the fiber web is affected by the speed at which the collector moves, with a slower speed causing an increase in thickness and a further reduction in pore size.<sup>185</sup> Kara and Molnár<sup>174</sup> conducted a study in which they investigated the impact of various parameters on the pore size and porosity of melt-blown PP fibers (Fig. 15). The research discovered that the overall porosity and the pore size of melt-blown fibers are influenced by DCD, air temperature, and air pressure. When DCD increased, pore size first decreased until 150 mm but then increased with higher DCD. Increased air turbulence at extended DCD led fibers to spread out over a larger area, reducing fiber packing density, and creating a softer texture. As the air temperature increased, the fiber diameter shrank and resulted in fluctuating porosity and overall reduced pore sizes, and at 125 °C (the lowest tested temperature) the fibers exhibited the highest porosity with large pore size. Elevated air pressure constricted fiber flow, leading to increased mat thickness and fiber packing density, which subsequently caused smaller pores and a thicker mat.

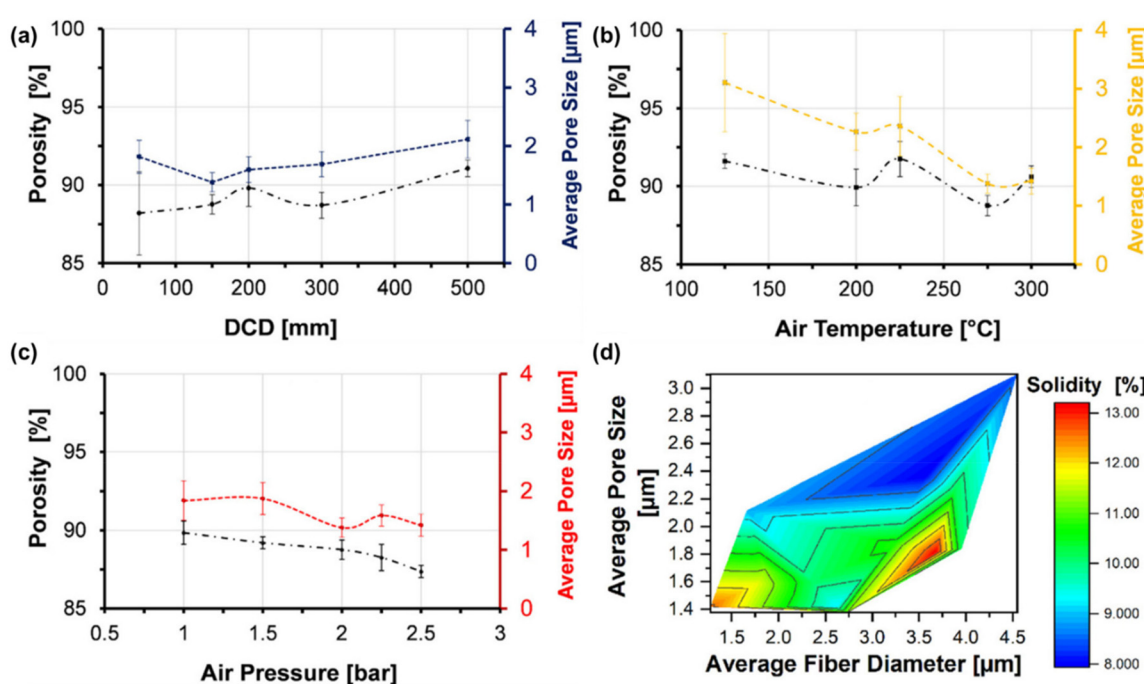


**Fig. 15** Porosity and pore size of PP melt-blown fibers as a function of (a) die-to-collector distance, (b) air temperature, (c) air pressure; (d) 2D contour plot of fiber solidity and pore size as a function of fiber diameter. (Reproduced from ref. 174. Copyright 2021 John Wiley & Sons, Inc.)



The pore size of melt-blown fibers ( $\bar{D}$ ) can be represented by employing eqn (9) and (10).<sup>186</sup>

$$\bar{D} = d_f \sqrt{\frac{32}{(1-c)^2 f(c)}} \quad (9)$$

$$f(c) = \frac{5.6c}{-\ln c + 2c - 0.5c^2 - 1.5} \quad (10)$$

where  $d_f$  is average fiber diameter,  $c$  is fiber packing density,  $(1 - c)$  is porosity, and  $f(c)$  is the function of fiber packing density given by Langmuir.<sup>187</sup>

Fiber morphology and pore size in melt-blown materials are shaped by parameters like air pressure, temperature, die-to-collector distance (DCD), and fiber packing density. High-speed air jets create finer fibers with smaller pores, enhancing filtration performance. Increased DCD initially decreases pore size but eventually raises it due to fiber spread and reduced packing density. High air temperatures yield finer fibers and fluctuating porosities, while low temperatures result in larger pores. Higher air pressure compresses fibers, increasing mat thickness and reducing pore size. Collector speed also influences thickness and pore size, with slower speeds producing thicker, denser fiber webs and smaller pores.

### 5.5. Melt-blown fibers for oil sorption

Nonwoven sheets of micro- and nanofibers produced *via* the melt-blowing process are highly effective as oil sorbents. The fibrous structure created by this melt-blowing allows for a highly porous surface area and is especially suitable for applications such as oil/water separation and oil sorption.<sup>188</sup> One of the most extensively studied polymers, melt-blown polypropylene (PP) non-wovens, provides enhanced oil adsorption performance, as PP inherently repels water and adsorbs oil.<sup>189</sup> By employing melt-blowing technology, ultrafine PP fibers are formed to create a specific structure characterized by micro-scale roughness and exceptional wetting properties. The PP

melt-blown fibers exhibit high breakthrough pressure and exceptional separation efficiency with stability and reusability in a range of demanding environments.<sup>190</sup>

Recently, Lee *et al.*<sup>191</sup> developed a novel approach to produce nonwoven fiber mats using a highly elastic tri-block copolymer SEBS, enhanced with low-concentration polypropylene (PP) loading. This study revealed that incorporating a small amount (10 wt%) of PP significantly improved the melt-blowing process, acting as a lubricant and resulting in the production of fine and continuous fiber mats. Notably, a formulation composed of 90% SEBS and 10% PP showed excellent performance in oil/water separation, isolating nearly 100% of oil from a 1:6 oil/water mixture, thus confirming the feasibility of using such nonwoven mats for environmental applications.

Furthermore, the study emphasized the unique oil gelation properties of SEBS. The gelation, occurring when SEBS interacts with oil, serves as an effective barrier, immobilizing the oil and preventing further spread, a crucial advantage over PP-based mats that rely solely on oil adsorption. Once PP-based mats reach their saturation point, they can no longer adsorb additional oil, leading to potential leakage or dispersion. In contrast, SEBS-based mats, by leveraging their oil gelation properties and the enhanced surface area from the melt-blown process, offer a highly effective sealing alternative when accidental oil leakage is a concern (Fig. 16).

Zhang *et al.*<sup>190</sup> fabricated a PP membrane through a facile melt-blowing process. The PP membrane showed exceptional oil-water separation capabilities, high flux, and improved intrusion pressure. The membrane's hydrophobic nature, along with the coarse and porous structure created by the interlacing of low-surface-energy fibers of different sizes contributed to its ability to selectively permeate oil over water. These membranes excelled at separating oils like pump and crude oil from various aqueous solution compositions, achieving over 99% separation efficiency. They remain functional in

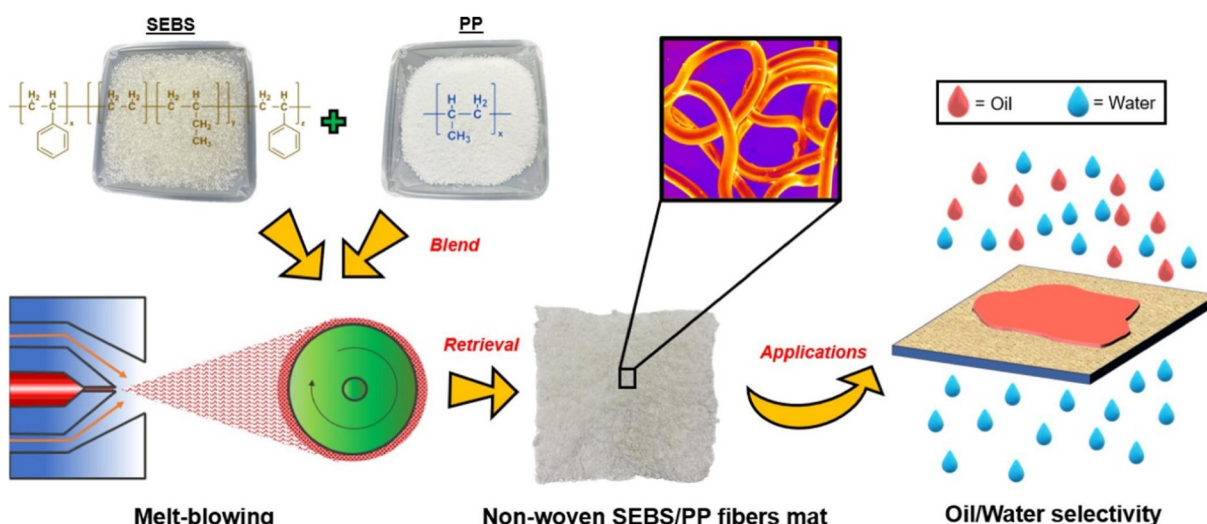


Fig. 16 Schematic diagram of SEBS/PP fibers mat fabricated through melt-blowing. Reproduced from ref. 191, Copyright 2023 Elsevier Inc.



harsh environments and are reusable for at least 20 cycles while preserving their effectiveness.

Meng *et al.*<sup>192</sup> examined the impact of varying melt flow indexes (MFIs) on the oil absorption capacity and diameters of PP melt-blown fibers. Four types of PP with different MFIs (800 g per 10 min, 1100 g per 10 min, 1300 g per 10 min, and 1800 g per 10 min) were prepared. PP resins are divided into two groups: (1) unblended PP resins with 4 different MFIs and (2) blended PP resins, in which each resin consists of two different PP types with distinct MFIs, combined in a 50:50 ratio. Both groups of PP resins were melt-blown into fibers using a swirl die melt-blowing apparatus. A blended PP fiber web consisting of 50% PP with an MFI of 1800 g per 10 min and 50% PP with an MFI of 800 g per 10 min demonstrated the highest oil adsorption capacity at 94.05 g g<sup>-1</sup>. In contrast, unblended PP webs with MFIs of 800 g per 10 min and 1800 g per 10 min exhibited oil adsorption capacities of approximately 50 g g<sup>-1</sup> and 70 g g<sup>-1</sup>, respectively. This can be attributed to the variations in porosity and fiber diameter. Unblended PP fiber web with low MFI (800 g per 10 min) created a large average fiber diameter (5.68  $\mu$ m), while that of a high MFI (1800 g per 10 min) created a small average fiber diameter (1.97  $\mu$ m). The high porosity and large disparities in fiber diameter for a blended PP fiber web ensured a rapid oil

sorption rate and large storage space for the adsorbed oil. Moreover, this blended PP fiber displayed good reusability, maintaining a sorption capacity of 18.36 g g<sup>-1</sup> after five cycles. It was found that blended PP fiber combined with different MFIs presented a promising option for oil spill remediation.

Sun *et al.*<sup>193</sup> blended PP and titanium dioxide (TiO<sub>2</sub>) through an extruder and then created PP/TiO<sub>2</sub> fibers through melt-blowing designed for oil/water separation and photocatalysis. Differential scanning calorimetry (DSC) and thermogravimetric analysis (TGA) results revealed that the presence of TiO<sub>2</sub> increased crystallinity and raised the thermal decomposition temperature. Scanning electron microscopy (SEM) images demonstrated a uniform dispersion of TiO<sub>2</sub> within the PP matrices, leading to a larger fiber diameter and rougher surface. The study overall showed crystallization, thermal stability, and photocatalytic performance due to an increase in TiO<sub>2</sub> content. The addition of TiO<sub>2</sub> increased oil/water separation efficiency (Fig. 17(a)), and oil flux (about 15 000 L m<sup>-2</sup> h<sup>-1</sup>), and the fibers remained stable after 6 hours of ultraviolet exposure. Fig. 17(b) shows that the PP/TiO<sub>2</sub> fiber mat has superhydrophobicity. Fig. 17(c) displays the surface tension of different acetone solutions on the fiber mat, where the surface tension increased with the water content, which also confirmed the superhydrophobicity of the synthesized oil absorption materials.

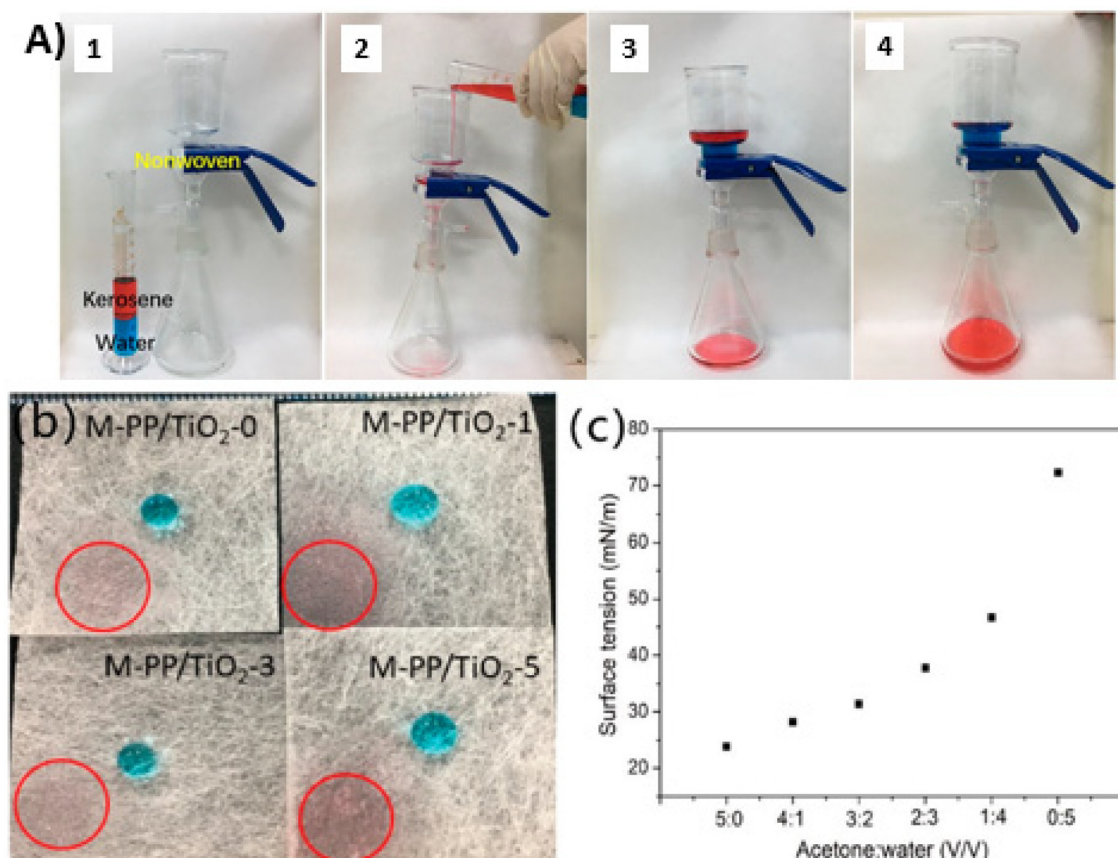


Fig. 17 (a) The oil–water separation process of M-PP/TiO<sub>2</sub>, (b) the oil and water drip on the melt-blown membrane (the red circle is kerosene, the blue drop is water), and (c) the surface tension of different acetone solutions. Reproduced from ref. 193, Copyright 2019 MDPI.



**Table 4** Comparison between polymer foams and melt-blown fibers for oil sorption

Items for comparison	Polymer foams	Melt-blown fibers
Porous structure	Open-cell structure with optimized capillary action channel required <sup>48,51</sup>	Fibrous structure with up to 100% interconnected tunnels <sup>181</sup>
Oil absorption capacity	High, due to the porous open-cell structure <sup>140</sup>	High, due to the fine fibers and large surface area <sup>194</sup>
Surface treatment	Surfactants, coatings, plasma treatments, and chemical grafting procedures can be used <sup>136</sup>	The polymer fiber surface may be required to be modified with additives or treatments to increase the contact angle with water and decrease the contact angle with oil <sup>194,195</sup>
Reusability	Limited, may cause leakage once saturated <sup>144</sup>	Limited, can be broken down due to the flexibility and poor mechanical strength <sup>195</sup>
Recyclability	Have to desorb before recycling; cured polymer foams can be hard to recycle <sup>197</sup>	Have to desorb before recycling; recyclable for the thermoplastics-based fibers
Processing parameters adjustment	Type of blowing agents, blowing agent content, pressure, foaming temperature <sup>85</sup>	Temperature, pressure, air velocity, due to collector distance <sup>166,191</sup>
Processing difficulty	Easy to fabricate, and many alternative processing methods; the foaming process can be slow <sup>85</sup>	The rapid fabrication process, high temperature, and pressure required <sup>154,198</sup>
Investment	Low, depending on the accessible equipment <sup>85</sup>	High, may need special handling and skills for processing <sup>162</sup>

Melt-blown fibers, such as polypropylene (PP) and SEBS/PP fibers, offer notable oil absorption capabilities but face challenges in selectivity, adaptability, and real-world performance.<sup>197</sup> Their efficiency across diverse oil types and environmental conditions needs further exploration, particularly regarding reusability and contamination resistance. Despite promising lab results, the complexity and cost of current modification techniques limit large-scale deployment. Research must focus on developing simpler, cost-effective methods without compromising performance. Additionally, extensive field testing is necessary to validate their practical application and ensure compliance with environmental regulations.

### 5.6. Comparison between polymer foam and melt-blown fibers for oil sorption

For oil absorption purposes, the porous structure, oil absorption capacity, processing difficulty, reusability, recyclability, and investment requirements of polymer foams and melt-blown fibers are listed in Table 4. The open-cell porous structure is required for polymer foams to be used for oil adsorption, thus the processing control (e.g., foaming agent, temperature, pressure) would be crucial.<sup>48</sup> For the melt-blown fibers, they would form a mat that has connected tunnels inside, so the porous structure is ideal for oil absorption and oil/water separation. Both the open-cell polymer foams and melt-blown fibers would have high oil absorption capacity, due to the porous structure. However, for the melt-blown fibers, the fine-blown fibers and the large surface area are ideal for oil capture and storage.<sup>194</sup>

Surfactants, coatings, plasma treatments, and chemical grafting procedures offer viable means for surface functionalization,<sup>136</sup> enhancing both the hydrophobicity and oil absorption capacity of polymer foams and melt-blown fibers. For optimal performance, modifications to the surface of melt-blown polymer fibers may involve the incorporation of additives or specific treatments aimed at augmenting the contact angle with water and diminishing it with oil. Given the size-

dependent effects of fibers and pores, the surface treatment protocols must be carefully calibrated to optimize modification efficiency.<sup>194,195</sup>

The reusability of both polymer foams and melt-blown fibers requires further improvement since they are unstable once the porous structure gets saturated.<sup>144,196</sup> For the polymer foams, the overloading oil may cause secondary pollution; for the melt-blown fibers, the limited stiffness or mechanical strength may cause structural damage during service.<sup>195</sup> Both polymer foam and melt-blown fibers need to be fully desorbed before reuse or recycling. The recycling of cured polymer foams is still a challenge,<sup>197</sup> but for thermoplastic polymer foams and melt-blown fibers, it is fairly straightforward apart from the desorption efficiency.

The polymer foams are easy to prepare and customize, and the required facilities are accessible, but the foaming can be time-consuming because the foaming gases dissolve (chemical decomposition) and the bubble stabilization processes usually take time.<sup>85</sup> Melt-blowing on the other hand can be rapid, but the temperature and pressure need to be optimized.<sup>154,166,198</sup> In addition, the capital investment for melt-blowing is high, since the processing may need special handling and skills to deal with the high temperature and pressure control.

## 6. Conclusion and future prospects

Polymer foams are low-density, porous materials with a spongy cellular structure created by entrapping gas in a polymer matrix. They offer numerous advantages over non-foamed polymers. The foam's large surface area and cellular structure enable effective oil ab/adsorption, while their lightweight and low-density properties help contain and prevent oil spreading. Foaming agents can be physical or chemical, with physical agents being eco-friendly, cost-effective, and safe, but causing post-shrinkage problems in thermoplastic elastomers. Chemical foaming prevents post-shrinkage but may cause pol-



lution from gas release. Various foaming processes, such as extrusion foaming, batch foaming, foam injection molding, compression foaming, and freeze-drying have been developed. The viscoelastic properties of molten polymers play a significant role in the foaming process, and higher melt strength results in more extensive foam expansion. Various polymer foams have been developed for oil sorption, including PP, PE, PU, and PS-based thermoplastic foams and EPDM- and EVA-based thermoplastic elastomeric foams.

Recent trends involve modifying PU foams with nano-materials for improved oil sorption and developing biodegradable polymer foams. Nano carbon-based materials have been proved to be effective as fillers in polyurethane foam for oil absorption purposes. Interest in oil-absorbing polymeric foam made from bio-based and biodegradable substances has been growing, as the consumption of non-renewable resources has caused severe environmental issues. The surface properties can be modified by adding additives, surfactants, coatings, plasma, or chemical treatments to the foams. The surface modifications for polymer foams for oil absorption showed that hydrophobicity can be improved *via* various kinds of treatments and the oil absorption properties would be enhanced.

Melt-blown creates fine fibers from thermoplastic resins by melting the resin, extruding it through nozzles, and using high-velocity heated air to form droplets that solidify into fibers. Melt-blown fibers are effective for oil sorption due to their hydrophobic nature and porous structure. Using hydrophobic polymers, such as PP, creates a water-repelling membrane with varied fiber diameters. Due to their rough and porous structure, the nonwoven fibers enable selective oil permeation and serve as excellent materials for oil spill cleanup and contaminated water filtration. Key components of the melt-blowing process include polymer feed, a metering pump system, die assembly, air assembly, and fiber collection and winding system. Extensive research on fiber dynamics during melt-blowing is crucial for controlling fiber properties. Factors such as die-to-collector distance, polymer viscoelasticity, air temperature, air pressure, and airflow rate determine fiber motion, diameter, crystallization, porosity, and pore size. Melt-blown nonwoven sheets are highly effective oil sorbents due to their porous surface area. Melt-blowing technology creates ultrafine PP fibers with microscale roughness and excellent wetting properties, resulting in high breakthrough pressure, separation efficiency, stability, and reusability. While there is limited research on melt-blown fibers as oil sorbents, recent studies have highlighted the enhancement of oil adsorption capacity and stability by blending PP with different melt flow index polymers or by increasing surface roughness through the addition of reinforcing fillers.

Overall, the prospects for both polymer foam and melt-blown fibers appear promising as ongoing research focuses on enhancing their performance and expanding their applications in oil sorption and other areas. To facilitate research, it is essential to establish standardized testing methods for sorbent materials that account for the unique oil uptake

mechanisms of each sorbent material and provide a more accurate understanding of their real-world potential. For instance, a thorough understanding of the core technology to separate oil and water effectively is still pending. Understanding the core impact and comparisons of optimized capillary action channels in foams and the surface effects for oil absorption and remediation is still under investigation. The environmental conditions of the oil-water mixture, such as pH, salinity, viscosity, and emulsion type, also affect real-world applications. These conditions affect the stability and separation efficiency of the foams while coping with different types of oil and water contaminants. Moreover, enhancing the ease of retrieval and reuse of sorbents will contribute to practicality and cost-effectiveness. Additionally, the adoption of bio-based and biodegradable materials will play a vital role in promoting sustainability.

## Data availability

No primary data were used for this review article.

## Conflicts of interest

There are no conflicts to declare.

## Acknowledgements

The financial support of the Natural Science and Engineering Research Council of Canada (NSERC) and Ontario Centre for Innovation (OCI) is greatly appreciated.

## References

- 1 J. S. Sinninghe Damsté and S. Schouten, *Biological Markers for Anoxia in the Photic Zone of the Water Column, in Marine Organic Matter: Biomarkers, Isotopes and DNA*, Springer-Verlag, Berlin/Heidelberg, 2006, pp. 127–163. DOI: [10.1007/978-3-540-31205-1](https://doi.org/10.1007/978-3-540-31205-1).
- 2 B. Zhang, E. J. Matchinski, B. Chen, X. Ye, L. Jing and K. Lee, *Marine Oil Spills—Oil Pollution, Sources and Effects, in World Seas: An Environmental Evaluation*, Elsevier, 2019, pp. 391–406. DOI: [10.1016/B978-0-12-805052-1.00024-3](https://doi.org/10.1016/B978-0-12-805052-1.00024-3).
- 3 P. Burgherr, In-depth analysis of accidental oil spills from tankers in the context of global spill trends from all sources, *J. Hazard. Mater.*, 2007, **140**, 245–256, DOI: [10.1016/j.jhazmat.2006.07.030](https://doi.org/10.1016/j.jhazmat.2006.07.030).
- 4 S. M. J. Baban and S. Jules-Moore, An Evaluation of Water Circulation and Contaminant Transport Models for the Intra-American Seas, *West Indian Journal of Engineering*, 2005, **27**(2), 1–27.
- 5 C. Harris, The Sea Empress Incident: Overview And Response At Sea, in *International Oil Spill Conference*



*Proceedings*, 1997, vol. 1997, pp. 177–184. DOI: [10.7901/2169-3358-1997-1-177](https://doi.org/10.7901/2169-3358-1997-1-177).

6 Q. Zheng, Q. Zhao, W. Nan and C. Li, Oil spill in the Gulf of Mexico and spiral vortex, *Acta Oceanol. Sin.*, 2010, **29**, 1–2, DOI: [10.1007/s13131-010-0044-9](https://doi.org/10.1007/s13131-010-0044-9).

7 A. Zafirakou, S. Themeli, E. Tsami and G. Aretoulis, Multi-Criteria Analysis of Different Approaches to Protect the Marine and Coastal Environment from Oil Spills, *J. Mar. Sci. Eng.*, 2018, **6**, 125, DOI: [10.3390/jmse6040125](https://doi.org/10.3390/jmse6040125).

8 S. Mishra, G. Chauhan, S. Verma and U. Singh, The emergence of nanotechnology in mitigating petroleum oil spills, *Mar. Pollut. Bull.*, 2022, **178**, 113609, DOI: [10.1016/j.marpolbul.2022.113609](https://doi.org/10.1016/j.marpolbul.2022.113609).

9 M. Baniasadi and S. M. Mousavi, A Comprehensive Review on the Bioremediation of Oil Spills, in *Microbial Action on Hydrocarbons*, Springer Singapore, Singapore, 2018, pp. 223–254. DOI: [10.1007/978-981-13-1840-5\\_10](https://doi.org/10.1007/978-981-13-1840-5_10).

10 A. C. S. V. de Negreiros, I. D. Lins, C. B. S. Maior and M. J. d. C. Moura, Oil spills characteristics, detection, and recovery methods: A systematic risk-based view, *J. Loss Prev. Process Ind.*, 2022, **80**, 104912, DOI: [10.1016/j.jlp.2022.104912](https://doi.org/10.1016/j.jlp.2022.104912).

11 R. C. Prince, T. J. Amande and T. J. McGenity, Prokaryotic Hydrocarbon Degraders, in *Taxonomy, Genomics and Ecophysiology of Hydrocarbon-Degrading Microbes*, Springer International Publishing, Cham, 2019, pp. 1–39. DOI: [10.1007/978-3-030-14796-9\\_15](https://doi.org/10.1007/978-3-030-14796-9_15).

12 R. C. Prince and J. D. Butler, A protocol for assessing the effectiveness of oil spill dispersants in stimulating the biodegradation of oil, *Environ. Sci. Pollut. Res.*, 2014, **21**, 9506–9510, DOI: [10.1007/s11356-013-2053-7](https://doi.org/10.1007/s11356-013-2053-7).

13 R. P. J. Swannell and F. Daniel, Effect of Dispersants on Oil Biodegradation Under Simulated Marine Conditions, in *International Oil Spill Conference Proceedings*, 1999, vol. 1999, pp. 169–176. DOI: [10.7901/2169-3358-1999-1-169](https://doi.org/10.7901/2169-3358-1999-1-169).

14 R. M. Atlas, Microbial hydrocarbon degradation-bioremediation of oil spills, *J. Chem. Technol. Biotechnol.*, 2007, **52**, 149–156, DOI: [10.1002/jctb.280520202](https://doi.org/10.1002/jctb.280520202).

15 A. Tuan Hoang, V. Viet Pham and D. Nam Nguyen, *A Report of Oil Spill Recovery Technologies*, 2018. <https://www.ripulation.com>.

16 X. Wang and R. Bartha, Effects of bioremediation on residues, activity and toxicity in soil contaminated by fuel spills, *Soil Biol. Biochem.*, 1990, **22**, 501–505, DOI: [10.1016/0038-0717\(90\)90185-3](https://doi.org/10.1016/0038-0717(90)90185-3).

17 P. J. Sheppard, K. L. Simons, E. M. Adetutu, K. K. Kadali, A. L. Juhasz, M. Manefield, P. M. Sarma, B. Lal and A. S. Ball, The application of a carrier-based bioremediation strategy for marine oil spills, *Mar. Pollut. Bull.*, 2014, **84**, 339–346, DOI: [10.1016/j.marpolbul.2014.03.044](https://doi.org/10.1016/j.marpolbul.2014.03.044).

18 A. A. Allen and R. J. Ferek, Advantages And Disadvantages Of Burning Spilled Oil, in *International Oil Spill Conference Proceedings*, 1993, vol. 1993, pp. 765–772. DOI: [10.7901/2169-3358-1993-1-765](https://doi.org/10.7901/2169-3358-1993-1-765).

19 J. V. Mullin and M. A. Champ, Introduction/Overview to In Situ Burning of Oil Spills, *Spill Sci. Technol. Bull.*, 2003, **8**, 323–330, DOI: [10.1016/S1353-2561\(03\)00076-8](https://doi.org/10.1016/S1353-2561(03)00076-8).

20 R. Lazès, A study on the effects of oil fires on fire booms employed during the in situ burning of oil, *Spill Sci. Technol. Bull.*, 1994, **1**, 85–87, DOI: [10.1016/1353-2561\(94\)90011-6](https://doi.org/10.1016/1353-2561(94)90011-6).

21 P. E. Ndimele, A. O. Saba, D. O. Ojo, C. C. Ndimele, M. A. Anetekhai and E. S. Erondu, Remediation of Crude Oil Spillage, in *The Political Ecology of Oil and Gas Activities in the Nigerian Aquatic Ecosystem*, Elsevier, 2018, pp. 369–384. DOI: [10.1016/B978-0-12-809399-3.00024-0](https://doi.org/10.1016/B978-0-12-809399-3.00024-0).

22 F. Muttin, R. Campbell, A. Ouansafi and Y. Benelmostafa, *Numerical modelling and experimentation of oil-spill curtain booms: Application to a harbor*, 2017, p. 020104. DOI: [10.1063/1.4972696](https://doi.org/10.1063/1.4972696).

23 A. O. Ifelebuegu and A. Johnson, Nonconventional low-cost cellulose- and keratin-based biopolymeric sorbents for oil/water separation and spill cleanup: A review, *Crit. Rev. Environ. Sci. Technol.*, 2017, **47**, 964–1001, DOI: [10.1080/10643389.2017.1318620](https://doi.org/10.1080/10643389.2017.1318620).

24 A. Bayat, S. F. Aghamiri, A. Moheb and G. R. Vakili-Nezaad, Oil Spill Cleanup from Sea Water by Sorbent Materials, *Chem. Eng. Technol.*, 2005, **28**, 1525–1528, DOI: [10.1002/ceat.200407083](https://doi.org/10.1002/ceat.200407083).

25 J. Ge, H.-Y. Zhao, H.-W. Zhu, J. Huang, L.-A. Shi and S.-H. Yu, Advanced Sorbents for Oil-Spill Cleanup: Recent Advances and Future Perspectives, *Adv. Mater.*, 2016, **28**, 10459–10490, DOI: [10.1002/adma.201601812](https://doi.org/10.1002/adma.201601812).

26 D. Loche, L. Malfatti, D. Carboni, V. Alzari, A. Mariani and M. F. Casula, Incorporation of graphene into silica-based aerogels and application for water remediation, *RSC Adv.*, 2016, **6**, 66516–66523, DOI: [10.1039/C6RA09618B](https://doi.org/10.1039/C6RA09618B).

27 Q. F. Wei, R. R. Mather, A. F. Fotheringham and R. D. Yang, Evaluation of nonwoven polypropylene oil sorbents in marine oil-spill recovery, *Mar. Pollut. Bull.*, 2003, **46**, 780–783, DOI: [10.1016/S0025-326X\(03\)00042-0](https://doi.org/10.1016/S0025-326X(03)00042-0).

28 J. Wang, Y. Zheng and A. Wang, Superhydrophobic kapok fiber oil-absorbent: Preparation and high oil absorbency, *Chem. Eng. J.*, 2012, **213**, 1–7, DOI: [10.1016/j.cej.2012.09.116](https://doi.org/10.1016/j.cej.2012.09.116).

29 R. Lin, A. Li, T. Zheng, L. Lu and Y. Cao, Hydrophobic and flexible cellulose aerogel as an efficient, green and reusable oil sorbent, *RSC Adv.*, 2015, **5**, 82027–82033, DOI: [10.1039/C5RA15194E](https://doi.org/10.1039/C5RA15194E).

30 Z. Rahmani, M. T. Samadi, A. Kazemi, A. M. Rashidi and A. R. Rahmani, Nanoporous graphene and graphene oxide-coated polyurethane sponge as a highly efficient, superhydrophobic, and reusable oil spill absorbent, *J. Environ. Chem. Eng.*, 2017, **5**, 5025–5032, DOI: [10.1016/j.jece.2017.09.028](https://doi.org/10.1016/j.jece.2017.09.028).

31 J. A. Pavlova, A. V. Ivanov, N. V. Maksimova, K. V. Pokholok, A. V. Vasiliev, A. P. Malakho and V. V. Avdeev, Two-stage preparation of magnetic sorbent based on exfoliated graphite with ferrite phases for sorption of oil and liquid hydrocarbons from the water surface, *J. Phys. Chem. Solids*, 2018, **116**, 299–305, DOI: [10.1016/j.jpcs.2018.01.044](https://doi.org/10.1016/j.jpcs.2018.01.044).

32 H. Liu and Y. Kang, Superhydrophobic and superoleophilic modified EPDM foam rubber fabricated by a facile



approach for oil/water separation, *Appl. Surf. Sci.*, 2018, **451**, 223–231, DOI: [10.1016/j.apsusc.2018.04.179](https://doi.org/10.1016/j.apsusc.2018.04.179).

33 Q. Ma, H. Cheng, A. G. Fane, R. Wang and H. Zhang, Recent Development of Advanced Materials with Special Wettability for Selective Oil/Water Separation, *Small*, 2016, **12**, 2186–2202, DOI: [10.1002/smll.201503685](https://doi.org/10.1002/smll.201503685).

34 L. Yan, Q. Li, X. Wang, H. Song, H. Chi, Y. Qiao, Y. Zhai and D. Liu, Synthesis and Absorption Performance of Acrylic Ester and Hollow Fiber MgO Nanoparticle Resin Composite, *Polym. Plast. Technol. Eng.*, 2017, **56**, 1857–1865, DOI: [10.1080/03602559.2017.1295310](https://doi.org/10.1080/03602559.2017.1295310).

35 C. Lin, Y.-J. Hong and A. H. Hu, Using a composite material containing waste tire powder and polypropylene fiber cut end to recover spilled oil, *Waste Manage.*, 2010, **30**, 263–267, DOI: [10.1016/j.wasman.2009.03.001](https://doi.org/10.1016/j.wasman.2009.03.001).

36 W. Zhai, J. Jiang and C. B. Park, *A review on physical foaming of thermoplastic and vulcanized elastomers*, 2021, DOI: [10.1080/15583724.2021.1897996](https://doi.org/10.1080/15583724.2021.1897996).

37 G. Chen, A. Gupta and T. H. Mekonnen, Effects of wood fiber loading, silane modification and crosslinking on the thermomechanical properties and thermal conductivity of EPDM biocomposite foams, *Ind. Crops Prod.*, 2023, **200**, 116911, DOI: [10.1016/j.indcrop.2023.116911](https://doi.org/10.1016/j.indcrop.2023.116911).

38 G. Chen and H. Luo, Acoustic emission of the fracture behaviors of epoxy foam composites reinforced by bamboo fibers, *Eur. J. Mech. - A/Solids*, 2023, **99**, 104911, DOI: [10.1016/j.euromechsol.2023.104911](https://doi.org/10.1016/j.euromechsol.2023.104911).

39 F. Rahimidehgolan and W. Altenhof, Compressive behavior and deformation mechanisms of rigid polymeric foams: A review, *Composites, Part B*, 2023, **253**, 110513, DOI: [10.1016/j.compositesb.2023.110513](https://doi.org/10.1016/j.compositesb.2023.110513).

40 J. Saleem, M. Adil Riaz and M. Gordon, Oil sorbents from plastic wastes and polymers: A review, *J. Hazard. Mater.*, 2018, **341**, 424–437, DOI: [10.1016/j.jhazmat.2017.07.072](https://doi.org/10.1016/j.jhazmat.2017.07.072).

41 H. T. T. Duong and R. P. Burford, Effect of foam density, oil viscosity, and temperature on oil sorption behavior of polyurethane, *J. Appl. Polym. Sci.*, 2006, **99**, 360–367, DOI: [10.1002/app.22426](https://doi.org/10.1002/app.22426).

42 R. J. Spontak and N. P. Patel, Thermoplastic elastomers: fundamentals and applications, *Curr. Opin. Colloid Interface Sci.*, 2000, **5**, 333–340, DOI: [10.1016/S1359-0294\(00\)00070-4](https://doi.org/10.1016/S1359-0294(00)00070-4).

43 L. Fan, R. Wang, Q. Zhang, S. Liu, R. He, R. Zhang, M. Shen, X. Xiang and Y. Zhou, *In situ* self-foaming preparation of hydrophobic polyurethane foams for oil/water separation, *New J. Chem.*, 2021, **45**, 13902–13908, DOI: [10.1039/DONJ05208F](https://doi.org/10.1039/DONJ05208F).

44 X. Qin, B. Wang, X. Zhang, Y. Shi, S. Ye, Y. Feng, C. Liu and C. Shen, Superelastic and Durable Hierarchical Porous Thermoplastic Polyurethane Monolith with Excellent Hydrophobicity for Highly Efficient Oil/Water Separation, *Ind. Eng. Chem. Res.*, 2019, **58**, 20291–20299, DOI: [10.1021/acs.iecr.9b03717](https://doi.org/10.1021/acs.iecr.9b03717).

45 Z. C. Ng, R. A. Roslan, W. J. Lau, M. Gürsoy, M. Karaman, N. Jullok and A. F. Ismail, A Green Approach to Modify Surface Properties of Polyurethane Foam for Enhanced Oil Absorption, *Polymers*, 2020, **12**, 1883, DOI: [10.3390/polym12091883](https://doi.org/10.3390/polym12091883).

46 H. Ding, W. Yang, W. Yu, T. Liu, H. Wang, P. Xu, L. Lin and P. Ma, High hydrophobic poly(lactic acid) foams impregnating one-step Si-F modified lignin nanoparticles for oil/organic solvents absorption, *Compos. Commun.*, 2021, **25**, 100730, DOI: [10.1016/j.coco.2021.100730](https://doi.org/10.1016/j.coco.2021.100730).

47 Y. Wang, H. Yang, Z. Chen, N. Chen, X. Pang, L. Zhang, T. Minari, X. Liu, H. Liu and J. Chen, Recyclable Oil-Absorption Foams via Secondary Phase Separation, *ACS Sustainable Chem. Eng.*, 2018, **6**, 13834–13843, DOI: [10.1021/acssuschemeng.8b01950](https://doi.org/10.1021/acssuschemeng.8b01950).

48 E. Lopez-Gonzalez, C. Saiz-Arroyo and M. A. Rodriguez-Perez, Low-density open-cell flexible polyolefin foams as efficient materials for oil absorption: influence of tortuosity on oil absorption, *Int. J. Environ. Sci. Technol.*, 2020, **17**, 1663–1674, DOI: [10.1007/s13762-019-02576-0](https://doi.org/10.1007/s13762-019-02576-0).

49 Y. C. López, G. A. Ortega and E. Reguera, Applications of engineered magnetite nanoparticles for water pollutants removal, in *Green Sustainable Process for Chemical and Environmental Engineering and Science*, Elsevier, 2023, pp. 23–68. DOI: [10.1016/B978-0-443-18746-9.00008-X](https://doi.org/10.1016/B978-0-443-18746-9.00008-X).

50 S. A. Rackley, Units, Acronyms, and Glossary, in *Carbon Capture and Storage*, Elsevier, 2010, pp. 353–372. DOI: [10.1016/B978-1-85617-636-1.00017-1](https://doi.org/10.1016/B978-1-85617-636-1.00017-1).

51 H. Liu, W. Zhai and C. B. Park, Biomimetic hydrophobic plastic foams with aligned channels for rapid oil absorption, *J. Hazard. Mater.*, 2022, **437**, 129346, DOI: [10.1016/j.jhazmat.2022.129346](https://doi.org/10.1016/j.jhazmat.2022.129346).

52 I. Karakutuk and O. Okay, Macroporous rubber gels as reusable sorbents for the removal of oil from surface waters, *React. Funct. Polym.*, 2010, **70**, 585–595, DOI: [10.1016/j.reactfunctpolym.2010.05.015](https://doi.org/10.1016/j.reactfunctpolym.2010.05.015).

53 M. Nandi, S. Banerjee and P. De, Stearyl-appended pendant amino acid-based hyperbranched polymers for selective gelation of oil from oil/water mixtures, *Polym. Chem.*, 2019, **10**, 1795–1805, DOI: [10.1039/C9PY00105K](https://doi.org/10.1039/C9PY00105K).

54 A. Prathap and K. M. Sureshan, Sugar-Based Organogelators for Various Applications, *Langmuir*, 2019, **35**, 6005–6014, DOI: [10.1021/acs.langmuir.9b00506](https://doi.org/10.1021/acs.langmuir.9b00506).

55 A. Pal, Y. K. Ghosh and S. Bhattacharya, Molecular mechanism of physical gelation of hydrocarbons by fatty acid amides of natural amino acids, *Tetrahedron*, 2007, **63**, 7334–7348, DOI: [10.1016/j.tet.2007.05.028](https://doi.org/10.1016/j.tet.2007.05.028).

56 S. R. Churipard, K. S. Kanakikodi, D. A. Rambhia, C. S. K. Raju, A. B. Halgeri, N. V. Choudary, G. S. Ganesh, R. Ravishankar and S. P. Maradur, Porous polydivinylbenzene (PDVB) as an efficient adsorbent for hydrocarbons: Effect of porogens on adsorption capacity, *Chem. Eng. J.*, 2020, **380**, 122481, DOI: [10.1016/j.cej.2019.122481](https://doi.org/10.1016/j.cej.2019.122481).

57 K. T. Kim, C. Park, G. W. M. Vandermeulen, D. A. Rider, C. Kim, M. A. Winnik and I. Manners, Gelation of Helical Polypeptide-Random Coil Diblock Copolymers by a Nanoribbon Mechanism, *Angew. Chem., Int. Ed.*, 2005, **44**, 7964–7968, DOI: [10.1002/anie.200502809](https://doi.org/10.1002/anie.200502809).



58 H. Lee, B. M. Trinh and T. H. Mekonnen, Fabrication of Triblock Elastomer Foams and Gelation Studies for Oil Spill Remediation, *Macromol. Rapid Commun.*, 2024, **45**, 2400232, DOI: [10.1002/marc.202400232](https://doi.org/10.1002/marc.202400232).

59 L. Gong, S. Kyriakides and W.-Y. Jang, Compressive response of open-cell foams. Part I: Morphology and elastic properties, *Int. J. Solids Struct.*, 2005, **42**, 1355–1379, DOI: [10.1016/j.ijсолstr.2004.07.023](https://doi.org/10.1016/j.ijсолstr.2004.07.023).

60 J. L. Ruiz-Herrero, M. A. Rodríguez-Pérez and J. A. de Saja, Effective diffusion coefficient for the gas contained in closed cell polyethylene-based foams subjected to compressive creep tests, *Polymer*, 2005, **46**, 3105–3110, DOI: [10.1016/j.polymer.2005.01.093](https://doi.org/10.1016/j.polymer.2005.01.093).

61 J. A. Reglero Ruiz, P. Viot and M. Dumon, Microcellular foaming of polymethylmethacrylate in a batch supercritical CO<sub>2</sub> process: Effect of microstructure on compression behavior, *J. Appl. Polym. Sci.*, 2010, **118**, 320–331, DOI: [10.1002/app.32351](https://doi.org/10.1002/app.32351).

62 B. Xiang, Y. Jia, Y. Lei, F. Zhang, J. He, T. Liu and S. Luo, Mechanical properties of microcellular and nanocellular silicone rubber foams obtained by supercritical carbon dioxide, *Polym. J.*, 2019, **51**, 559–568, DOI: [10.1038/s41428-019-0175-6](https://doi.org/10.1038/s41428-019-0175-6).

63 S.-K. Yeh, Z.-E. Liao, K.-C. Wang, Y.-T. Ho, V. Kurniawan, P.-C. Tseng and T.-W. Tseng, Effect of molecular weight to the structure of nanocellular foams: Phase separation approach, *Polymer*, 2020, **191**, 122275, DOI: [10.1016/j.polymer.2020.122275](https://doi.org/10.1016/j.polymer.2020.122275).

64 D. Eaves, *Handbook of Polymer Foams*, Rapra Technology Ltd, 2004.

65 P. Stevenson, Inter-bubble gas diffusion in liquid foam, *Curr. Opin. Colloid Interface Sci.*, 2010, **15**, 374–381, DOI: [10.1016/j.cocis.2010.05.010](https://doi.org/10.1016/j.cocis.2010.05.010).

66 M. Nofar, J. Utz, N. Geis, V. Altstädt and H. Ruckdäschel, Foam 3D Printing of Thermoplastics: A Symbiosis of Additive Manufacturing and Foaming Technology, *Adv. Sci.*, 2022, **9**, 2105701, DOI: [10.1002/advs.202105701](https://doi.org/10.1002/advs.202105701).

67 N. S. Ramesh, D. H. Rasmussen and G. A. Campbell, Numerical and experimental studies of bubble growth during the microcellular foaming process, *Polym. Eng. Sci.*, 1991, **31**, 1657–1664, DOI: [10.1002/pen.760312305](https://doi.org/10.1002/pen.760312305).

68 R. Höfer, Processing and Performance Additives for Plastics, in *Polymer Science: A Comprehensive Reference*, Elsevier, 2012, pp. 369–381. DOI: [10.1016/B978-0-444-53349-4.00272-7](https://doi.org/10.1016/B978-0-444-53349-4.00272-7).

69 J. Štěpek and H. Daoust, Chemical and Physical Blowing Agents, in *Additives for Plastics*, Springer, New York, New York, NY, 1983, pp. 112–123. DOI: [10.1007/978-1-4419-8481-4\\_7](https://doi.org/10.1007/978-1-4419-8481-4_7).

70 L. Wang, Y. Hikima, M. Ohshima, A. Yusa, S. Yamamoto and H. Goto, Development of a Simplified Foam Injection Molding Technique and Its Application to the Production of High Void Fraction Polypropylene Foams, *Ind. Eng. Chem. Res.*, 2017, **56**, 13734–13742, DOI: [10.1021/acs.iecr.7b03382](https://doi.org/10.1021/acs.iecr.7b03382).

71 S. K. Goel and E. J. Beckman, Generation of microcellular polymeric foams using supercritical carbon dioxide. I: Effect of pressure and temperature on nucleation, *Polym. Eng. Sci.*, 1994, **34**, 1137–1147, DOI: [10.1002/pen.760341407](https://doi.org/10.1002/pen.760341407).

72 Y. Zhou, Y. Tian and X. Peng, Applications and Challenges of Supercritical Foaming Technology, *Polymers*, 2023, **15**, 402, DOI: [10.3390/polym15020402](https://doi.org/10.3390/polym15020402).

73 Z. Xu, G. Wang, J. Zhao, A. Zhang, G. Dong and G. Zhao, Anti-shrinkage, high-elastic, and strong thermoplastic polyester elastomer foams fabricated by microcellular foaming with CO<sub>2</sub> & N<sub>2</sub> as blowing agents, *J. CO<sub>2</sub> Util.*, 2022, **62**, 102076, DOI: [10.1016/j.jcou.2022.102076](https://doi.org/10.1016/j.jcou.2022.102076).

74 J. Lu, H. Zhang, Y. Chen, Y. Ge and T. Liu, Effect of chain relaxation on the shrinkage behavior of TPEE foams fabricated with supercritical CO<sub>2</sub>, *Polymer*, 2022, **256**, 125262, DOI: [10.1016/j.polymer.2022.125262](https://doi.org/10.1016/j.polymer.2022.125262).

75 J.-H. Kim, K.-C. Choi and J.-M. Yoon, *The Foaming Characteristics and Physical Properties of Natural Rubber Foams: Effects of Carbon Black Content and Foaming Pressure*, 2006.

76 M. Amran, Y. Huei Lee, N. Vatin, R. Fediuk, S. Poi-Ngian, Y. Yong Lee and G. Murali, Design Efficiency, Characteristics, and Utilization of Reinforced Foamed Concrete: A Review, *Crystals*, 2020, **10**, 948, DOI: [10.3390/crys10100948](https://doi.org/10.3390/crys10100948).

77 J. A. Kosin, J. M. Huber and C. L. Tice, Novel Endothermic Chemical Foaming Agents and Their Applications, *Journal of Cellular Plastics*, 1990, **26**(4), 332–344.

78 R. L. Heck, A Review of Commercially Used Chemical Foaming Agents for Thermoplastic Foams, *J. Vinyl Addit. Technol.*, 1998, **4**, 113–116, DOI: [10.1002/vnl.10027](https://doi.org/10.1002/vnl.10027).

79 F.-L. Jin, M. Zhao, M. Park and S.-J. Park, Recent Trends of Foaming in Polymer Processing: A Review, *Polymers*, 2019, **11**(6), 953, DOI: [10.3390/polym11060953](https://doi.org/10.3390/polym11060953).

80 C. B. Park and L. K. Cheung, A study of cell nucleation in the extrusion of polypropylene foams, *Polym. Eng. Sci.*, 1997, **37**, 1–10, DOI: [10.1002/pen.11639](https://doi.org/10.1002/pen.11639).

81 B. Del Saz-Orozco, M. Oliet, M. V. Alonso, E. Rojo and F. Rodríguez, Formulation optimization of unreinforced and lignin nanoparticle-reinforced phenolic foams using an analysis of variance approach, *Compos. Sci. Technol.*, 2012, **72**, 667–674, DOI: [10.1016/j.compscitech.2012.01.013](https://doi.org/10.1016/j.compscitech.2012.01.013).

82 G. Wypych, Dispersion And Solubility Of Blowing Agents, in *Handbook of Foaming and Blowing Agents*, Elsevier, 2017, pp. 45–49. DOI: [10.1016/B978-1-895198-99-7.50006-4](https://doi.org/10.1016/B978-1-895198-99-7.50006-4).

83 W. L. Kong, J. B. Bao, J. Wang, G. H. Hu, Y. Xu and L. Zhao, Preparation of open-cell polymer foams by CO<sub>2</sub> assisted foaming of polymer blends, *Polymer*, 2016, **90**, 331–341, DOI: [10.1016/J.POLYMER.2016.03.035](https://doi.org/10.1016/J.POLYMER.2016.03.035).

84 Y. Pang, S. Wang, M. Wu, W. Liu, F. Wu, P. C. Lee and W. Zheng, Kinetics study of oil sorption with open-cell polypropylene/polyolefin elastomer blend foams prepared via continuous extrusion foaming, *Polym. Adv. Technol.*, 2018, **29**, 1313–1321, DOI: [10.1002/pat.4243](https://doi.org/10.1002/pat.4243).

85 C. Okoliecha, D. Raps, K. Subramaniam and V. Altstädt, Microcellular to nanocellular polymer foams: Progress (2004–2015) and future directions – A review, *Eur. Polym. J.*, 2015, **72**, 1–18, DOI: [10.1016/j.eurpolymj.2015.09.014](https://doi.org/10.1016/j.eurpolymj.2015.09.014).

J., 2015, 73, 500–519, DOI: [10.1016/j.eurpolymj.2015.11.001](https://doi.org/10.1016/j.eurpolymj.2015.11.001).

86 M. Sauceau, J. Fages, A. Common, C. Nikitine and E. Rodier, New challenges in polymer foaming: A review of extrusion processes assisted by supercritical carbon dioxide, *Prog. Polym. Sci.*, 2011, 36, 749–766, DOI: [10.1016/j.progpolymsci.2010.12.004](https://doi.org/10.1016/j.progpolymsci.2010.12.004).

87 G. Wang, G. Zhao, L. Zhang, Y. Mu and C. B. Park, Lightweight and tough nanocellular PP/PTFE nanocomposite foams with defect-free surfaces obtained using in situ nanofibrillation and nanocellular injection molding, *Chem. Eng. J.*, 2018, 350, 1–11, DOI: [10.1016/j.cej.2018.05.161](https://doi.org/10.1016/j.cej.2018.05.161).

88 Y. Liu, G. Huang, C. Gao, L. Zhang, M. Chen, X. Xu, J. Gao, C. Pan, N. Yang and Y. Liu, Biodegradable polylactic acid porous monoliths as effective oil sorbents, *Compos. Sci. Technol.*, 2015, 118, 9–15, DOI: [10.1016/j.compscitech.2015.08.005](https://doi.org/10.1016/j.compscitech.2015.08.005).

89 W. Xiao, B. Niu, M. Yu, C. Sun, L. Wang, L. Zhou and Y. Zheng, Fabrication of foam-like oil sorbent from poly-lactic acid and Calotropis gigantea fiber for effective oil absorption, *J. Cleaner Prod.*, 2021, 278, 123507, DOI: [10.1016/j.jclepro.2020.123507](https://doi.org/10.1016/j.jclepro.2020.123507).

90 C. Brondi, E. Di Maio, L. Bertuccelli, V. Parenti and T. Mosciatti, Competing bubble formation mechanisms in rigid polyurethane foaming, *Polymer*, 2021, 228, 123877, DOI: [10.1016/j.polymer.2021.123877](https://doi.org/10.1016/j.polymer.2021.123877).

91 A. Rizvi, R. K. M. Chu, J. H. Lee and C. B. Park, Superhydrophobic and Oleophilic Open-Cell Foams from Fibrillar Blends of Polypropylene and Polytetrafluoroethylene, *ACS Appl. Mater. Interfaces*, 2014, 6, 21131–21140, DOI: [10.1021/am506006v](https://doi.org/10.1021/am506006v).

92 G. Wang, G. Wan, J. Chai, B. Li, G. Zhao, Y. Mu and C. B. Park, Structure-tunable thermoplastic polyurethane foams fabricated by supercritical carbon dioxide foaming and their compressive mechanical properties, *J. Supercrit. Fluids*, 2019, 149, 127–137, DOI: [10.1016/j.supflu.2019.04.004](https://doi.org/10.1016/j.supflu.2019.04.004).

93 Y.-M. Corre, A. Maazouz, J. Duchet and J. Reignier, Batch foaming of chain extended PLA with supercritical CO<sub>2</sub>: Influence of the rheological properties and the process parameters on the cellular structure, *J. Supercrit. Fluids*, 2011, 58, 177–188, DOI: [10.1016/j.supflu.2011.03.006](https://doi.org/10.1016/j.supflu.2011.03.006).

94 S. Yeh, Y. Tsai, K. F. Gebremedhin, T. Chien, R. Chang and K. Tung, Preparation of polypropylene/high-melt-strength PP open-cell foam for oil absorption, *Polym. Eng. Sci.*, 2021, 61, 1139–1149, DOI: [10.1002/pen.25654](https://doi.org/10.1002/pen.25654).

95 C. Hopmann, F. Lemke and Q. Nguyen Binh, Foaming of EPDM with water as blowing agent in injection molding, *J. Appl. Polym. Sci.*, 2016, 133, 43613, DOI: [10.1002/app.43613](https://doi.org/10.1002/app.43613).

96 H. A. Kharbas, J. D. McNulty, T. Ellingham, C. Thompson, M. Manitiu, G. Scholz and L.-S. Turng, Comparative study of chemical and physical foaming methods for injection-molded thermoplastic polyurethane, *J. Cell. Plast.*, 2017, 53, 373–388, DOI: [10.1177/0021955X16652107](https://doi.org/10.1177/0021955X16652107).

97 J. Zhao, G. Wang, Z. Chen, Y. Huang, C. Wang, A. Zhang and C. B. Park, Microcellular injection molded outstanding oleophilic and sound-insulating PP/PTFE nanocomposite foam, *Composites, Part B*, 2021, 215, 108786, DOI: [10.1016/j.compositesb.2021.108786](https://doi.org/10.1016/j.compositesb.2021.108786).

98 A. Serrano, A. M. Borreguero, J. Catalá, J. F. Rodríguez and M. Carmona, Effect of Foaming Formulation and Operating Pressure on Thermoregulating Polyurethane Foams, *Polymers*, 2021, 13, 2328, DOI: [10.3390/polym13142328](https://doi.org/10.3390/polym13142328).

99 H. Lee, A. Gupta and T. H. Mekonnen, Fabrication of Triblock Elastomer Foams for Oil Absorption Applications: Effects of Crosslinking, Composition, and Rheology Factors, *ACS Appl. Polym. Mater.*, 2023, 5(7), 5026–5027, DOI: [10.1021/acsapm.3c00567](https://doi.org/10.1021/acsapm.3c00567).

100 W. Abdelwahed, G. Degobert, S. Stainmesse and H. Fessi, Freeze-drying of nanoparticles: Formulation, process and storage considerations, *Adv. Drug Delivery Rev.*, 2006, 58, 1688–1713, DOI: [10.1016/j.addr.2006.09.017](https://doi.org/10.1016/j.addr.2006.09.017).

101 X. Wang, Y. Pan, X. Liu, H. Liu, N. Li, C. Liu, D. W. Schubert and C. Shen, Facile Fabrication of Superhydrophobic and Eco-Friendly Poly(lactic acid) Foam for Oil–Water Separation via Skin Peeling, *ACS Appl. Mater. Interfaces*, 2019, 11, 14362–14367, DOI: [10.1021/acsami.9b02285](https://doi.org/10.1021/acsami.9b02285).

102 K. Ashida, *Polyurethane and Related Foams Chemistry and Technology*, CRC Press, 2006.

103 . Polymer Foam Market Size, Share & Trends Analysis Report By Type (Polystyrene, Polyurethane, Polyolefin, Melamine, Phenolic, PVC), By Application, By Region, And Segment Forecasts, 2022–2030, San Francisco, CA, United States, 2020.

104 B. R. Thompson, T. S. Horozov, S. D. Stoyanov and V. N. Paunov, Hierarchically structured composites and porous materials from soft templates: fabrication and applications, *J. Mater. Chem. A*, 2019, 7, 8030–8049, DOI: [10.1039/C8TA09750J](https://doi.org/10.1039/C8TA09750J).

105 M. Li, X. Dai, W. Gao and H. Bai, Ice-Templated Fabrication of Porous Materials with Bioinspired Architecture and Functionality, *Acc. Mater. Res.*, 2022, 3, 1173–1185, DOI: [10.1021/accountsmr.2c00169](https://doi.org/10.1021/accountsmr.2c00169).

106 S. Zheng, Y. Wang, X. Wang and H. Lu, Ingenious construction of three-dimensional porous carbon foams and their polymer composites using template-based strategies, *Polym. Test.*, 2024, 135, 108469, DOI: [10.1016/j.polymertesting.2024.108469](https://doi.org/10.1016/j.polymertesting.2024.108469).

107 L. Kong, Y. Li, F. Qiu, T. Zhang, Q. Guo, X. Zhang, D. Yang, J. Xu and M. Xue, Fabrication of hydrophobic and oleophilic polyurethane foam sponge modified with hydrophobic Al<sub>2</sub>O<sub>3</sub> for oil/water separation, *J. Ind. Eng. Chem.*, 2018, 58, 369–375, DOI: [10.1016/j.jiec.2017.09.050](https://doi.org/10.1016/j.jiec.2017.09.050).

108 S. Xiong, Y. Yang, Z. Zhong and Y. Wang, One-Step Synthesis of Carbon-Hybridized ZnO on Polymeric Foams by Atomic Layer Deposition for Efficient Absorption of Oils from Water, *Ind. Eng. Chem. Res.*, 2018, 57, 1269–1276, DOI: [10.1021/acs.iecr.7b03939](https://doi.org/10.1021/acs.iecr.7b03939).

109 D. Yuan, T. Zhang, Q. Guo, F. Qiu, D. Yang and Z. Ou, A novel hierarchical hollow  $\text{SiO}_2$  @ $\text{MnO}_2$  cubes reinforced elastic polyurethane foam for the highly efficient removal of oil from water, *Chem. Eng. J.*, 2017, **327**, 539–547, DOI: [10.1016/j.cej.2017.06.144](https://doi.org/10.1016/j.cej.2017.06.144).

110 H. Li, L. Liu and F. Yang, Hydrophobic modification of polyurethane foam for oil spill cleanup, *Mar. Pollut. Bull.*, 2012, **64**, 1648–1653, DOI: [10.1016/j.marpolbul.2012.05.039](https://doi.org/10.1016/j.marpolbul.2012.05.039).

111 A. Visco, A. Quattrocchi, D. Nocita, R. Montanini and A. Pistone, Polyurethane Foams Loaded with Carbon Nanofibers for Oil Spill Recovery: Mechanical Properties under Fatigue Conditions and Selective Absorption in Oil/Water Mixtures, *Nanomaterials*, 2021, **11**, 735, DOI: [10.3390/nano11030735](https://doi.org/10.3390/nano11030735).

112 X. He, S. Lin, X. Feng and Q. Pan, Synthesis and Modification of Polyurethane Foam Doped with Multi-walled Carbon Nanotubes for Cleaning up Spilled Oil from Water, *J. Polym. Environ.*, 2021, **29**, 1271–1286, DOI: [10.1007/s10924-020-01942-1](https://doi.org/10.1007/s10924-020-01942-1).

113 T. Zhang, B. Gu, F. Qiu, X. Peng, X. Yue and D. Yang, Preparation of Carbon Nanotubes/Polyurethane Hybrids as a Synergistic Absorbent for Efficient Oil/Water Separation, *Fibers Polym.*, 2018, **19**, 2195–2202, DOI: [10.1007/s12221-018-8399-1](https://doi.org/10.1007/s12221-018-8399-1).

114 A. Keshavarz, H. Zilouei, A. Abdolmaleki and A. Asadinezhad, Enhancing oil removal from water by immobilizing multi-wall carbon nanotubes on the surface of polyurethane foam, *J. Environ. Manage.*, 2015, **157**, 279–286, DOI: [10.1016/j.jenvman.2015.04.030](https://doi.org/10.1016/j.jenvman.2015.04.030).

115 M. Anju and N. K. Renuka, Magnetically actuated graphene coated polyurethane foam as potential sorbent for oils and organics, *Arabian J. Chem.*, 2020, **13**, 1752–1762, DOI: [10.1016/j.arabjc.2018.01.012](https://doi.org/10.1016/j.arabjc.2018.01.012).

116 Z. Lv, N. Zhao, Z. Wu, C. Zhu and Q. Li, Fabrication of Novel Open-Cell Foams of Poly( $\epsilon$ -caprolactone)/Poly(lactic acid) Blends for Tissue-Engineering Scaffolds, *Ind. Eng. Chem. Res.*, 2018, **57**, 12951–12958, DOI: [10.1021/acs.iecr.8b02233](https://doi.org/10.1021/acs.iecr.8b02233).

117 S. Wang, W. Yang, X. Li, Z. Hu, B. Wang, M. Li and W. Dong, Preparation of high-expansion open-cell polylactic acid foam with superior oil-water separation performance, *Int. J. Biol. Macromol.*, 2021, **193**, 1059–1067, DOI: [10.1016/j.ijbiomac.2021.11.033](https://doi.org/10.1016/j.ijbiomac.2021.11.033).

118 B. Li, G. Zhao, G. Wang, L. Zhang, J. Gong and Z. Shi, Biodegradable PLA/PBS open-cell foam fabricated by supercritical  $\text{CO}_2$  foaming for selective oil-adsorption, *Sep. Purif. Technol.*, 2021, **257**, 117949, DOI: [10.1016/j.seppur.2020.117949](https://doi.org/10.1016/j.seppur.2020.117949).

119 K. Ru, S. Zhang, X. Peng, J. Wang and H. Peng, Fabrication of Poly(butylene succinate) phosphorus-containing ionomers microcellular foams with significantly improved thermal conductivity and compressive strength, *Polymer*, 2019, **185**, 121967, DOI: [10.1016/j.polymer.2019.121967](https://doi.org/10.1016/j.polymer.2019.121967).

120 M. Zhu, X. Wei, M. Zhang, H. Zhou, X. Wang and J. Hu, Adsorption characteristics of amphiphilic open-cell poly (butylene succinate) foams with ultrahigh porosity, *J. Supercrit. Fluids*, 2023, **200**, 106002, DOI: [10.1016/j.supflu.2023.106002](https://doi.org/10.1016/j.supflu.2023.106002).

121 M. Xu, M. Wu, X. Li, J. Tang, W. Ma, X. Zhu, Q. Ren, L. Wang and W. Zheng, Biodegradable nanofibrillated microcellular PBS/PLA foams for selective oil absorption, *Int. J. Biol. Macromol.*, 2024, **254**, 127844, DOI: [10.1016/j.ijbiomac.2023.127844](https://doi.org/10.1016/j.ijbiomac.2023.127844).

122 S. Liu, Q. Wang, S. Zhang, Z. Yao, L.-C. Tang and K. Cao, Study on the Foaming Behaviors of PBS and Its Modification with PA6IcoT Assisted by  $\text{scCO}_2$ , *Adv. Eng. Mater.*, 2022, **24**, 2100713, DOI: [10.1002/adem.202100713](https://doi.org/10.1002/adem.202100713).

123 A. Gupta, B. Chudasama, B. P. Chang and T. Mekonnen, Robust and sustainable PBAT – Hemp residue biocomposites: Reactive extrusion compatibilization and fabrication, *Compos. Sci. Technol.*, 2021, **215**, 109014, DOI: [10.1016/j.compscitech.2021.109014](https://doi.org/10.1016/j.compscitech.2021.109014).

124 D. Hu, K. Xue, Z. Liu, Z. Xu and L. Zhao, The essential role of PBS on PBAT foaming under supercritical  $\text{CO}_2$  toward green engineering, *J.  $\text{CO}_2$  Util.*, 2022, **60**, 101965, DOI: [10.1016/j.jcou.2022.101965](https://doi.org/10.1016/j.jcou.2022.101965).

125 X. Gao, R. Li, L. Hu, J. Lin, Z. Wang, C. Yu, Y. Fang, Z. Liu, C. Tang and Y. Huang, Preparation of boron nitride nanofibers/PVA composite foam for environmental remediation, *Colloids Surf. A*, 2020, **604**, 125287, DOI: [10.1016/j.colsurfa.2020.125287](https://doi.org/10.1016/j.colsurfa.2020.125287).

126 Q. Hou and X. Wang, The effect of PVA foaming characteristics on foam forming, *Cellulose*, 2017, **24**, 4939–4948, DOI: [10.1007/s10570-017-1452-1](https://doi.org/10.1007/s10570-017-1452-1).

127 R. Zhang, W. Wan, L. Qiu, Y. Wang and Y. Zhou, Preparation of hydrophobic polyvinyl alcohol aerogel via the surface modification of boron nitride for environmental remediation, *Appl. Surf. Sci.*, 2017, **419**, 342–347, DOI: [10.1016/j.apsusc.2017.05.044](https://doi.org/10.1016/j.apsusc.2017.05.044).

128 Z. He, H. Wu, Z. Shi, Z. Kong, S. Ma, Y. Sun and X. Liu, Facile Preparation of Robust Superhydrophobic/Superoleophilic  $\text{TiO}_2$ -Decorated Polyvinyl Alcohol Sponge for Efficient Oil/Water Separation, *ACS Omega*, 2022, **7**, 7084–7095, DOI: [10.1021/acsomega.1c06775](https://doi.org/10.1021/acsomega.1c06775).

129 S. Jin, X. Wei, Z. Yu, J. Ren, Z. Meng and Z. Jiang, Acoustic-Controlled Bubble Generation and Fabrication of 3D Polymer Porous Materials, *ACS Appl. Mater. Interfaces*, 2020, **12**, 22318–22326, DOI: [10.1021/acsami.0c02118](https://doi.org/10.1021/acsami.0c02118).

130 M. V. Lorevice, E. O. Mendonça, N. M. Orra, A. C. Borges and R. F. Gouveia, Porous Cellulose Nanofibril-Natural Rubber Latex Composite Foams for Oil and Organic Solvent Absorption, *ACS Appl. Nano Mater.*, 2020, **3**, 10954–10965, DOI: [10.1021/acsanm.0c02203](https://doi.org/10.1021/acsanm.0c02203).

131 U. Hwang, B. Lee, B. Oh, H. S. Shin, S. S. Lee, S. G. Kang, D. Kim, J. Park, S. Shin, J. Suhr, S.-H. Kim and J.-D. Nam, Hydrophobic lignin/polyurethane composite foam: An eco-friendly and easily reusable oil sorbent, *Eur. Polym. J.*, 2022, **165**, 110971, DOI: [10.1016/j.eurpolymj.2021.110971](https://doi.org/10.1016/j.eurpolymj.2021.110971).

132 A. Chamas, H. Moon, J. Zheng, Y. Qiu, T. Tabassum, J. H. Jang, M. Abu-Omar, S. L. Scott and S. Suh, Degradation Rates of Plastics in the Environment, *ACS*



*Sustainable Chem. Eng.*, 2020, **8**, 3494–3511, DOI: [10.1021/acssuschemeng.9b06635](https://doi.org/10.1021/acssuschemeng.9b06635).

133 J. Gonzalez Ausejo, J. Rydz, M. Musioł, W. Sikorska, M. Sobota, J. Włodarczyk, G. Adamus, H. Janeczek, I. Kwiecień, A. Hercog, B. Johnston, H. R. Khan, V. Kannappan, K. R. Jones, M. R. Morris, G. Jiang, I. Radecka and M. Kowalcuk, A comparative study of three-dimensional printing directions: The degradation and toxicological profile of a PLA/PHA blend, *Polym. Degrad. Stab.*, 2018, **152**, 191–207, DOI: [10.1016/j.polymdegradstab.2018.04.024](https://doi.org/10.1016/j.polymdegradstab.2018.04.024).

134 A. Z. Naser, I. Deiab and B. M. Darras, Poly(lactic acid) (PLA) and polyhydroxyalkanoates (PHAs), green alternatives to petroleum-based plastics: a review, *RSC Adv.*, 2021, **11**, 17151–17196, DOI: [10.1039/D1RA02390J](https://doi.org/10.1039/D1RA02390J).

135 S. Qian, T. Igarashi and K. Nitta, Thermal degradation behavior of polypropylene in the melt state: molecular weight distribution changes and chain scission mechanism, *Polym. Bull.*, 2011, **67**, 1661–1670, DOI: [10.1007/s00289-011-0560-6](https://doi.org/10.1007/s00289-011-0560-6).

136 J. Pinto, A. Athanassiou and D. Fragouli, Surface modification of polymeric foams for oil spills remediation, *J. Environ. Manage.*, 2018, **206**, 872–889, DOI: [10.1016/j.jenvman.2017.11.060](https://doi.org/10.1016/j.jenvman.2017.11.060).

137 B. Li, X. Liu, X. Zhang, J. Zou, W. Chai and J. Xu, Oil-absorbent polyurethane sponge coated with KH-570-modified graphene, *J. Appl. Polym. Sci.*, 2015, **132**, 41821, DOI: [10.1002/app.41821](https://doi.org/10.1002/app.41821).

138 C. A. Pal, G. K. R. Angaru, L. P. Lingamdinne, Y.-L. Choi, Z. H. Momin, R. Kulkarni, J. R. Koduru and Y.-Y. Chang, Fabrication of plasma-treated superhydrophobic polydimethylsiloxane (PDMS) – Coated melamine sponge for enhanced adhesion capability and sustainable oil/water separation, *Sep. Purif. Technol.*, 2024, **330**, 125483, DOI: [10.1016/j.seppur.2023.125483](https://doi.org/10.1016/j.seppur.2023.125483).

139 V. O. A. Tanobe, T. H. D. Sydenstricker, S. C. Amico, J. V. C. Vargas and S. F. Zawadzki, Evaluation of flexible postconsumed polyurethane foams modified by polystyrene grafting as sorbent material for oil spills, *J. Appl. Polym. Sci.*, 2009, **111**, 1842–1849, DOI: [10.1002/app.29180](https://doi.org/10.1002/app.29180).

140 V. H. Pham and J. H. Dickerson, Superhydrophobic Silanized Melamine Sponges as High Efficiency Oil Absorbent Materials, *ACS Appl. Mater. Interfaces*, 2014, **6**, 14181–14188, DOI: [10.1021/am503503m](https://doi.org/10.1021/am503503m).

141 Q. Ke, Y. Jin, P. Jiang and J. Yu, Oil/Water Separation Performances of Superhydrophobic and Superoleophilic Sponges, *Langmuir*, 2014, **30**, 13137–13142, DOI: [10.1021/la502521c](https://doi.org/10.1021/la502521c).

142 L. Qiu, A. D. Phule, W. Zhong, S. Wen and Z. Zhang, Degradable Superhydrophilic Iron-Pillared Bentonite Doped with Polybutylene Adipate/Terephthalate Open-Cell Foam: Its Application in Dye Degradation, Removal of Heavy Metal Ions, and Oil-Water Separation, *Macromol. Mater. Eng.*, 2021, **306**, 2100481, DOI: [10.1002/mame.202100481](https://doi.org/10.1002/mame.202100481).

143 C. Ruan, K. Ai, X. Li and L. Lu, A Superhydrophobic Sponge with Excellent Absorbency and Flame Retardancy, *Angew. Chem., Int. Ed.*, 2014, **53**, 5556–5560, DOI: [10.1002/anie.201400775](https://doi.org/10.1002/anie.201400775).

144 M. Q. Seah, Z. C. Ng, W. J. Lau, M. Gürsoy, M. Karaman, T.-W. Wong and A. F. Ismail, Development of surface modified PU foam with improved oil absorption and reusability via an environmentally friendly and rapid pathway, *J. Environ. Chem. Eng.*, 2022, **10**, 106817, DOI: [10.1016/j.jece.2021.106817](https://doi.org/10.1016/j.jece.2021.106817).

145 A. Uricchio, T. Lasalandra, E. R. G. Tamborra, G. Caputo, R. P. Mota and F. Fanelli, Atmospheric Pressure Plasma-Treated Polyurethane Foam as Reusable Absorbent for Removal of Oils and Organic Solvents from Water, *Materials*, 2022, **15**, 7948, DOI: [10.3390/ma15227948](https://doi.org/10.3390/ma15227948).

146 G. Wang, Z. Zeng, X. Wu, T. Ren, J. Han and Q. Xue, Three-dimensional structured sponge with high oil wettability for the clean-up of oil contaminations and separation of oil–water mixtures, *Polym. Chem.*, 2014, **5**, 5942–5948, DOI: [10.1039/C4PY00552J](https://doi.org/10.1039/C4PY00552J).

147 H. Li, L. Liu and F. Yang, Oleophilic Polyurethane Foams for Oil Spill Cleanup, *Procedia Environ. Sci.*, 2013, **18**, 528–533, DOI: [10.1016/j.proenv.2013.04.071](https://doi.org/10.1016/j.proenv.2013.04.071).

148 L. Zhang, Z. Zhang and P. Wang, Smart surfaces with switchable superoleophilicity and superoleophobicity in aqueous media: toward controllable oil/water separation, *NPG Asia Mater.*, 2012, **4**, e8–e8, DOI: [10.1038/am.2012.14](https://doi.org/10.1038/am.2012.14).

149 Z. Lei, G. Zhang, Y. Deng and C. Wang, Surface modification of melamine sponges for pH-responsive oil absorption and desorption, *Appl. Surf. Sci.*, 2017, **416**, 798–804, DOI: [10.1016/j.apsusc.2017.04.165](https://doi.org/10.1016/j.apsusc.2017.04.165).

150 E. S. Medeiros, G. M. Glenn, A. P. Klamczynski, W. J. Orts and L. H. C. Mattoso, Solution blow spinning: A new method to produce micro- and nanofibers from polymer solutions, *J. Appl. Polym. Sci.*, 2009, **113**, 2322–2330, DOI: [10.1002/app.30275](https://doi.org/10.1002/app.30275).

151 B. Zhao, Experimental study and numerical simulation the air jet flow field of a dual slot sharp blunt die in the melt blowing nonwoven process, *Polym. Eng. Sci.*, 2017, **57**, 417–423, DOI: [10.1002/pen.24436](https://doi.org/10.1002/pen.24436).

152 B. O. Lee, J. A. Ko and S. W. Han, Characteristics of PP/PET Bicomponent Melt Blown Nonwovens as Sound Absorbing Material, *Adv. Mater. Res.*, 2010, **123–125**, 935–938, DOI: [10.4028/www.scientific.net/AMR.123-125.935](https://doi.org/10.4028/www.scientific.net/AMR.123-125.935).

153 Y. Wang and X. Wang, Numerical analysis of new modified melt-blowing dies for dual rectangular jets, *Polym. Eng. Sci.*, 2014, **54**, 110–116, DOI: [10.1002/pen.23536](https://doi.org/10.1002/pen.23536).

154 Y. Kara and K. Molnár, A review of processing strategies to generate melt-blown nano/microfiber mats for high-efficiency filtration applications, *J. Ind. Text.*, 2022, **51**, 137S–180S, DOI: [10.1177/15280837211019488](https://doi.org/10.1177/15280837211019488).

155 H. Zhang, Q. Zhen, Z.-Y. Liu, J.-Q. Cui and X.-M. Qian, Facile fabrication of polylactic acid/polyethylene glycol micro-nano fabrics with aligned fibrous roughness for enhancing liquid anisotropic wetting performance via double-stage drafting melt blowing process, *Colloids*



*Surf., A*, 2022, **648**, 129174, DOI: [10.1016/j.colsurfa.2022.129174](https://doi.org/10.1016/j.colsurfa.2022.129174).

156 F. Sun, T.-T. Li, X. Zhang, B.-C. Shiu, Y. Zhang, H.-T. Ren, H.-K. Peng, J.-H. Lin and C.-W. Lou, In situ growth polydopamine decorated polypropylene melt-blown membrane for highly efficient oil/water separation, *Chemosphere*, 2020, **254**, 126873, DOI: [10.1016/j.chemosphere.2020.126873](https://doi.org/10.1016/j.chemosphere.2020.126873).

157 M. Wehmann and W. J. G. McCulloch, *Melt blowing technology*, 1999, pp. 415–420. DOI: [10.1007/978-94-011-4421-6\\_58](https://doi.org/10.1007/978-94-011-4421-6_58).

158 L. Zhang, J. Wu, X. Yang, Y. Di and X. Zhuang, Melt-blown of silicane-modified phenolic fibrous mat for personal thermal protection, *Colloids Surf., A*, 2023, **663**, 131076, DOI: [10.1016/j.colsurfa.2023.131076](https://doi.org/10.1016/j.colsurfa.2023.131076).

159 J. E. Spruiell and E. Bond, *Melt spinning of polypropylene*, 1999, pp. 427–439. DOI: [10.1007/978-94-011-4421-6\\_60](https://doi.org/10.1007/978-94-011-4421-6_60).

160 I. M. Hutten, Processes for Nonwoven Filter Media, in *Handbook of Nonwoven Filter Media*, Elsevier, 2007, pp. 195–244. DOI: [10.1016/B978-185617441-1/50020-2](https://doi.org/10.1016/B978-185617441-1/50020-2).

161 N. Mao, Nonwoven fabric filters, in *Advances in Technical Nonwovens*, Elsevier, 2016, pp. 273–310. DOI: [10.1016/B978-0-08-100575-0.00010-3](https://doi.org/10.1016/B978-0-08-100575-0.00010-3).

162 R. (Rongguo) Zhao, Melt Blown Dies: A Hot Innovation Spot, *Int. Nonwovens J.*, 2002, **os-11**, 1558925002OS-01, DOI: [10.1177/1558925002OS-01100409](https://doi.org/10.1177/1558925002OS-01100409).

163 D. Duran, Investigation of the Physical Characteristics of Polypropylene Meltblown Nonwovens Under Varying Production Parameters, in *Thermoplastic Elastomers*, InTech, 2012. DOI: [10.5772/36798](https://doi.org/10.5772/36798).

164 J. V. Galaviz, E. H. Rodriguez, M. R. Torrentera and J. J. A. Saiz, Mechanical Design of Primary Air System, Meltblown Banks Machine TL02, *J. Manage. Poli Pract.*, 2015, **3**, 69–83, DOI: [10.15640/jmpp.v3n1a9](https://doi.org/10.15640/jmpp.v3n1a9).

165 G. Sun, W. Han, Y. Wang, S. Xin, J. Yang, F. Zou, X. Wang and C. Xiao, Overview of the Fiber Dynamics during Melt Blowing, *Ind. Eng. Chem. Res.*, 2022, **61**, 1004–1021, DOI: [10.1021/acs.iecr.1c03972](https://doi.org/10.1021/acs.iecr.1c03972).

166 X. Hao and Y. Zeng, A Review on the Studies of Air Flow Field and Fiber Formation Process during Melt Blowing, *Ind. Eng. Chem. Res.*, 2019, **58**, 11624–11637, DOI: [10.1021/acs.iecr.9b01694](https://doi.org/10.1021/acs.iecr.9b01694).

167 S. Xie and Y. Zeng, Turbulent Air Flow Field and Fiber Whipping Motion in the Melt Blowing Process: Experimental Study, *Ind. Eng. Chem. Res.*, 2012, **51**, 5346–5352, DOI: [10.1021/ie202938b](https://doi.org/10.1021/ie202938b).

168 S. Xie, W. Han, G. Jiang and C. Chen, Turbulent air flow field in slot-die melt blowing for manufacturing microfibrous nonwoven materials, *J. Mater. Sci.*, 2018, **53**, 6991–7003, DOI: [10.1007/s10853-018-2008-y](https://doi.org/10.1007/s10853-018-2008-y).

169 E. M. Moore, R. L. Shambaugh and D. V. Papavassiliou, Analysis of isothermal annular jets: Comparison of computational fluid dynamics and experimental data, *J. Appl. Polym. Sci.*, 2004, **94**, 909–922, DOI: [10.1002/app.20963](https://doi.org/10.1002/app.20963).

170 B. Zhu, S. Xie, W. Han and G. Jiang, Swirling Diffused Air Flow and Its Effect on Helical Fiber Motion in Swirl-Die Melt Blowing, *Fibers Polym.*, 2021, **22**, 1594–1600, DOI: [10.1007/s12221-021-0809-0](https://doi.org/10.1007/s12221-021-0809-0).

171 M. A. J. Uyttendaele and R. L. Shambaugh, Melt blowing: General equation development and experimental verification, *AIChE J.*, 1990, **36**, 175–186, DOI: [10.1002/aic.690360203](https://doi.org/10.1002/aic.690360203).

172 R. S. Rao and R. L. Shambaugh, Vibration and stability in the melt blowing process, *Ind. Eng. Chem. Res.*, 1993, **32**, 3100–3111, DOI: [10.1021/ie00024a020](https://doi.org/10.1021/ie00024a020).

173 V. T. Marla and R. L. Shambaugh, Three-Dimensional Model of the Melt-Blowing Process, *Ind. Eng. Chem. Res.*, 2003, **42**, 6993–7005, DOI: [10.1021/ie030517u](https://doi.org/10.1021/ie030517u).

174 Y. Kara and K. Molnár, Revealing of process–structure–property relationships of fine polypropylene fiber mats generated via melt blowing, *Polym. Adv. Technol.*, 2021, **32**, 2416–2432, DOI: [10.1002/pat.5270](https://doi.org/10.1002/pat.5270).

175 R. R. Bresee and W.-C. Ko, Fiber Formation during Melt Blowing, *Int. Nonwovens J.*, 2003, **os-12**, 1558925003os-12, DOI: [10.1177/1558925003os-1200209](https://doi.org/10.1177/1558925003os-1200209).

176 E. M. Moore, D. V. Papavassiliou and R. L. Shambaugh, Air Velocity, Air Temperature, Fiber Vibration and Fiber Diameter Measurements on a Practical Melt Blowing Die, *Int. Nonwovens J.*, 2004, **os-13**, 1558925004os-13, DOI: [10.1177/1558925004os-1300309](https://doi.org/10.1177/1558925004os-1300309).

177 T. Chen, X. Wang and X. Huang, Effects of Processing Parameters on the Fiber Diameter of Melt Blown Nonwoven Fabrics, *Text. Res. J.*, 2005, **75**, 76–80, DOI: [10.1177/004051750507500114](https://doi.org/10.1177/004051750507500114).

178 D. Moyo, A. Patanaik and R. D. Anandjiwala, Process control in nonwovens production, in *Process Control in Textile Manufacturing*, Elsevier, 2013, pp. 279–299. DOI: [10.1533/9780857095633.3.279](https://doi.org/10.1533/9780857095633.3.279).

179 D. H. Tan, C. Zhou, C. J. Ellison, S. Kumar, C. W. Macosko and F. S. Bates, Meltblown fibers: Influence of viscosity and elasticity on diameter distribution, *J. Non-Newton. Fluid Mech.*, 2010, **165**, 892–900, DOI: [10.1016/j.jnnfm.2010.04.012](https://doi.org/10.1016/j.jnnfm.2010.04.012).

180 H. Yin, Z. Yan, W.-C. Ko and R. R. Bresee, Fundamental Description of the Melt Blowing Process, *Int. Nonwovens J.*, 2000, **os-9**, 1558925000OS-90, DOI: [10.1177/1558925000OS-900408](https://doi.org/10.1177/1558925000OS-900408).

181 Y. Yesil and G. S. Bhat, Porosity and barrier properties of polyethylene meltblown nonwovens, *J. Text. Inst.*, 2017, **108**, 1035–1040, DOI: [10.1080/00405000.2016.1218109](https://doi.org/10.1080/00405000.2016.1218109).

182 G. Sun, Y. Chen, Y. Ruan, G. Li, W. Hu and S. Xin, Modeling and experimental study of pore structure in melt-blown fiber assembly, *J. Ind. Text.*, 2022, **51**, 6051S–6064S, DOI: [10.1177/15280837211011776](https://doi.org/10.1177/15280837211011776).

183 L. Zhang and J. Y. Chen, Comparative study on compressional recovery performance of vertically laid and cross-laid highloft nonwovens, *J. Ind. Text.*, 2022, **51**, 1372S–1391S, DOI: [10.1177/1528083720925828](https://doi.org/10.1177/1528083720925828).

184 R. R. Bresee, A. Qureshi and M. C. Pelham, Influence of Processing Conditions on Melt Blown Web Structure: Part 2–Primary Airflow Rate, *Int. Nonwovens J.*, 2005, **os-14**, 1558925005os-14, DOI: [10.1177/1558925005os-1400202](https://doi.org/10.1177/1558925005os-1400202).



185 A. Ghosal, S. Sinha-Ray, A. L. Yarin and B. Pourdeyhimi, Numerical prediction of the effect of uptake velocity on three-dimensional structure, porosity and permeability of meltblown nonwoven laydown, *Polymer*, 2016, **85**, 19–27, DOI: [10.1016/j.polymer.2016.01.013](https://doi.org/10.1016/j.polymer.2016.01.013).

186 P. P. Tsai, Characterization of Melt Blown Web Properties using Air Flow Technique, *Int. Nonwovens J.*, 1999, **08-8**, 1558925099OS-80, DOI: [10.1177/1558925099OS-800216](https://doi.org/10.1177/1558925099OS-800216).

187 I. Langmuir, *Report on smokes and filters*, 1942.

188 M. Guo, H. Liang, Z. Luo, Q. Chen and W. Wei, Study on melt-blown processing, web structure of polypropylene nonwovens and its BTX adsorption, *Fibers Polym.*, 2016, **17**, 257–265, DOI: [10.1007/s12221-016-5592-y](https://doi.org/10.1007/s12221-016-5592-y).

189 W. Wu, T. Hirogaki, E. Aoyama, M. Ikegaya and H. Sota, Investigation of Oil Adsorption Performance of Polypropylene Nanofiber Nonwoven Fabric, *J. Eng. Mater. Technol.*, 2019, **141**, 021004, DOI: [10.1115/1.4041853](https://doi.org/10.1115/1.4041853).

190 Z. Zhang, D. Yu, X. Xu, H. Li, T. Mao, C. Zheng, J. Huang, H. Yang, Z. Niu and X. Wu, A polypropylene melt-blown strategy for the facile and efficient membrane separation of oil–water mixtures, *Chin. J. Chem. Eng.*, 2021, **29**, 383–390, DOI: [10.1016/j.cjche.2020.03.033](https://doi.org/10.1016/j.cjche.2020.03.033).

191 H. Lee, B. M. Trinh, E. A. Crawford and T. H. Mekonnen, Thermoplastic elastomer melt-blown fiber mats for oil spill remediation: Fabrication, oil uptake, and gel formation studies, *Sep. Purif. Technol.*, 2023, **326**, 124761, DOI: [10.1016/j.seppur.2023.124761](https://doi.org/10.1016/j.seppur.2023.124761).

192 X. H. Meng, H. H. Wu and Y. C. Zeng, Blended Polypropylene Fiber of Various MFR via a Melt-Blowing Device for Oil Spill Cleanup, *Appl. Mech. Mater.*, 2014, 624, 669–672, DOI: [10.4028/www.scientific.net/AMM.624.669](https://doi.org/10.4028/www.scientific.net/AMM.624.669).

193 F. Sun, T.-T. Li, H. Ren, Q. Jiang, H.-K. Peng, Q. Lin, C.-W. Lou and J.-H. Lin, PP/TiO<sub>2</sub> Melt-Blown Membranes for Oil/Water Separation and Photocatalysis: Manufacturing Techniques and Property Evaluations, *Polymers*, 2019, **11**, 775, DOI: [10.3390/polym11050775](https://doi.org/10.3390/polym11050775).

194 B. Qi, X. Hu, S. Cui, H. Liu, Y. Li, J. Lu and M. Bao, Rapid fabrication of superhydrophobic magnetic melt-blown fiber felt for oil spill recovery and efficient oil–water separation, *Sep. Purif. Technol.*, 2023, **306**, 122486, DOI: [10.1016/j.seppur.2022.122486](https://doi.org/10.1016/j.seppur.2022.122486).

195 B. Qi, N. Wang, X. Hu, S. Cui, H. Liu, R. He, J. Lian, Y. Li, J. Lu, Y. Li and M. Bao, Melt-blown fiber felt for efficient all-weather recovery of viscous oil spills by Joule heating and photothermal effect, *J. Hazard. Mater.*, 2023, **460**, 132523, DOI: [10.1016/j.jhazmat.2023.132523](https://doi.org/10.1016/j.jhazmat.2023.132523).

196 J. A. Kadili, A. H. Abdullah, I. S. Johari, N. Zainuddin and S. N. A. M. Jamil, Highly efficient and reusable superhydrophobic 3D polyurethane nanocomposite foam for remediation of oil polluted water, *J. Porous Mater.*, 2023, **31**, 449–461, DOI: [10.1007/s10934-023-01529-w](https://doi.org/10.1007/s10934-023-01529-w).

197 E. Morici and N. Tz, Dintcheva, Recycling of Thermoset Materials and Thermoset-Based Composites: Challenge and Opportunity, *Polymers*, 2022, **14**, 4153, DOI: [10.3390/polym14194153](https://doi.org/10.3390/polym14194153).

198 J. Drabek and M. Zatloukal, Meltblown technology for production of polymeric microfibers/nanofibers: A review, *Phys. Fluids*, 2019, **31**, 091301, DOI: [10.1063/1.5116336](https://doi.org/10.1063/1.5116336).

